THE TEMPORAL DYNAMICS OF VISION

FOR ACTION AND PERCEPTION

SUMMARY

INDEX OF FIGURES:

RIASSUNTO GENERALE *(Italiano)*

L'obiettivo del presente lavoro è quello di analizzare i meccanismi di integrazione sensorimotoria e – in particolare – il ruolo dei ritmi cerebrali (oscillazioni) nella modulazione delle nostre azioni e percezioni. Nel **primo studio** abbiamo indagato le dinamiche temporali di sensibilità visiva al contrasto durante l'esecuzione libera di movimenti saccadici. Abbiamo quindi testato l'ipotesi che un movimento oculare volontario possa sincronizzare oscillazioni nella visibilità, con lo scopo di analizzare nel dettaglio le proprietà dei sottostanti ritmi percettivi. In un **secondo studio** abbiamo investigato l'effetto dell'esecuzione di movimenti saccadici sulla risposta pupillare. Si sono quindi analizzate le dinamiche di risposta della pupilla e, confrontandole con quelle percettive, si è cercata una possibile correlazione tra i due tipi di risposte. In un **terzo studio** è stato analizzato l'effetto di una semplice azione motoria (la pressione di un tasto) sulla sensibilità visiva al contrasto, verificando anche il possibile ruolo modulatorio di fattori di luminanza ambientale. Infine, nel **quarto studio** (composto a sua volta da tre esperimenti) abbiamo affrontato in maniera sistematica l'effetto della luminanza ambientale sui fenomeni oscillatori del cervello, attraverso uno studio elettrofisiologico e psicofisico. Una discussione generale tenterà – in ultimo – di sintetizzare il significato e la portata dei risultati presentati, suggerendo su tale base nuovi possibili scenari o progetti di ricerca.

GENERAL ABSTRACT *(English)*

The aim of the present thesis is to investigate the mechanisms of sensorimotor integration, and - in particular - the role of oscillations in action and perception. In the **first study**, we considered the contrast sensitivity dynamics during the execution of free saccades. We tested the hypothesis that a voluntary eye movement could trigger behavioral oscillations, with the aim to study in depth the properties of these perceptual rhythmicity. The **second study** investigated the effect of saccades on the pupillary response. We studied the perceptual and the pupillary dynamics at around the time of a saccade, looking for possible correlation between the perceptual response and the pupillary constriction. In the **third study**, we moved to analyze the effect of a simple hand action (button press) over contrast sensitivity, investigating also some possible modulatory effects of ambient luminance. Finally, in the **fourth study** (comprising three experiments), we enucleated the modulatory effects of ambient luminance via an electrophysiological and psychophysical investigation. A general conclusion will sum up the present findings shown here, suggesting possible future directions.

0 GENERAL INTRODUCTION

0.1 COORDINATING ACTION AND PERCEPTION

The sensory systems are traditionally conceived as passive mechanisms, stimulus-driven, receiving and reacting to external information according to a certain set of rules, and mainly dependent on solely external stimulation events. This interpretation is grounded on very old philosophical investigations on the human perception, and it is implicitly assumed as a fundamental principle of psychology. One of the first philosophers that systematically investigated this very crucial aspect was Aristotle. In his *De Anima*, the Stagirite claimed that perception was nothing but an imprint of external events. For centuries, this became the mainstream view and drove very important researchers in understanding the basic rules of perception under passive viewing. In the 50s of the last century, Gibson proposed a different and ecological approach on perception: he proposed a view in which perception results from the combination of the environmental stimulation and how perceivers interact with the environment[1]. This approach has led to a development of a new field of studies on perception, with the goal to understand the *active sensing* processes and discovering the causal links between action and perception. For example, it is widely known that cortical neurons in primary sensory areas are spontaneously active in the absence of external input, and their activity reveals a strong and highly coherent synchronous ongoing dynamical patterns[2,3]. Traditionally, this input-free

activity was considered as a noisy and stochastic process, unlikely being informative regarding the actual perceptual mechanisms and processes involved in the input recording and elaboration[4]. However, in recent years many evidence has revealed a close link between this ongoing activity and perception[5–7], discarding the thesis of a dissociation between the dynamic internal state of the brain and its actual functioning. Thus, human brain started to be conceived as a dynamical system in which the instantaneous state of cortical networks (governed by both external or bottom-up, and internal or top-down processes) plays a key role in determining the nature of the neural processes[8]. It has been shown that even neurons in the primary sensory areas (e.g. in V1) are not exhaustively characterized by their receptive field properties, but instead both contextual information and internal states have a profound influence on their response properties[9]. The analysis of these top-down influences on perception suggested to consider perception as a Bayesian inference orchestrated by the brain[10].

At each moment, our perceptual systems are exposed to an incredible amount of information about the environment that needs to be processed and elaborated in order to create a good representation of the world. However, there is a trade-off between the quantity of information that can be processed and the quality of the perceptual representation: our brain has not enough energy and resources to process every single information, so there is the biological necessity to filter the information to be processed. It is widely known that our sensory systems adopt several bottom-up filters, represented by simple and complex receptive fields of

the sensitive neurons[11–15]. However, there are more complex filters that are not driven by the present stimulation (i.e. the stimulus properties) but by past events and future predictions. These top-down filters influence very low-level stages of sensory processing[9,16–20], and are supposed to be driven by automatic Bayesian inferences that strongly modulate the neuronal response independently from the external stimulation[21]. These modulations are very effective and superimposed on the bottom-up responses: a crystal clear example is the *change blindness*, a phenomenon in which motion transients mask huge changes in the visual scene that subjects fail to see[22,23]. A wide variety of visual illusions revealed the importance of predictive-coding strategies in perception, and its influence in determining the functioning of our primary brain processes. Several models and theories have proposed to describe visual perception in terms of predictive coding[10,24–26]: vision weights the present inputs on the basis of the past events, and makes predictions about the upcoming stimulations. In this view, perception is fundamentally an inference process – rather than a passive imprint of the inputs – that dampens the quantity\quality dichotomy by selecting and processing only those inputs that are meaningful at the moment. Moreover, the meaning of a percept is well defined by its link with the perceiver actions: we do perceive to act and react to environmental events. This intimate and dynamic relationship between action and perception, together with the idea of an oscillatory brain mechanism that acts to synchronize these dynamics, represents the theoretical core of the present thesis.

It has been suggested that neuronal coherence and synchrony could play a key role in integrating action and perception[27–29], and – in this sense - neural oscillations are the most obvious candidates to consider. Neural oscillations are ubiquitous in the brain and they represent the basic strategy to coordinate in time the activity of different neuronal populations. Moreover, they include a wide range of events, that are quite different and independent one from the others. From single cell, to EEG recording, the neural activity possesses some intrinsic rhythmic activity varying from very slow to very fast frequencies. Specific processes have been linked to specific frequency ranges, and the amplitude, as well as the phase, of these oscillations was connected with different functional aspects[30].

0.2 OSCILLATIONS AND THE TEMPORAL BINDING MODEL

Neuronal oscillations are supposed to play a key role in determining the temporal structure of neural responses[27]. Electrophysiological experiments have suggested that gamma oscillations (at about 40 Hz) represent a marker of stimulus processing and a vehicle for bottom-up information. On the other hand, it has been shown that theta and alpha oscillations (between 3-12 Hz) play an important role in feedback processing and do actively modulate gamma activity, resulting in a cross-frequency coupling[31–34]. Consistently with this evidence, several theories have been advanced to explain the coupling between slow and fast oscillations[35–40]. These theories agree in assuming neural synchrony as a crucial event for object representation, response selection, attention,

memory, and sensorimotor integration. In general, it is assumed that slow oscillations act by rhythmically modulating the inhibition influxes over feedforward processing. This modulation is nested in a faster oscillation that reflects bottom-up stimulus processing dynamics. Crucially, slow oscillations are considered top-down processes mostly driven by expectations. In this way, the saliency of the neural response is enhanced thanks to the neural synchrony, as neuronal populations discharging together have a stronger impact than uncorrelated populations. Another crucial ingredient is that the top-down effect can be modulated by implicit Bayesian inference generating expectations based on contextual influences and also action goals[27]. These models imply that perception – as the resultant of discrete processing – would be discontinuous in time[7]. In agreement with the idea of a discrete perception, several data have shown that our perceptual abilities are not constant over time, but they do oscillate rhythmically creating perceptual cycles[6]. It has been shown that the amplitude, as well as the phase, of the theta and alpha oscillations modulates our visual sensibility (at about 10-20% of modulation) and motor reaction times[5,41–44]. This modulation is normally referred as a top-down effect driven by expectation, thus, it is likely that different expectations would produce different oscillations (possibly modulating the frequency or the phase of the oscillation). Accordingly, we might hypothesize that our top-down mechanisms will enhance the expected population of neurons at the expected moment, generally acting like a reset of relevant oscillations to achieve the maximal efficiency at the exact timing. It follows that if an event can phase-lock

this rhythmical processes, we should be able to employ psychophysical measurements to reconstruct the behavioral oscillations[45]. In fact, several behavioral studies have shown that oscillations can be reset by external sensory stimuli and behavioral oscillations have been reported for several visual tasks[46–49]. These oscillations are in the theta-alpha range and are traditionally interpreted as attentional modulatory effects over visual processing. In this sense, it has been proposed that attentional rhythms can lock their activity to external sensory events to synchronize the perceptual systems with salient environmental events. In other words, this oscillatory mechanism can be interpreted as a dynamical predictive process that rhythmically samples sensory information following top-down modulations. Moreover, these top-down modulations have the goal to optimize the perceptual processing by aprioristically selecting specific time windows of interest over time. Thus, one may speculate that an efficient visual system should be able to modulate this oscillatory effect depending on the peculiar characteristics of the neural population to synchronize. Accordingly, it has recently proposed that distinct oscillations can coexist and cooperate[6]. To oversimplify, it has been suggested that whenever the system is required to synchronize different sensorial events, perceptual oscillations are likely driven by alpha activity. On the other hand, if the system has to synchronize perception with attentional events, these oscillations are likely driven by slower oscillations in the theta range[6]. This selectivity does not only reveal oscillations as a basic communication brain protocol, but implies that this mechanism is adaptive and specific.

0.3 DOES ACTION SHAPE PERCEPTION?

Is it legit to hypothesize the presence of a similar specific mechanism for action-perception coupling? In this regard, we might speculate the presence of a common "pacemaker" between the motor and the perceptual system, synchronizing their activity. According to this hypothesis, a sensorimotor integration model has been developed by Bland[29,50] proposing that:

> "…*components of the neural circuitry in hippocampus and associated structures function in the capacity of providing voluntary motor systems with continually updated feedback on their performance relative to changing environmental (sensory) conditions. […]. The components of the neural circuitry involved in sensorimotor integration are those underlying the production of oscillation and synchrony (theta) in the hippocampus and associated structures.*" [51].

The model proposes that theta oscillations, generated by the hippocampus, play a key role in sensorimotor information during sensorimotor behaviors. Hippocampal formation continuously integrates sensorimotor information and updates both motor and sensory systems via a precise rhythmical dynamic within the theta range[52]. Accordingly, a recent experiment has shown in rats that hippocampal theta rhythm can actively entrain primary somatosensory areas suggesting that theta oscillations entrainment provides a mechanism by which activity in

neocortical and hippocampal networks can be temporally coordinated[53]. Moreover, it has been shown that the frequency of rat's and guinea pig's hippocampal theta rhythm is related to speed of locomotion[54,55]. Invasive recordings have demonstrated movement-related theta oscillations in the human neocortex[28,56], and theta oscillations are suggested to reflect a putative neural mechanism for human sensorimotor integration[57–59], although these oscillations cannot be easily related to the human hippocampal theta rhythm[60,61].

Independently from the actual biological substrate involved in this sensorimotor coupling, we should expect that such a functional mechanism would modulate perception (in a sensorimotor task) in an oscillatory fashion at around the theta range. Moreover, we might hypothesize these oscillations be phase-locked with internal action planning activities: the motor and the sensory systems have to be coordinated even before the actual action execution, and it is likely that the phase-reset would act in a motor preparatory stage. Consistently with this hypothesis, a recent psychophysical experiment has shown for the first time that contrast sensitivity at around the time of a simple motor action (grasping) is not constant over time, but it oscillates in the theta range (at around 5 Hz) in synchrony with the action onset[62]. The experiment consisted in a visual orientation discrimination task recorded around the time of a voluntary reaching movement (±600 ms from action onset). Authors reported that contrast sensibility oscillated rhythmically in cycles of about 200 ms. Crucially, this oscillation was phase-locked with action execution and started at least 600 ms before the movement onset.

This suggests that voluntary actions can reset the phases of ongoing endogenous oscillations, and possibly revealing crucial properties of sensorimotor integration processes.

0.4 STRUCTURE OF THE THESIS

The aim of the present thesis is to further investigate the mechanisms of sensorimotor integration, and - in particular - the role of oscillations in action and perception. In the **first study**, we considered the contrast sensitivity dynamics during the execution of free saccades. We tested the hypothesis that a voluntary eye movement could trigger behavioral oscillations, with the aim to study in depth the properties of these perceptual rhythmicity. The **second study** investigated the effect of saccades on the pupillary response. We studied the perceptual and the pupillary dynamics at around the time of a saccade, looking for possible correlation between the perceptual response and the pupillary constriction. In the **third study**, we moved to analyze the effect of a simple hand action (button press) over contrast sensitivity, investigating also some possible modulatory effects of ambient luminance. Finally, in the **fourth study** (comprising three experiments), we enucleated the modulatory effects of ambient luminance via an electrophysiological and psychophysical investigation.

A general conclusion will sum up the present findings shown here, suggesting possible future directions.

0.4.1 Research abstracts

0.4.1.1 *Saccadic suppression is embedded within extended oscillatory modulation of sensitivity*

Action and perception are intimately coupled systems; one clear case is saccadic suppression, the reduced visibility around the time of saccades, important in mediating visual stability; another is the oscillatory modulation of visibility synchronized with hand action. To suppress effectively the spurious retinal motion generated by the eye movements, it is crucial that saccadic suppression and saccadic onset be temporally synchronous. However, the mechanisms that determine this temporal synchrony are unknown. We investigated the effect of saccades on contrast discrimination sensitivity over a long period stretching over more than 1 second before and after saccade execution. Human subjects made horizontal saccades at will to two stationary saccadic targets separated by 20 degrees. At a random interval, a brief Gabor patch was displayed between the two fixations in either the upper or lower visual field, and the subject had to detect its location. Strong saccadic suppression was measured between -50 and 50 ms from saccadic onset. However, the suppression was systematically embedded in a trough of oscillations of contrast sensitivity that fluctuated rhythmically in the delta range (at about 3 Hz), commencing about one second before saccade execution and lasting for up to one second after the saccade. The results show that saccadic preparation and visual sensitivity oscillations are coupled, and the coupling might be instrumental in temporally aligning the initiation of the saccade with the visual suppression.

0.4.1.2   Dissociable saccadic suppression of pupillary and perceptual responses to light

We measured pupillary constrictions in response to full-screen flashes of variable luminance, occurring either at the onset of a saccadic eye movement or well before/after it. A large fraction of perisaccadic flashes were undetectable to the subjects, consistent with saccadic suppression of visual sensitivity. Likewise, pupillary responses to perisaccadic flashes were strongly suppressed. However, the two phenomena appear to be dissociable. Across subjects and luminance levels of the flash stimulus, there were cases in which conscious perception of the flash was completely depleted yet the pupillary response was clearly present, as well as cases in which the opposite occurred. On one hand, the fact that pupillary light responses are subject to saccadic suppression reinforces evidence that this is not a simple reflex but depends on the integration of retinal illumination with complex "extraretinal" cues. On the other hand, the relative independence of pupillary and perceptual responses suggests that suppression acts separately on these systems—consistent with the idea of multiple visual pathways that are differentially affected by saccades.

0.4.1.3   Rhythmic modulation of visual contrast discrimination triggered by action

Recent evidence suggests that ongoing brain oscillations may be instrumental in binding and integrating multisensory signals. In this experiment, we investigated the temporal dynamics of visual–motor integration processes. We show that action modulates sensitivity to

visual contrast discrimination in a rhythmic fashion at frequencies of about 5 Hz (in the theta range), for up to 1 s after execution of action. To understand the origin of the oscillations, we measured oscillations in contrast sensitivity at different levels of luminance, which is known to affect the endogenous brain rhythms, boosting the power of alpha-frequencies. We found that the frequency of oscillation in sensitivity increased at low luminance, probably reflecting the shift in mean endogenous brain rhythm towards higher frequencies. Importantly, both at high and at low luminance, contrast discrimination showed a rhythmic motor-induced suppression effect, with the suppression occurring earlier at low luminance. We suggest that oscillations play a key role in sensory–motor integration, and that the motor-induced suppression may reflect the first manifestation of a rhythmic oscillation.

0.4.1.4 *Luminance changes modulate oscillatory properties of the visual system*

We investigated the effects of ambient luminance changes on neural oscillation dynamics. Brain oscillations, particularly in the alpha range (~10 Hz), are important in determining our percepts. Crucially, ambient luminance changes drastically modulate neural processing. However, the influence of luminance over brain rhythmicity is still not clear. Here, we investigated the effect of ambient luminance on EEG alpha during spontaneous brain activity at rest (experiment 1) and during the measurement of echo functions (i.e. EEG "impulse-response functions", IRF) or evoked alpha (experiment 2). Results show that during resting, alpha amplitude increased at low luminance, while luminance changes

did not affect alpha frequency. In the second experiment, we found that under low-luminance viewing the IRF amplitude was lower, and its frequency was slightly faster. Crucially, the evoked alpha activity behaved differently from IRF: while evoked alpha and perceptual echoes showed a similar amplitude modulation, luminance changes influenced the echo peak frequency but not that of evoked EEG alpha. Finally, we explored the behavioral effects of these modulations in a monocular critical flicker frequency task (experiment 3), reporting a facilitatory effect of contralateral dark ambient luminance over temporal thresholds. Globally, we found that ambient luminance changes affect neural oscillatory dynamics and greatly impact on the occipital alpha expression. Moreover, we found that the alpha frequency of the perceptual echo increases at low luminance, and this shift correlates with a psychophysical enhancement of the critical flicker frequency. These results suggest that the visual system adapts its oscillatory dynamics to fit the environmental light conditions.

1 SACCADIC SUPPRESSION IS EMBEDDED WITHIN EXTENDED OSCILLATORY MODULATION OF SENSITIVITY[*][63]

1.1 INTRODUCTION

Action and perception are tightly coupled in everyday life. Although these sensorimotor integration mechanisms are pervasive in the brain, they are still poorly understood. Brain oscillations might be important in binding and integrating sensorimotor information[27] via a shared internal oscillator that coordinates the two systems. Recent experiments have shown that voluntary movements can synchronize oscillations of visual performance[62,64]. So, action not only interferes with perception through a single transient suppression at around movement time (a phenomenon called *motor-induced suppression*), but rhythmically interacting long before and after action execution. These rhythmical interferences may result from endogenous brain rhythms synchronized by the intention-to-move signal. On this view the motor-induced suppression might be a stronger manifestation of a more general sensorimotor modulation.

The best-known example of *motor-induced suppression* is saccadic suppression. Visually driven saccadic eye movements are known to

---

produce strong visual suppression at time of saccades[65–68]. This suppression is transient, but highly precise in time, starting about 50 ms before saccadic onset and maximal at saccadic onset[68]. This contrasts with the highly variable saccadic reaction time that can be higher than 80 ms[44,69,70]. The suppression is present also in conditions of no visual references and with simulated saccades (for a review see Morrone[71]) demonstrating that it does not arise from visual masking.

Physiological and psychophysical studies[67,68,72–76] have demonstrated that suppression is followed by an enhancement, 100-200 ms after saccades. Both suppression and enhancement are independent of stimulus eccentricity[76], and hence unlikely generated by spatial attention which shifts from fixation to saccadic target very early, about 300 ms before saccadic onset[77–79]. The peri-saccadic suppression and the subsequent enhancement form a cycle of an oscillation at about 3 Hz, suggesting that they might be part of a more prolonged oscillation linked to saccadic preparation, similarly to the visual oscillation demonstrated in preparation of an hand action[62,64].

How the brain ensures that the suppression occurs at saccadic onset is unknown. An active mechanism (*efference copy* or *corollary discharge)* probably mediates the suppression[68,80,81], which is an anticipatory signal[82]. However, we do not know whether it is a temporally punctual signal informing vision about the incoming saccades, or it is a sluggish signal that builds up during the preparation of the saccade. Many voluntary action onsets are preceded by a readiness potential that have

a gradual build-up over 500 ms or more[83–87]. It is likely that also for saccades there is a long build-up of the corollary discharge signal. In all cases, oscillations during the motor preparation phase might be a means to propagate in time the corollary discharge signal and to keep a precise representation of movement onset. Interestingly, recently it has been shown that spatial attention[88] and temporal integration or segregation[89] oscillate rhythmically and in synchrony with saccades, reinforcing this suggestion.

To test whether saccadic suppression and post-saccadic facilitation are part of an ongoing oscillatory modulation of vision, we measured contrast discrimination over a long peri-saccadic period. Results show that peri-saccadic contrast sensitivity is modulated in the delta range (2-3 Hz) and, crucially, saccadic suppression and enhancement are embedded in phase with these oscillations.

1.2 MATERIAL AND METHODS

1.2.1 Participants

Eight volunteers (three women; mean age: 28±4 years, including author AB) performed the experiment. All had normal or corrected-to-normal vision. Participants gave informed consent in accordance with the Declaration of Helsinki.

1.2.2 Apparatus

The experiment was performed in a quiet, dark room. Subjects sat in front of a monitor screen (40x30 cm) at a distance of 57 cm, with their head stabilized by a chin rest. Stimuli were generated with the ViSaGe (Cambridge Research System) in MATLAB (MATLAB r2010a, The MathWorks) and presented on a CRT monitor (Barco Calibrator) with a resolution of 800x600 pixels and a refresh rate of 100 Hz. Two-dimensional position of the left eye was monitored at 1 kHz with an EyeLink 1000 system (SR Research) with an infrared camera mounted below the screen. Horizontal eye position recordings were linearized by means of a linear calibration performed at the beginning of each session.

1.2.3 Stimuli and procedure

Two red square saccadic targets (0.25°), vertically aligned and horizontally separated by 20°, appeared at the beginning of the experiment and persisted until the end of the session. The stimulus was a horizontal sinusoidal grating (1 cpd, pedestal contrast 10%, random phase) presented for 10 ms in a 5° circular window with Gaussian

smoothed edge on the center of the screen at 10° distance from both fixation points (figure 1A). The contrast was incremented in a Gaussian window in the upper or lower half of the circular stimulus. The luminance *l(x,y)* was given by:

$$l(x,y) = \sin(x\omega + \varphi)\left(K + \Delta K\, e^{-\left[\left(\frac{x}{\sigma_x}\right)^2 + \left(\frac{y \pm \mu_y}{\sigma_y}\right)^2\right]} \right) G(x,y)$$

Where *x* and *y* and are the spatial coordinates; K is the pedestal contrast (10%) and ΔK is the contrast increment; σ_x=1.5° and σ_y=0.75° are the space constants and μ_y=1.25° is the spatial vertical offset; ω=1 c/° is the spatial frequency, φ the random phase, and the function G(*x,y*) is a circular step function of diameter 5° convolved with a Gaussian function of constant equal to 0.5° to smooth the stimulus-background edges.

Individual thresholds for contrast increment were obtained during a training session, with a QUEST procedure. The contrast increment value that elicited about 75% correct responses was selected and kept constant within each block. In order to balance perceptual learning improvement, the contrast increment was adjusted slightly from block to block to maintain 75% correct response. For the whole duration of each session, participants made 20° horizontal saccades at will from one stationary saccadic target to the other (figure 1A). After each saccade, they were instructed to maintain fixation for at least 3 s before performing a new saccade towards the opposite saccadic target. At a random interval, the stimulus was displayed, with a probability of about 1 presentation every 3 saccades (inter-stimulus interval, ISI: 12±5 s; fixation duration: 4.3±0.4

s). This was established to avoid an automatic allocation of attention at the center of the screen for every saccade. The ISI was random and controlled by the experimenter in order to maximize the amount of collectable data. Subjects were required to detect by 2AFC a threshold contrast increment in either the upper or lower field, and verbally report the response to the experimenter after the execution of the next saccade. Each session lasted for 5 minutes, single participants performed on average 3 hours of eye movement recordings over different days (37±10 sessions per participant).

1.2.4   Data analysis

In an offline analysis, eye-position traces were examined and individual saccade modelled with a trapezoidal function. A positive slope segment, with two abutting constant segments were used to fit the saccade trace and derive the saccadic onset and offset. We included in further analysis only saccades with inter-saccadic separation greater than 3 s and that were fit well by the trapezoidal model ($R^2 > 0.99$, ~80% of the saccades). To disentangle the contribution of saccadic preparation from the saccadic execution to the contrast sensitivity data, we restricted the analysis only to a temporal window of ±1.5 s from the saccadic onset and pooled together the data for the leftward and rightward saccades. The eye-movement recording traces were also automatically analyzed to detect microsaccades, on the basis of speed and amplitude criteria (events faster than 20°/s and shorter than 2°). Subsequently, individual microsaccades were validated via visual inspection.

To evaluate the presence of oscillations, we performed several analyses at a group level, where the individual subject data were first binned and then averaged across subjects; and also by pooling all data together in a single dataset (hereafter termed the *aggregate observer*) and subsequently binned. For the aggregate observer data, we computed the percentage of correct responses in 80 ms independent bins. The variability was assessed via a bootstrap procedure performed before the binning (1000 iterations, with replacement and standard deviation of the bootstrap reported as standard error of the mean, s.e.m.).

Spectral analyses were conducted using the fast Fourier transform (FFT). We computed the spectral variability via a bootstrap procedure for the aggregate observer (1000 iterations, with replacement). A two-dimensional statistical significance test was run on the real and imaginary components for each frequency. A nonparametric two-tailed sign test was run to determine whether the distribution of data points was different from zero in at least one of the two components, implying that the two-dimensional cloud of bootstrapped data was not centered at the origin. These analyses were conducted separately for the pre-saccadic response (-1.46 to 0.08 s), for the post-saccadic response (0.08 to 1.13 s) and for the whole signal (from -1.46 to 1.13 s). For the whole signal, the relative p-values were corrected for multiple comparison using the False Discovery Rate methods (FDR[90]). Note that both pre- and post-saccadic responses FFT excluded peri-saccadic data within 80 ms from saccadic onset (peri-saccadic gap of 80 ms).

Beside the FFT, we also used a different approach that requires that the oscillations are stationary in time. The pre- (from -1.38 s) and post-saccadic (to 1.22 s) time series were separately fitted with two independent sinusoidal functions. The best-fit statistical significance was evaluated using a bootstrap procedure on surrogate data obtained by randomly shuffling the time-stamps (-1.38 to 1.22 s) of the single trial and then performing the standard binning procedure. The surrogate data were fit with a sinusoidal waveform of the same frequency as the original data, with amplitude and phase as free parameters. A one-tail nonparametric bootstrap t-test was run to assess whether the R^2 of the best fit of the data was statistically higher than the 95% of the R^2 distribution obtained from the bootstrapped surrogate data. To evaluate the effect of saccadic suppression on the oscillatory performance, we ran the same analysis on both pre- and post-saccadic responses by extending the peri-saccadic gap from 80 ms to 400 ms, in steps of 80 ms. For the gap of 160 ms we also ran a more stringent statistical test: the surrogate data were fit with a sinusoidal waveform with all free parameters (frequency varying between 1.5 and 6 Hz) and the real data best fit was compared against the best fit of the noise distribution independently of the frequency. Finally, we tested the statistical significance of all the possible sinusoidal models from 1.5 to 6 Hz (in steps of 0.1 Hz) using the same procedure described above that take into account the correction for multiple comparison. For both FFT and best-fitting analysis, phase angles are calculated respect the origin set at 0 ms and are relative to a cosine function.

In order to evaluate the oscillatory effect on single subjects, we computed d-prime in bins of 160ms, overlapped by 90% with the adjoining one. The group-mean d-prime (d') was fit by sinusoidal waveforms, with the same procedure described above, for the pre-saccadic and post-saccadic intervals. A one-tail nonparametric bootstrap t-test was run to assess whether the R^2 of the best fit of the data was statistically higher than the 95% of the R^2 distribution obtained from the bootstrapped surrogate data for each individual subject.

1.3 RESULTS

Subjects made saccades at their own pace to stationary saccadic targets. At random times, we sporadically presented a brief Gabor stimulus with a contrast increment that subjects had to localize in a two-alternative force choice procedure (2AFC, figure 1A). We measured how contrast discrimination accuracy varied as a function of stimulus presentation from the saccadic onset. Figure 1B shows the result obtained by pooling together the data from all subjects (aggregate observer). A strong peri-saccadic suppression is evident, being maximal at saccadic onset, similar to that commonly observed for visually driven saccades. Subjects performed nearly at chance level for peri-saccadic stimuli (±40 ms), and around 75% away from the saccade. However, for times long before and long after the saccade, performance was not constant but oscillated with about 10% of modulation. To quantitatively assess the nature of these oscillations, we best-fitted the performance timecourse with sinusoidal waveforms. To avoid possible biases in the frequency and phase estimation introduced by the strong minima of saccadic suppression, we fitted independently the pre-saccadic and post-saccadic responses, excluding the ±160ms around the saccadic onset. The best sinusoidal model was obtained at a frequency around 3 Hz for the pre-saccadic performance (2.9±0.4 Hz, mean and 95% confidence bounds, red curve in figure 1B), and around 2Hz (2.3±0.4 Hz, mean and 95% confidence bounds, green curve in figure 1B) for the post-saccadic performance.

Figure 1.1: paradigm and main results
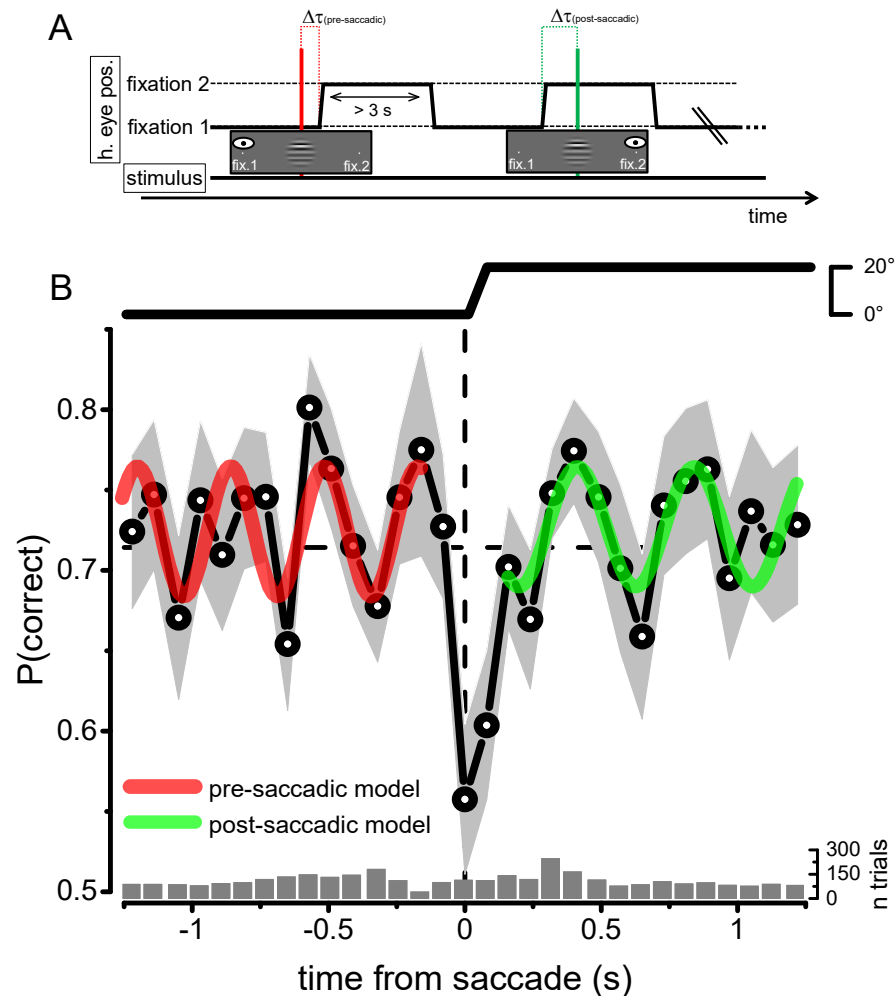
A. Illustration of the experimental procedure. Participants performed saccades at their own pace to stationary saccadic targets (fixation 1 and fixation 2). At random delay from the saccadic onset (Δt), a brief Gabor stimulus with a contrast increment was presented in its upper or lower side, and participants were asked to report the location of the increment. **B**. Pre- and post- saccadic contrast discrimination performance as a function of time from saccadic onset. Aggregate observer, pooling together the single trial data of 8 individual subjects. The bar plot shows the number of observations for each bin (106±38). The gray area represents ±1 s.e.m. from bootstrapping; thick lines represent the best sinusoidal fit to the data for pre-saccadic responses (in red at around 3 Hz) and for post-saccadic responses (in green at around 2 Hz). Dashed vertical and horizontal lines report the time from saccadic onset and the median probability of correct response, respectively. Top trace shows the mean horizontal eye position.

To evaluate the significance of both these models, we compared the R^2 values of these fits with the distribution of the R^2 obtained by fitting a sinusoidal waveform of the same frequency to surrogate data (obtained by shuffling the time-stamps of each trial). Figure 2A shows the results of this analysis for the pre-saccadic (left panel) and the post-saccadic model (right panel). For both models, the goodness of fit was statistically higher than that expected from a noise distribution (pre-saccadic model: $R^2=0.49$, $p=0.007$; post-saccadic model: $R^2=0.62$, $p=0.005$).

Similar results were obtained for a range of peri-saccadic gaps between 80 and 400 ms, in five steps of 80 ms (figure 2C). All the best sinusoidal fits were statistically significant, with the exception of the pre-saccadic model with 400 ms gap that was marginally significant (p-values for different peri-saccadic gaps for pre- and post-saccadic responses, respectively: gap=0.08 s, p=[0.009 0.032]; gap=0.16 s, p=[0.007 0.005]; gap=0.24 s, p=[0.028 0.007]; gap =0.32 s, p=[0.044 0.02]; gap =0.4 s, p=[0.07 0.026]). We also evaluated the significance of the oscillation with a more stringent test, comparing the R^2 of the best fitting sinusoidal model against the R^2 distribution of the best fitting of the surrogate data across all possible frequencies. Figure 2B shows that for both models the R^2 obtained from the aggregate observer data was statistically higher than the R^2 surrogated distribution (pre-saccadic response: p=0.041; post-saccadic response: p=0.019), for the best fit across all frequencies. For the pre-saccadic data, no other frequency of the model in the range between 1.5 and 6 Hz (in steps of 0.1 Hz) survived statistical significance with this stringent test (figure 2B left), while for the post-saccadic

oscillations were significant (p< 0.05) in the range between 2.2 and 2.5 Hz (with a peak of significance at 2.3 Hz). No single frequency model fitted significantly both periods, indicating the presence of long lasting delta oscillatory modulation of contrast discrimination of different frequencies for the pre- and the post-saccadic range.

Figure 1.2: best-fit model analysis
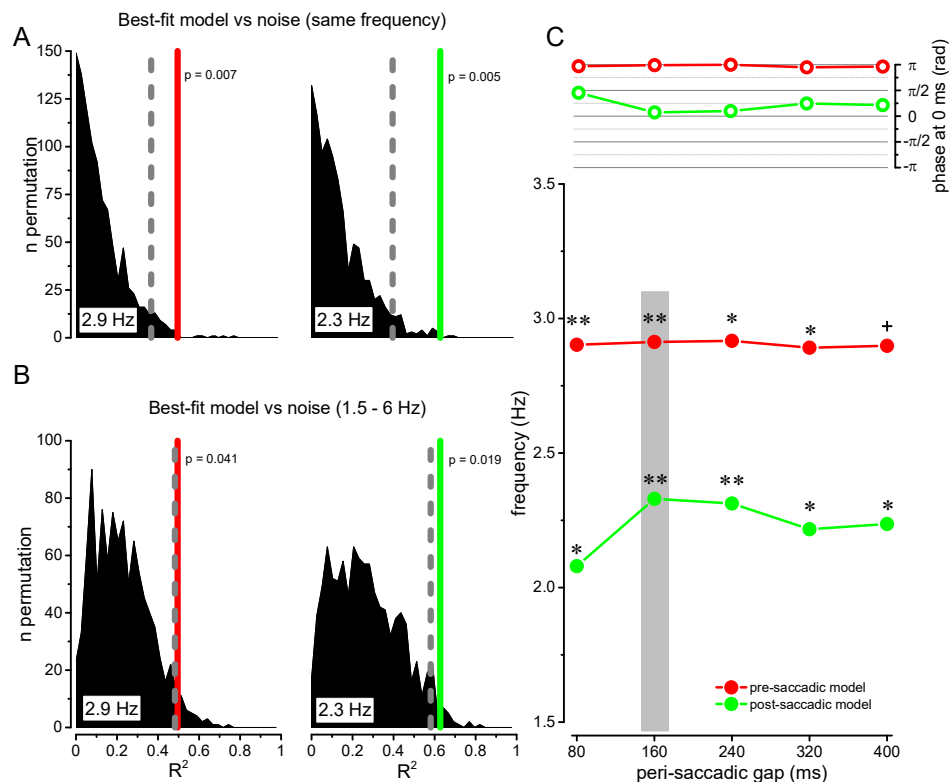
A. R^2 distribution obtained by fitting the random shuffled data with the sinusoidal functions from figure 1 with amplitude and phases as free parameters (peri-saccadic gap set to 160 ms); thick lines mark the R^2 for the pre-saccadic model (red, 2.9 Hz, p = 0.007) and the post-saccadic model (green, 2.3 Hz, p = 0.005). Dashed lines mark 0.95 probability; **B**. Same analysis as reported in A, but with an R^2 permuted distribution obtained by best fitting the random shuffled data with frequency as a free parameter. The best fit was statistically higher than noise level for both pre-saccadic response (red, p = 0.041) and post-saccadic response (green, p = 0.019). **C**. Best fitting frequency and phase of the aggregate data as function of different peri-saccadic gaps The phase is calculated respect to 0 ms origin and reported for a cosine function. Asterisks indicate significant points following the procedure in A (0.1 > + > 0.05 > * > 0.01 > ** > 0.001).

Subjects saccaded at their own pace. In principle, the oscillations observed before the saccadic onset might have been related to the execution of the previous saccade or even to the spurious retinal motion generated by the previous saccadic execution. To control for this possible confound, we aligned the responses to the previous saccade excluding the response to stimuli that were closer than about 100 ms to the following saccade onset. Figure 3 shows that the performance, after the first 1.5 s from saccadic onset, was randomly modulated around the average value of 75%. The best fitting of the data of figure 3 (between 0.08 and 3 s) with a single sinusoidal function was not statistically significant (R^2=0.07, p=0.31) for any frequency in the range 1.5 and 6 Hz, while the modulation of the first second was qualitatively well captured by the best fit of the post-saccadic modulation of figure 1 (green curve, figure 3). This suggests that pre-saccadic oscillations were not related to the previous saccade, but were genuinely phase-locked to the preparation of the upcoming saccade.

Figure 1.3: post-saccadic oscillations
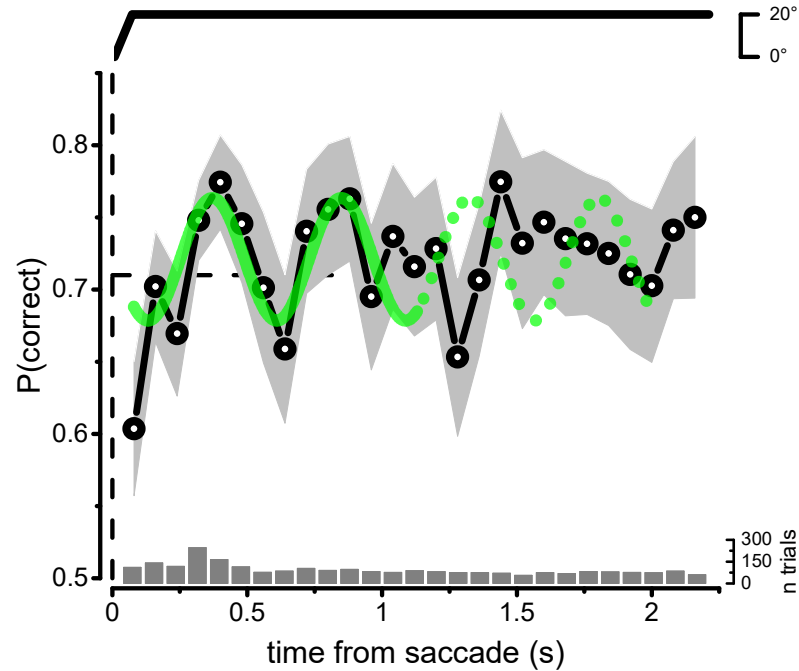
Post-saccadic contrast discrimination performance as function of delay from the onset of the previous saccade. The gray area represents ±1 s.e.m. from bootstrapping; thick line represents the best sinusoidal fit of figure 1B (green curves), dotted line shows that after about the first second the model does not fit well the dataset. Note that the first 1.5 s corresponds to the post-saccadic data of figure 1. Data from saccades with latency less than 3s are not included. Dashed vertical and horizontal lines report the time from saccadic onset and the median probability of correct response, respectively. Top trace is the mean horizontal eye position.

Having confirmed that a separation of 3 seconds is sufficient to disentangle the effect of the previous saccade from that of the following one, we performed a spectral analysis on the whole signal of figure 1B (without peri-saccadic gap). Two main frequency peaks were detected at about 2 and 3 Hz in the FFT (figure 4), confirming the fitting results of figure 1B. We ran the 2D spectral statistical analysis for each frequency (see methods) and the obtained p-values were corrected for multiple

comparisons using a FDR procedure. A two-tailed sign test showed that only these two components were statistically significant (1.9 Hz: p=0.006 after FDR correction: p=0.048; 3 Hz: p=0.004 after FDR correction: p=0.048).

Figure 1.4: global FFT analysis
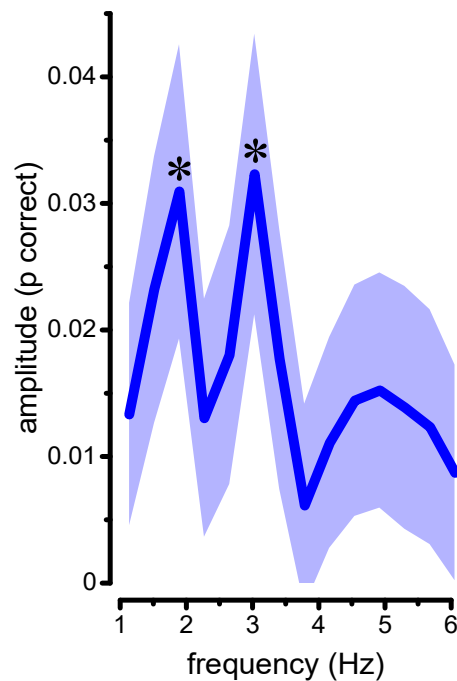
FFT spectral analysis for the aggregate observer. Amplitude spectra of the signal ± 1 s.e.m. The local maxima at 1.9 and 3 Hz are the only to reach statistical significance (1.9 Hz: p = 0.006; 3 Hz: p = 0.004). Asterisks indicate the significance after FDR correction (0.1 > + > 0.05 > * > 0.01).

Figure 5 shows a similar spectral analysis performed separately for the pre-saccadic (figure 5A, red curve, interval -1.46 to -0.08 s) and the post-saccadic (figure 5A, green curve, interval 0.08 and 1.13 s) responses, with gap of 80 ms. Amplitude peaks were present at 2.8 and 1.8 Hz for

the two intervals, respectively. The bootstrapped amplitude and phase evaluations clustered away from the zero amplitude, indicating that the oscillations were statistically significant (2.8 Hz: p=0.014, figure 5B; 1.8 Hz: p=0.012, figure 5C) and different from random noise. The average phase, computed respect to the origin at 0 ms, of these significant frequencies (black vectors in Fig 5B and C) were 2.81±0.4 rad and 2.23±0.45 rad, respectively.

Figure 1.5: pre- and post-saccadic FFT analysis
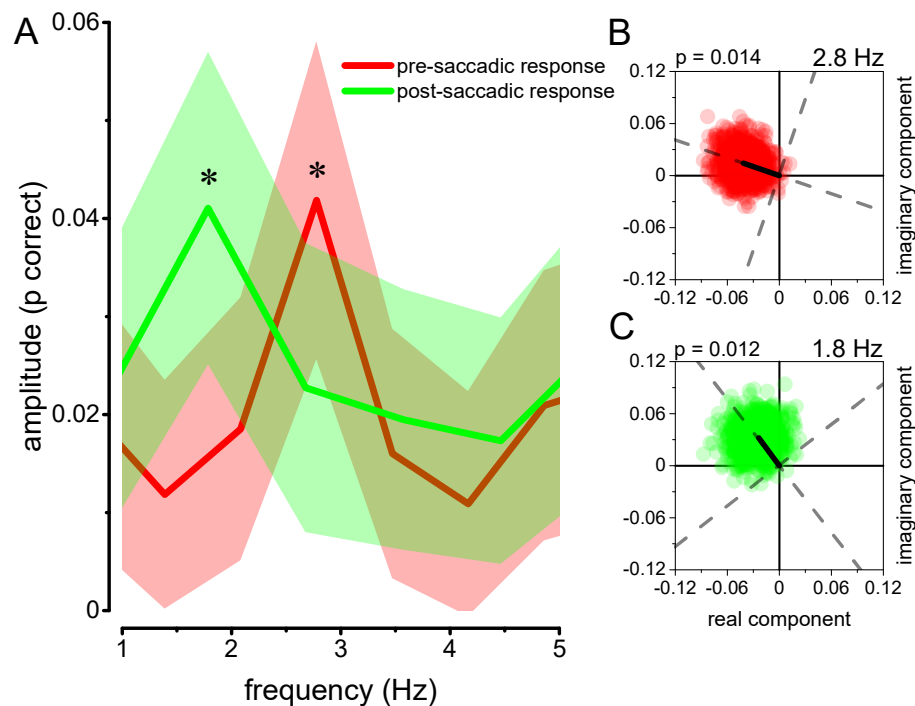
A. FFT mean amplitude spectra ±1 s.e.m for pre-saccadic (red curves) and post-saccadic responses (green curve). **B** and **C**. 2D bootstrap analysis performed for pre-saccadic response at 2.8 Hz (**B**, p = 0.014), and post-saccadic response at 1.8 Hz (**C**, p = 0.012). The black vectors show the average amplitudes and phases at 2.8 and 1.8 Hz. The phases are calculated respect to 0 ms origin and reported for a cosine function. Asterisks indicate the significance (0.1 > + > 0.05 > * > 0.01 > ** > 0.001).

An important question is whether the period of saccadic suppression in embedded in phase with the oscillation. Saccadic suppression is usually reported to be maximally between 0 and 30 ms from saccadic onset[68,76,91]. This time is very close to the estimated time by the oscillation for the FFT analysis: the arrival time of the minimum of the 2.8 Hz pre-saccadic oscillation falls around the time of saccadic onset (19±23 ms). Similarly, the arrival time of the minimum of the post-saccadic 1.8 Hz oscillation is delayed of about 81±40 ms from saccadic onset. Interestingly, this time correspond to the bin including saccadic offset (mean saccadic duration was 62±6 ms), suggesting that saccadic suppression is embedded in phase with the pre-saccadic oscillations and that pre- and post-saccadic oscillation minima straddle the onset and offset of the saccades.

Oscillations might result from periodic microsaccades, that affect vision in a similar way to normal saccades, producing visual suppression and enhancement (for a review see Rucci and Poletti[92]). It is known that fixational eye movements have little effect on low spatial frequencies[92,93], and may not contribute to the visibility of our stimulus. However, to confirm that microsaccades were not relevant to the oscillation of sensitivity we measured the average frequency of microsaccades across subjects in bins of 20 ms (figure 6). The temporal distribution of microsaccades showed a peak at around 120 ms after saccadic execution, followed by a nearly constant rate with negligible (less than 0.5%) modulation.

Figure 1.6: microsaccadic rate
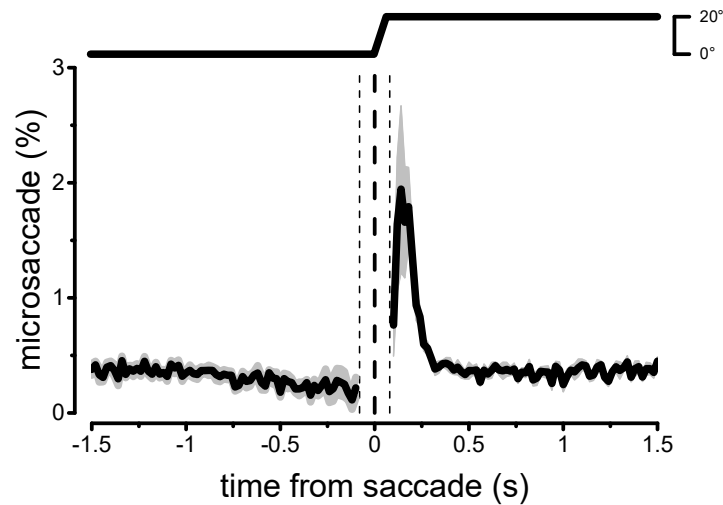
Horizontal microsaccadic frequency and s.e.m. as a function of time from saccadic onset, for group-level data (N=8) calculate in bin of 20 ms. The thick vertical line represents the saccadic onset, thin vertical lines delimit peri-saccadic boundaries. The microsaccadic rate decays rapidly in the first 120 ms after saccadic onset, being nearly constant before and after saccadic execution. The top trace shows a mean horizontal eye position.

Analysis of aggregate observer data is generally robust, and relatively unaffected by differences in the amount of data for different time bins and participants. However, it conceals individual differences, so the results could be driven by a few subjects with strong oscillations. To rule out this possibility, we calculated the group mean performance across the individual subjects (figure 7A). The group average analysis gave very similar results to the aggregate observer data, with significant oscillations at 3.1 and 2 Hz for pre- and post-saccadic responses respectively (pre-saccadic: 3.1 ± 0.12 Hz, $p = 0.008$; post-saccadic: 2 ± 0.11 Hz, $p=0.01$; figure 7B). Two individual subjects (figure 7C) also showed oscillations at frequencies similar to those measured in the aggregate observer data.

Figure 1.7: group level analysis
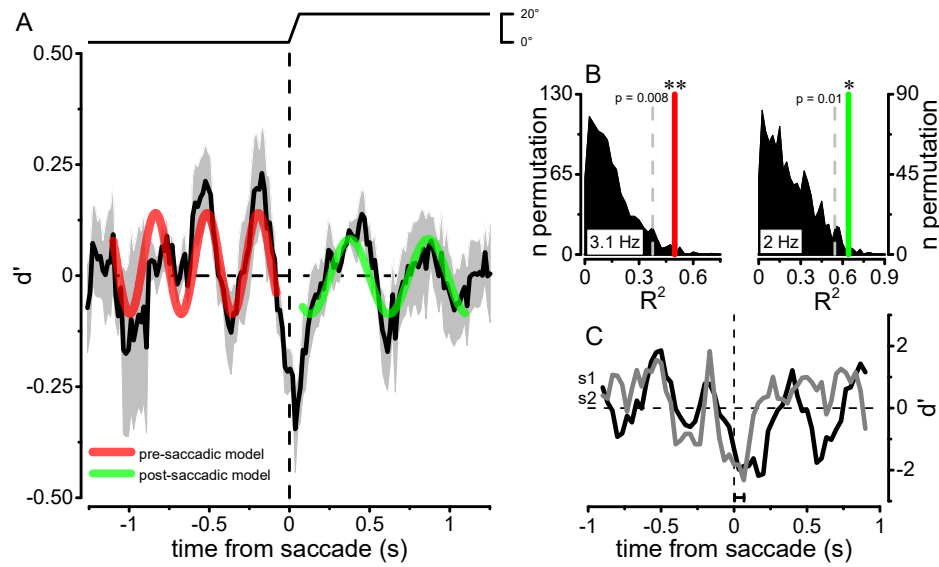
A, d-prime (d') averaged across subjects (n=8) as function of delay from saccadic onset. The gray area represents ±1 s.e.m.; thick lines represent the best sinusoidal fit to the data for pre-saccadic responses (in red at 3.1 Hz) and for post-saccadic responses (in green at 2 Hz). Dashed vertical and horizontal lines report the time from saccadic onset and the median probability of correct response, respectively. The top trace shows mean horizontal eye position. **B**, R^2 distribution obtained by fitting the random shuffled data with the sinusoidal functions from **A** with amplitude and phases as free parameters. Dashed lines mark 0.95 probability; thick lines mark the R^2 for the pre-saccadic model (left panel, 3.1 Hz, p = 0.008) and the post-saccadic model (right panel, 2 Hz, p = 0.01). Asterisks indicate significant points (0.05 > * > 0.01 > ** > 0.001). **C**, d-prime as a function of time from saccadic onset for two representative subjects.

1.4 DISCUSSION

The visual effects of saccades are traditionally analyzed within a narrow temporal window of few hundreds of milliseconds around saccadic onset. Here we analyzed the temporal dynamics of contrast sensitivity in a 3 s window centered at saccadic onset. Our data replicated the well-known effects of saccadic suppression and saccadic facilitation. Crucially, they show strong contrast sensitivity oscillations in the delta-range from about one second before to one second after saccadic execution, with saccadic suppression and saccadic enhancement embedded in the phase with these oscillations. The pre-saccadic oscillation was slightly faster than the post-saccadic one (2.9 Hz vs. 2.3 Hz) and slower than the oscillations measured for hand movements (reported roughly at 6 Hz[62,64]) for the same visual task.

Visual contrast sensitivity oscillations began at least one second before saccadic onset, lasting for up to one second after. Given that the saccades were not visually driven (subjects saccaded freely between two stationary small targets), we can exclude that oscillations were initiated by a transient appearance of the saccadic target. It is also unlikely that oscillations were generated by the transient retinal motion produced by the eye movement[68,76,94]. Aligning all the responses with the previous saccadic onset, we observed oscillations only around the first second. Thereafter, the oscillations disappeared gradually, confirming a decay with time from saccade execution[89]. This pattern of results indicates that the oscillations are synchronized with motor preparation, and not to the

transient appearance of perceptual stimuli, a phenomenon demonstrated by previous work[47,49]. It is also unlikely that oscillations are related to the spatial attentional allocation towards the stimulus position, as more than half of saccades were made without the presentation of the stimulus, and we do not detect any hazard rate[95]. We can also dismiss a role of microsaccades. In agreement with the evidence that fixational eye movements have little effect on the low spatial frequency stimuli[92,93] used here, we show that their rate is constant over time with the exception of a corrective microsaccades for the physiological saccadic overshooting[96].

Consistent with Tomassini et al.[62], the cyclic modulation of visual contrast sensitivity observed here is phase-locked with action planning (or the intention to move), corroborating the hypothesis that oscillations play a key role in binding action and perception[27,97,98]. This sensorimotor synchronization may be mediated by a time-keeping mechanism, shared between visual and motor processes. It is well known that humans are extremely good at producing repetitive movements[99] including saccadic eye movements[100], and we can perform saccades with precise timing also for intervals over seconds. The close link between time mechanisms and saccades is demonstrated by the profound alteration of time perception for peri-saccadic stimuli[101–103]. Interestingly, saccadic reaction times to abrupt visual stimuli are highly variable, and can be predicted by the phase of ongoing brain oscillations, as it has been observed for many other visual functions[5,7,43,104]. Thus, a system based on endogenous oscillations synchronized by an internal clock could produce the close

temporal alignment of perceptual and motor events at the face of the erratic saccadic reaction time.

Here we show that saccades are synchronous with long-lasting visual delta oscillations at about 3 Hz. We scan the world with at a similar rate of about 3 saccades per second, thought to be optimal timing given the temporal dynamics of visual perception[80,105]. Interestingly, also hand-onset actions are synchronous with oscillations of visual contrast thresholds[62,64]. However, for hand action, visual oscillations are at higher frequencies (around 6 Hz) and these frequencies correspond to the maximum hand movement rate while maintaining accurate timing[106]. All these results suggest that motor and sensory circuitry oscillates in synchrony in the brain, and that these periodicities may be orchestrated by effector-specific clocks. Our results are consistent with the hypothesis of a shared internal clock between action and perception, which helps to maintain visual stability and coordination between these two systems. This sensorimotor hypothesis is also corroborated by the fact that both saccadic suppression and saccadic enhancement are embedded in phase with visual oscillations: oscillations might play a key role in precisely inhibiting/enhancing vision according to the motor state of the subject.

The major motor mechanism that informs visual brain about the upcoming eye movement is a corollary discharge signal [107]. Electrophysiological evidence indicates that corollary discharge signals takes time to emerge, and can reverberate for several hundreds of

milliseconds[108,109]. It is still unknown whether this motor signal is short and punctate in time or long and rhythmically modulated. A punctate corollary discharge may directly lock the ongoing visual oscillation or, conversely, the corollary signal itself may be oscillatory, producing the modulatory effect on visual performance observed in our data. Both models can explain the oscillation observed here. However, both models imply that the corollary discharge is active 1 s before saccade, and not just 200 ms as it is commonly assumed by current research on eye-movements[71,81]. An anticipatory corollary discharge signal has been already proposed as a mechanism to explain the complex changes in oscillatory activity during eye movements. In monkeys an increase of high-frequency power and phase-reset of low-frequency oscillations have been observed after the execution of eye movements[110,111], and suggested to be responsible for the transient perceptual enhancement measured psychophysically at the new fixation onset[112]. The corollary discharge signal, generated at an early stage during motor preparation, could thus keep the ongoing activity in visual areas phase-locked.

The early emergence of corollary discharge is similar to the readiness potential observed in other voluntary actions[83–87]. A long-lasting *active sensing* process, which starts about 1 s before saccadic onset, might be important to prepare and organize the visual system for spatial and temporal patterns of visual inputs directly linked to oculomotor events[89,113]. Consistent with this interpretation, a recent study[89] has shown that saccadic onset locks the phases of 3 Hz oscillations for temporal integration or segregation of visual information. Here we

observed similar frequencies for a different, but equally important property: saccadic suppression. Also attention oscillates rhythmically in synchrony with saccades, but at a higher frequency than that observed here (at 4Hz; Hogendoorn[88]), for a period much closer to the saccadic onset (about 500 ms), and with a strong hazard rate. Inter alia, that narrower time window is consistent with the shift of the allocation of spatial attention to saccadic target that it known to take place about 300 ms before the saccadic onset. All these phenomena are not observed in the present data, suggesting that our results are linked to early visual processing mechanisms. Spurious retinal motion induced by the eye movement can modulate sensitivity, particularly post-saccadically[76]. It is reassuring that our data and those of Hogendoorn et al. - who used very different visual references (minimal for the present study and very strong for Hogendoorn et al.) - show similar post-saccadic oscillation, although at different frequencies and with different temporal decay. This reinforces the suggestion that the post-saccadic oscillation are not synchronized only by perceptual signals as demonstrated in previous studies[46,47].

In conclusion, our data are consistent with the idea of a supra-modal neuronal timing mechanism that synchronizes visual and motor oscillations. Motor oscillations determine the time of the saccade, and visual oscillations determine the time of saccadic suppression or enhancement. Oscillations may have the crucial role of coordinating visuo-motor information, helping not only in maintaining visual stability but also in defining our sense of agency. This may result in actions being constrained to start around particular phases of endogenous oscillations.

This would imply that we are not free to move the eyes when we want: the possible onset times may be pre-determined by internal mechanisms long time before the actual movement, as previously proposed by Libet et al.[86] However, further experiments are necessary to verify the fascinating idea of an oscillatory free-will.

2   DISSOCIABLE SACCADIC SUPPRESSION OF PUPILLARY AND PERCEPTUAL RESPONSES TO LIGHT[*][114]

2.1   INTRODUCTION

Saccades are rapid ballistic eye movements. While allowing for rapidly directing our high-resolution fovea to different objects of interest, they impose heavy costs on the visual system. These include the smearing and sudden displacement of retinal images. Many processes contribute to elimination of these disturbances; one of these is a transient suppression of visual sensitivity to low-frequency luminance modulations (which can attenuate the disruptive motion signals produced by the rotation of the eyes[115,116]). There is no consensus on the neural substrates of this suppression, but most agree that it spares the retina; it might be produced by a corollary discharge or copy of the oculomotor command, interacting with visual signals as early as in the thalamus[67,81]. In contrast with an early suppression site, however, there is evidence that suppression differentially affects conscious vision and unconscious visual processing[117] — visual stimuli that are completely suppressed from conscious perception may still affect subsequently presented images,

---

[*] This chapter refers to the published paper: A. Benedetto, P. Binda. (2016). *Dissociable saccadic suppression of pupillary and perceptual responses to light*. J. Neurophysiol.

creating a "shape contrast illusion." This fits with the notion that visual processing involves multiple pathways, relatively independent of each other[118,119]. This idea remains controversial despite numerous investigations; among these there is specific evidence that saccades have different effects on those supporting conscious vision and the others, e.g., pathways related to action planning[120,121].

Here we aimed to test for such dissociation by simultaneously measuring the effects of saccadic suppression on two kinds of responses to retinal stimulation: a perceptual response (the conscious detection of a light flash) and an automatic involuntary response (the pupillary constriction evoked by the flash).

Pupillary constriction in response to light is often thought of as a reflex behavior, supported by a mesencephalic circuit, directly fed by retinal signals[122,123]. However, there is growing evidence that this response in fact integrates complex information and depends on relatively high-level visual processing (for review see Binda and Murray[124]). Granted that the major determinant of pupil diameter is light[123], it has been shown that subtle pupillary constrictions can be evoked by stimuli that do not alter the level of retinal illumination, e.g., by changes of perceived brightness (during binocular rivalry[125,126] or with brightness illusions[127]) and even by simply evoking the idea of brightness (e.g., pictures of the sun[128,129]) or mental imagery of bright scenes[130]). Moreover, shifting attention to a brighter region[128,131–133] or feature[134]) is sufficient to induce pupillary

constriction, and the pupillary response to a luminance increment is enhanced when the stimulus is made behaviorally relevant[124].

These results strongly suggest that a brightness signal, relatively independent of retinal illumination, participates in the specification of the pupillary light response. Is this signal subject to the effect of saccadic suppression, like the luminance signal supporting conscious perception is? Work from the 1960s indicates that saccadic suppression does affect pupillary light responses[135,136]. These experiments showed that the pupillary constriction evoked by a briefly presented flash is substantially reduced when the flash occurs just before or during a saccade, i.e., when conscious detection of the stimulus is impaired. Interestingly, the data are suggestive of a differential effect of saccades on pupillary and perceptual responses: the suppression of pupillary responses extends over a much longer temporal window than the perceptual suppression. However, this difference of temporal dynamics alone could simply be put down to the slow temporal dynamics of the pupillary response[137] — the same extraretinal signal will give rise to a longer-lasting suppression when affecting a process with longer integration times, as modeled in Diamond et al.[138]. To more directly test for a dissociation between suppressive effects on the pupillary response and conscious detection, here we reexamined the work by Lorber and collaborators in conditions optimized for testing the relationship between the two phenomena: measuring both phenomena while varying the luminance of the flash about the subjective visibility threshold. This allows us to correlate pupillary and perceptual responses, obtaining a quantitative index of their interdependence.

2.2 Methods

2.2.1 Subjects

14 subjects (5 females, mean age ± standard deviation: 24.57 ± 2.06) participated in the study. All reported normal or corrected-to-normal vision. Experimental procedures were approved by the local ethics committee and were in accordance with the Declaration of Helsinki; participants gave their written informed consent.

2.2.2 Apparatus

The experiment was performed in a quiet, dark room. Subjects sat in front of a monitor screen (40x30 cm) at a distance of 57 cm, with their head stabilized by a chin rest. Viewing was binocular. Stimuli were generated with the PsychoPhysics Toolbox routines[139] for MATLAB (MATLAB r2010a, The MathWorks) and presented on a CRT monitor (Barco Calibrator) with a resolution of 1024x768 pixels and a refresh rate of 120 Hz, driven by a Mac Pro 4.1. Two-dimensional eye position and pupil diameter were monitored at 1000 Hz with an EyeLink 1000 system (SR Research) with an infrared camera mounted below the screen and recording from the left eye. Pupil diameter measures were transformed from pixels to millimeters with an artificial 4-mm pupil, positioned at the approximate location of the subjects' left eye. Eye position recordings were linearized by means of a standard 13-point calibration routine performed at the beginning of each session. Synchronization between eye recordings and visual presentations was ensured by the Eyelink toolbox for MATLAB[140].

2.2.3 Stimuli and procedure

Trial structure was simple (figure 1A), encompassing a fixation point (displaced to elicit a saccade) and a full-screen flash (presented at variable times around the saccade). Specifically, trials began with participants fixating a red dot (0.15° across) shown on the left side of the screen (-16° of eccentricity from screen center) against a gray background (luminance of 37.2 cd/m2). After a variable delay of 1500±100 ms, the fixation point disappeared and a similar dot appeared at the opposite side of the screen (+16° of eccentricity from the center of the screen). Subjects made a saccade to the rightmost dot (the saccade target) as quickly and precisely as they could. After the saccade, gaze was to be maintained on the saccade target until the end of the trial, which had an overall duration of 4 s; an intertrial interval (ITI) of variable duration was marked by the appearance of the mouse cursor (see below). Subjects were asked to refrain from blinking at all times except during the ITI. Except in "catch" trials (15% of all trials), a full-field flash was presented for one monitor frame. The flash could take one of five possible luminance values: 62, 68, 73, 82, or 88 cd/m2. The latter was the maximum attainable luminance. Flash presentation could immediately follow the detection of saccade onset (calculated online as the first of 2 consecutive time points where horizontal eye velocity exceeded 100°/s), or it could be delayed by 500 ms relative to it. Alternatively, the flash could be shown before the saccade — its presentation time defined a priori based on the subject's saccade latency (median across all the previous trials) and an average intended delay of

~500 ms. In a two-alternative forced-choice (2AFC) yes/no task, subjects reported whether they had or had not seen a flash. They did so by clicking on the top or bottom half of the screen with the mouse cursor. Collection of the response triggered the beginning of the following trial.

The experiment was run in two sessions, on different days. One session was completed by 10 participants and comprised the presentation of three luminance levels (68, 73, or 82 cd/m2) at three delays of flash presentation from the saccade (presaccadic, perisaccadic, or postsaccadic). Each run consisted of a randomized presentation of three trials per condition (3 repetitions 3 contrast levels 3 delays) plus three control trials with no flash presentation, for a total of 30 trials. The other session was completed by all subjects and comprised the presentation of two luminance levels (62 or 88 cd/m2) in the perisaccadic or postsaccadic time window. Each run consisted of a randomized presentation of six trials for each condition (6 repetitions 2 contrast levels 2 delays) plus six trials with no flash presentation, for a total of 30 trials. Each session lasted ~1 h, which allowed for a maximum of eight runs (240 trials).

Figure 2.1: methods
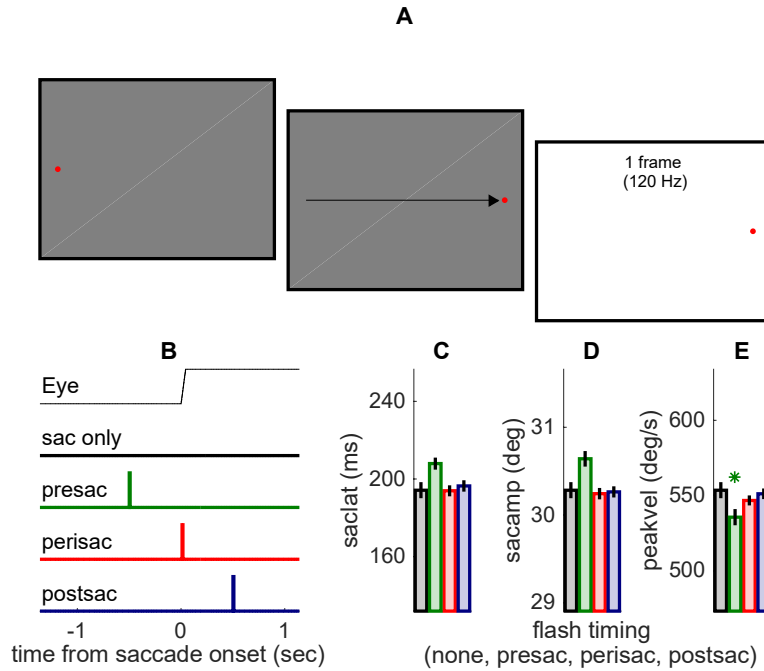
A: Subjects made saccades from the fixation point to the saccade target (red points), as illustrated by the arrow (not part of the display). The flash stimulus was a full-field luminance increment, lasting 1 monitor frame. **B**: timing of the flash relative to the saccade. Except in catch trials where it was not presented, the flash could occur perisaccadically (immediately upon online saccade onset detection), 500 ms postsaccadically, or ~500 ms presaccadically. **C**–**E**: saccade parameters (latency, amplitude and peak velocity) in the 4 conditions, averaged across trials and subjects. Presaccadic flashes tend to interfere with saccade planning, resulting in slightly delayed and larger saccades with significantly lower peak velocity, but saccade parameters were all well matched across the other conditions. Asterisk marks only significant difference (P < 0.05) between no-flash condition (black) and other conditions (color-coded as in B).

2.2.4 Data analysis

An off-line analysis examined the Eyelink output to exclude trials in which

one of the following conditions was met: i) no saccade could be detected

(mean ± SE across subjects: 4.4 ± 4%), ii) saccade latency was negative

(13.2 ± 4%), iii) saccade amplitude was smaller than 24°, i.e., 3/4 of the required amplitude (1.5 ± 0%), iv) a blink occurred in the interval [-1:2] s around saccade onset (10.5 ± 4%). The application of these criteria led to the inclusion of a total of 4092 trials, corresponding to 72.9 ± 7% trials on average, with considerable variability across subjects.

The off-line analysis confirmed that pre-, peri-, and postsaccadic flashes were presented in the intended time windows: -506.32±5.18, 11.99±0.35, and 512.31±0.32 ms from the saccade onset, respectively. For each valid trial, we studied the time course of pupil diameter in the [-1:2]-s interval around saccade onset, averaging samples into 10-ms-long bins and then subtracting the average pupil diameter in the first 500 ms of this interval. Finally, we took the minimum of each trace as an estimate of the peak pupillary response to the flash (or the peak saccade-related modulation in the catch trials with no flash) to be compared across conditions. The ultimate goal was to test whether pupillary responses to light flashes presented during the saccade are suppressed compared with postsaccadic or presaccadic flashes; for this purpose, it is important to realize that our pupil recordings reflect the combination of two influences: the pupillary light response evoked by the flash and the pupillary constriction that accompanies the execution of the saccade. Because the rules governing this combination are currently unknown, we analyzed the data according to two extreme hypotheses: 1) strong subadditivity, where pupil size reflects only the largest component, and 2) perfect additivity, where the two components add up linearly. Previous work on perisaccadic pupillary responses[135] followed the latter assumption

(hypothesis 2) and estimated the light response by subtracting from each trace the average pupil modulation observed in trials with no flash presentation, which implies assuming that they are independent and additively combined. We followed this approach in our main analyses, shown in figure 2B, figure 3, B and D, figure 4, and figure 5. Subtracting the no-flash trace from the response to perisaccadic flashes will underestimate the light response if the independence between light and saccade-related pupillary constrictions is not perfect — for example, if the light response inhibits the saccade-related modulation. One extreme example of such subadditivity is described by hypothesis 1 above, in which the light response completely inhibits the saccade-related modulation. This implies that the latter must not be subtracted from the traces, but responses to peri- and pre/postsaccadic flashes must be directly compared. This approach was taken to run additional data analyses (shown in figure 2A and figure 3A). Opposite to the approach described above, this procedure is biased toward overestimating the perisaccadic light response; thus, together, the two approaches estimate the upper and lower limits of the perisaccadic light response, and consequently of the saccadic suppression effect.

Statistical analyses relied mainly on a linear-mixed model approach, motivated by the considerable sample size variability across subjects. In this approach, individual trials from all subjects are compared with a model comprising both the effect of experimental variables ("fixed effects") and the variability across participants ("random effects"). The main fixed effects we analyzed are the categorical variable "delay" of

flash relative to the saccade, which takes four values: no flash and pre-, peri-, or postsaccadic flash; a continuous variable "luminance" coding the luminance of the flash; and a dichotomous variable "perceptual report" indicating whether the subject had indicated having seen/not seen a flash on each trial. Random effects were coded by allowing subject-by-subject variations of both the slope and intercept for each of the fixed effects; we also used random effects to represent further variables that were not manipulated as in a full factorial design. For example, our first analysis compared saccade parameters and pupillary constrictions across all levels of the factor "delay" and we modeled the effect of luminance as a random effect (given that luminance in the no-flash condition was necessarily distinct from all flash luminance levels in the other conditions). We used standard MATLAB functions provided with the Statistics and Machine Learning Toolbox (R2015b, The MathWorks). Specifically, the function "fitlme(data, model)" fit the linear-mixed model to the data, yielding an object "lme" with associated method "anova" that returns F statistics and P values for each of the fixed effect terms.

2.3 RESULTS

While subjects made large saccades, we showed a flash of variable luminance and variable delays from the saccade onset. Figure 1, C–E, show that the flash had a minor influence on saccade parameters relative to catch trials where no flash was presented; as expected (e.g., Reingold and Stampe[141]), a presaccadic flash could interfere with saccade execution, leading to nonsignificantly delayed and larger saccades with significantly lower peak velocity (fixed effect "condition" with luminance and subject as random effects and contrasts evaluating the difference between presaccadic flashes and no flash: $F_{(1,4088)} = 8.786$, $P < 0.01$). However, saccade parameters in the other conditions (peri- and postsaccadic flashes) were closely matched to the no-flash condition (all $P > 0.08$).

We compared pupillary responses across conditions, and average traces of pupil diameter over time from saccade onset are shown in figure 2. The top trace in figure 2A shows the pupil modulation accompanying saccade execution with no flash presented. This consists of a progressive dilation leading up to saccade onset, probably associated with saccade preparation, followed by a marked constriction, similar to a light-evoked response and with unknown cause; in addition, a systematic disturbance is produced during the saccade, and it matches a known artifact of video-based eye-tracking systems. The other traces in figure 2A show pupil modulations recorded in trials when a flash did occur, so that the saccade-related modulation was combined with a light-evoked pupil

response. Figure 2A shows traces averaged after subtracting the baseline pupil size for each trial (mean pupil size in the first 500 ms), whereas figure 2B shows the result of subtracting, from each trial, the average pupil trace in the no-flash condition. These correspond to two extreme hypotheses for describing the combination of the saccade-related and the light-evoked pupil modulation: 1) extreme subadditivity, where pupil size reflects only the largest component, or 2) perfect additivity, where the two components add up linearly and the pupil response to light is obtained by subtracting out the saccade-related modulation (as done in previous work[135]; see methods for the rationale behind the 2 analysis approaches).

Visual inspection of figure 2 indicates that, under either assumption, pupillary responses to perisaccadic flashes are smaller than for pre- and postsaccadic flashes (red traces are always less modulated than blue and green traces). The same conclusion is supported by the quantitative comparison of peak pupil constrictions, computed from traces in figure 2, A and B, and shown in figure 3, A and B, respectively. The delay of the flash relative to the saccade onset reliably affected pupillary constrictions (fixed effect "condition" with luminance and subject as random effects and contrasts evaluating the difference between peri- and pre/postsaccadic flashes); perisaccadic flashes evoked smaller responses compared with postsaccadic flashes ($F(1,4088) = 36.397$, $P < 0.001$ for figure 3A; $F(1,4088) = 39.119$, $P < 0.001$ for figure 3B) and compared with presaccadic flashes ($F(1,4088) = 7.783$, $P < 0.01$ for figure 3A; $F(1,4088) = 39.513$, $P < 0.001$ for figure 3B). Similar effects in figure 3, A and B,

imply that pupillary responses are suppressed perisaccadically, no matter whether we assume extreme subadditivity or perfect additivity between the different components of pupillary constrictions.

Figure 2.2: pupillary traces
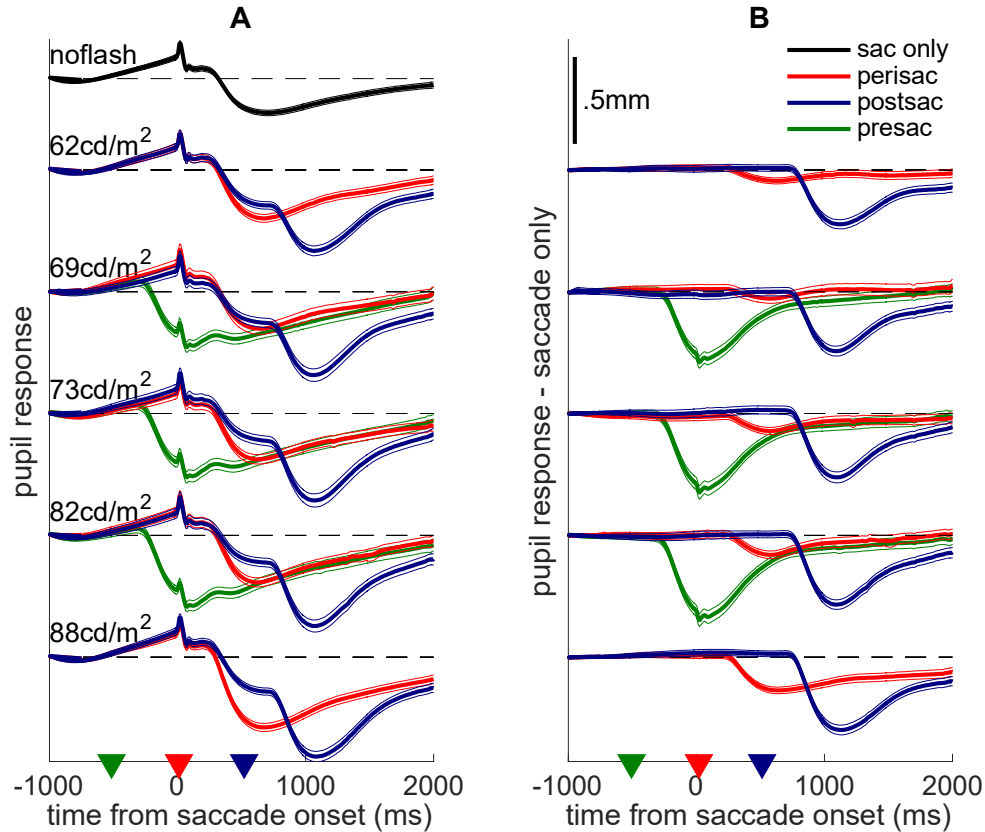
Pupil size change as a function of time from saccade onset, plotted separately for trials in which the flash occurred before/during/after the saccade or was withheld (different colors) and for the different luminance levels of the flash (y-offset; luminance as shown). Traces are averages across all trials from all subjects (with thin lines giving 95% confidence intervals), computed after subtracting from each trial the mean pupil size in the first 500 ms (**A**) and subtracting the average pupil trace in the saccade-only condition from each subject and experimental session (**B**). Black dashed lines mark 0 for each group of traces; triangles in x-axis mark the time of flash presentation. Scale is the same in A and B (shown in B, top).

The contrast of pre- vs. postsaccadic responses is significant, too (F(1,4088) = 5.336, P < 0.05 for figure 3A; F(1,4088) = 11.736, P < 0.001 for figure 3B). Figure 2 indicates that the constriction in response to presaccadic flashes peaks just when there is the maximum saccade-related dilation, whereas for peri- and postsaccadic flashes the light response co-occurs with the saccade-related constriction. If the saccade-related modulation is not factored out, the response to presaccadic flashes is bound to be strongly reduced compared with postsaccadic flashes, as seen in figure 3A. However, when we do subtract out the saccade-related modulation, the resulting pupillary responses become larger presaccadically than postsaccadically (figure 3B). One possibility is that this subtraction leads to overcorrecting the saccade-related dilation, which could be smaller in the presaccadic flash than in the no-flash condition. This would be consistent with the saccade metrics results (figure 1, C-E), which suggests that the presaccadic flash interfered with saccade preparation and might therefore have impaired the associated pupil dilation[142].

A second analysis focused on data where a flash did occur and studied the effect of flash luminance on pupillary responses. This confirmed a significant effect of condition (pre- vs. peri- vs. postsaccadic flashes, F(2,3411) = 6.583, P < 0.01 for figure 3A; F(2,3411) = 8.335, P < 0.001 for figure 3B) and showed the expected effect of flash luminance (F(1,3411) = 44.583, P < 0.001 for figure 3A; F(1,3411) = 38.795, P < 0.001 for figure 3B), with no interaction between the two factors (P > 0.6

in both cases). This suggests that saccadic suppression of pupillary responses is a subtractive effect, in contrast with the divisive effect typically found for saccadic suppression of perceptual thresholds[67,76,143] — but note that the luminance range tested here is small, and evidence for either model is weak.

Figure 2.3: suppression of pupillary light responses
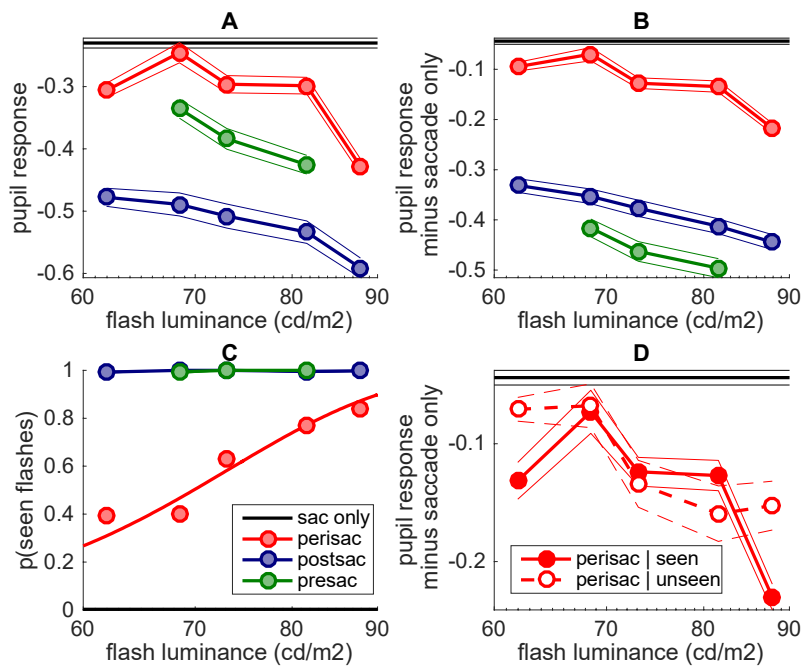
A and **B**: peak pupil response (i.e., minimum of pupil traces in Fig. 2, A and B, respectively) as a function of flash luminance, with black lines giving the response in the saccade-only (no flash) condition. Symbols and thick lines give the grand average across trials from all subjects, and thin lines give 95% confidence intervals. **C**: proportion of trials where the flash was reported as seen. The line gives the best-fit cumulative Gaussian function across the aggregate data from all subjects (symbols). See Fig. 4 for individual psychometric functions. **D**: pupillary response (same conventions as in B), computed separately for perisaccadic flashes that were reported as seen or as unseen.

The same analysis was applied to the other response we collected, the subjective visibility of the flashes (figure 3C, showing average proportions of "seen" responses as function of flash luminance and separately for each condition). While pre- and postsaccadic flashes were almost never missed (across all subjects, there were only 6 misses in 1932 trials), perisaccadic flashes were often missed, in a proportion that varied with luminance (note that in catch trials with no flash presentation, false alarms were extremely infrequent: 2 in 675 trials). This resulted in a significant condition x luminance interaction ($F(2,3411) = 288.654$, $P < 0.001$).

Figure 4A shows the results from individual subjects, showing the difference of detection rate and the difference of pupillary responses (mm) and comparing perisaccadic and postsaccadic flashes (figure 4A, left) or perisaccadic and presaccadic flashes (figure 4A, right). While there is considerable variability across subjects, the suppression of pupillary responses is statistically significant in all but one case (significance evaluated by performing 2-sample t-tests and comparing, for each subject, single trial responses to peri- and pre/postsaccadic flashes; the number of trials in the perisaccadic flash condition is shown in figure 5C, right, with the same color coding and order of subjects).

Next, we focused on trials with perisaccadic flash presentations. Despite the small variability of flash timing (in 95% of perisaccadic trials, the flash occurred between 6 and 18 ms from saccade onset), its exact delay from the saccade had a significant impact upon subjective reports of flash

visibility (significant interaction of fixed effects delay and luminance, with subjects as random effects: $F(1,1481) = 9.063$, $P < 0.01$). Figure 4B describes this interaction, plotting detection rate against the exact time of perisaccadic flashes from the saccadic onset, separately for flashes of different luminance: there is a negative trend, more pronounced for low-luminance flashes. The negative trend implies that the peak of suppression does not coincide with saccade onset but rather occurs 20 ms into the saccade. This is at odds with the time course of suppression typically found for detection of contrast patterns, peaking just before or at saccade onset[138]. However, such delayed suppression is consistent with the results of previous studies measuring detection of luminance flashes, where peak suppression clearly is delayed and occurs some 20-40 ms into the saccade[135,144,145].

In contrast with this effect on detection rate, the variation of pupillary responses with time (figure 4C) is less evident; coherently, the mixed-model analysis reveals no main effect of delay and no interaction between delay and luminance (both $P > 0.5$), only a main effect of luminance ($F(1,1481) = 16.103$, $P < 0.001$). These results are consistent with different time courses of suppression for detection judgments and pupillary responses: faster for detection, implying strong variation of detection rates over a short time window (5–20 ms into the saccade, as measured here), and slower for pupillary responses. This is in line with Lorber et al.'s observation[135] that the time course of saccadic suppression is different for perceptual and pupillary responses (tighter for

the former), suggesting that saccadic suppression of perceptual and pupillary responses may be dissociable at the individual trial level.

Figure 2.4: Suppression of individual light responses
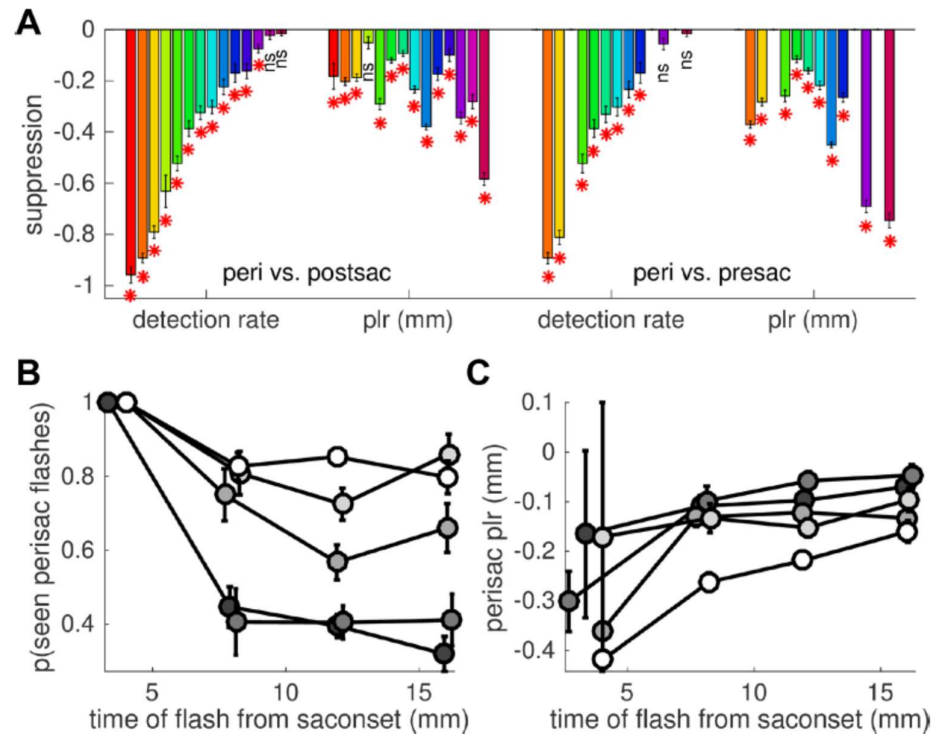
A: individual suppression indexes, computed as the difference between the detection rate or the pupillary response observed for perisaccadic flashes and the same responses for postsaccadic (left) or presaccadic (right) flashes. Subjects are ordered based on the suppression of detection rate; the same order and color coding is used in Fig. 5. Error bars are SE of the difference, computed from the SE of the means of the 2 conditions considering the propagation of errors. *P<0.05; ns, nonsignificant. **B** and **C**: average detection rate (B) and pupillary response (C) for perisaccadic flashes, plotted as a function of the exact flash time relative to the saccade onset (means in continuous nonoverlapping 5-ms bins) and shown separately for the different flash luminance levels (grayscale: highest luminance in white and lowest in dark gray). Error bars are SE; data pooled across subjects.

To directly explore this possibility, we started by comparing pupillary responses to perisaccadic flashes that were reported as seen or unseen (figure 3D). Once the obvious effect of luminance is taken into account (i.e., in a mixed model with perceptual report as fixed effect and luminance, flash timing, and subject as random effects), there is no reliable difference between pupillary responses to perisaccadic seen and unseen flashes ($F_{(1,1257)}$ = 3.789, $P > 0.05$). However, figure 5A shows that visibility thresholds varied considerably across participants (although all subjects were close to 100% correct in the no-flash and pre/postsaccadic flash conditions). We therefore narrowed trial selection further to look at luminance levels that, for each subject, led to an approximately equal number of trials with seen and unseen flashes; also in this case, we failed to find a statistically significant effect ($F_{(1,301)}$ = 1.768, $P > 0.05$).

This negative finding is not, of course, sufficient to conclude that pupillary and perceptual responses to perisaccadic flashes are independent. The ability to test this hypothesis depends on the specific model used to describe the relationship between the two responses, and at least some extreme possibilities can be excluded on the basis of our data.

First, we can rule out a model imposing the strongest possible relationship between perceptual reports and pupillary responses: where pupillary responses are intact vs. suppressed (in an all-or-none fashion) depending on the presence vs. absence of perceptual awareness. Besides predicting a difference between pupillary responses to seen and

unseen perisaccadic flashes (which we failed to measure, see above), this model also predicts that pupillary responses should be unaffected by suppression whenever flashes are reported as seen. This is clearly not the case (fixed effect of "condition" contrasting seen perisaccadic vs. seen postsaccadic flashes, with luminance and subject as random effects: $F_{(1,2354)} = 35.781$, $P < 0.001$).

Second, we can exclude a weaker model that releases the assumption of a direct mapping between the suppression of pupillary responses and presence/absence of perceptual awareness and simply assumes that pupillary responses should be absent when perceptual awareness is absent. We have strong evidence against this, too: even in the subset of trials where the perisaccadic flash is reported as unseen, pupillary responses are clearly detectable (fixed effect of "condition" contrasting unseen perisaccadic flashes vs. no-flash trials, with luminance and subject as random effects $F_{(1,1257)} = 3.960$, $P < 0.05$) and sensitive to flash luminance (effect of luminance on unseen perisaccadic flashes with subject as random effect: $F_{(1,582)} = 6.376$, $P < 0.05$).

Thus, whether seen or unseen, perisaccadic flashes lead to attenuated but still detectable pupillary responses; in other words, our data are only compatible with models in which the relationship between perceptual and pupillary responses has an unspecified (and small) effect size. We estimated this effect size by studying the correlation of pupillary and perceptual responses at the individual subject level. Figure 5 shows that both responses varied with flash luminance (as shown for the data pooled

across subjects discussed above) and were indeed well correlated with luminance (on average [95% confidence interval] R = 0.41 [0.24, 0.58] and 0.26 [0.17, 0.36], respectively, close to the 0.3 value defined as a "medium"-sized effect in Cohen's classification[146]). When this effect of luminance is controlled for, however, the remaining partial correlation between pupillary responses and perceptual reports becomes very small (on average R = 0.07 [95% CI -0.004, 0.14]), nonsignificantly different from 0 (1-sample t-test, t(13) = 1.92, P = 0.08) and close to the 0.1 value termed "small" in Cohen's classification[146]. In conclusion, even if there is no practical way of completely excluding a relationship between the suppression of perceptual and pupillary responses, our results indicate that if such relationship exists it is a trivially small one.

Figure 2.5: responses to peri-saccadic seen and unseen flashes
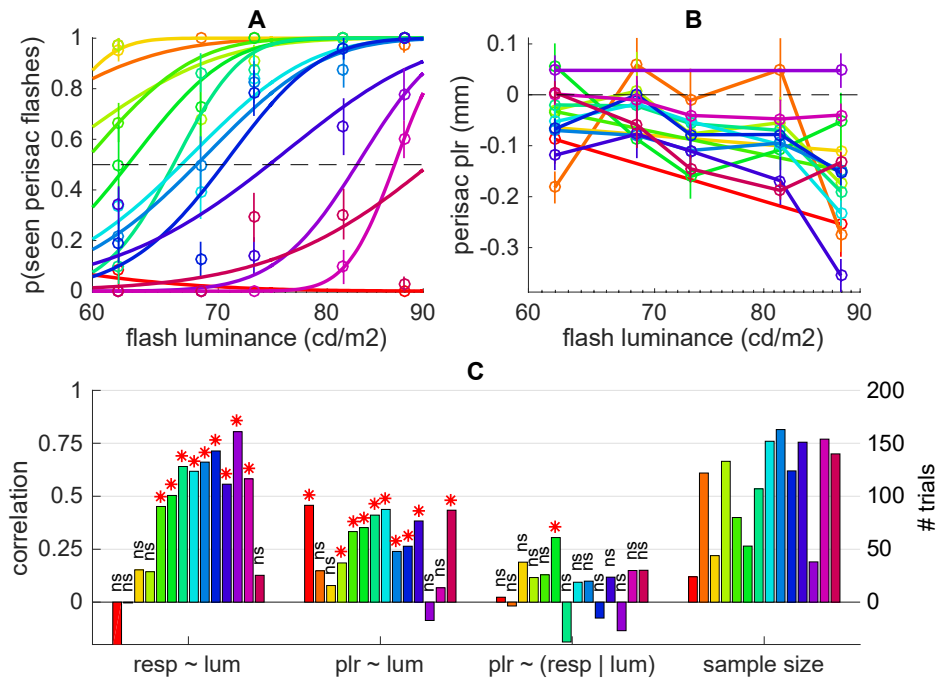
A: individual psychometric curves plotting, for each subject (color-coded, preserved across the 3 panels), the proportion of seen perisaccadic flashes against their luminance (symbols with error bars showing SE across trials) and the best- fit cumulative Gaussian function across the data. **B**: pupillary response to perisaccadic flashes (computed as in Fig. 3B). **C**: Spearman rank correlation between luminance of the flash and the seen/unseen report or the amplitude of the pupillary response (significant for most subjects; *P < 0.05), and partial correlation between the seen/unseen report and the pupillary response after controlling for the effect of luminance [nonsignificant (ns) with P > 0.05 in all but 1 subject]. Bars on right display the number of trials considered for these correlations. Error bars report SE of the correlation coefficient, computed as $SE = \sqrt{[(1 - r^2)/(n - 2)]}$.

2.4 DISCUSSION

We flashed lights during or before/after a saccade while monitoring pupil diameter. In agreement with previous observations[135,136], we find that the pupillary constrictions in response to light flashes are strongly suppressed during saccades. In control trials where no flash was presented, we find that the mere execution of a saccade is sufficient to generate a pupillary modulation — noted and described previously[135,136,147]. This implies that responses to flashes presented at saccade onset reflect the combination of two pupil responses, related to light and to the saccade. Previous work assumed that the combination was linear and factored out the second by subtracting, from the raw traces, the pupil modulation observed in saccade-only trials[135,136]. We show that releasing this linearity assumption does not change the conclusion: pupillary constrictions evoked by perisaccadic flashes are suppressed relative to pre- and postsaccadic flashes, even if we fail to discount the effect of the saccade-related modulation. Our figure 2 also confirms that subtracting the latter from the raw pupil traces has the advantage of reducing the complexity of waveforms, yielding traces that match the typical light response well[148]. This allows for summarizing pupillary responses with established indexes like the peak pupil constriction, which we use for all our analyses. These show that the suppression is approximately constant across the tested luminance range (~50 – 100 cd/m2, typical of everyday computer use and TV watching): a reduction of ~0.2 mm, which represents up to 90% of the pupillary responses evoked by the test flashes

Because we simultaneously monitored the subjective flash visibility (perceptual detection rate), our measurements offer an opportunity to test the relationship between the saccadic suppression of perceptual and pupillary responses. We find that such a relation is not tight. Our data are consistent with Lorber et al.'s report that the temporal dynamics of saccadic suppression of pupillary responses is different from that of perceptual responses[135]. In addition, we find that pupillary responses to perisaccadic flashes do not differ depending on the perceptual report — whether the flash was seen or not seen. Pupillary responses remain clearly detectable and show the expected luminance dependence even when flashes are suppressed from perceptual awareness. We cannot, of course, rule out all possible models that impose any arbitrarily small relationship between pupillary and perceptual responses. However, we can look at their trial-by-trial correlation to estimate the effect size of such a relationship. Once we factor out the effect of luminance, with which both perceptual and pupillary responses are expected to correlate, the residual correlation between the two responses is only ~0.1 — if at all present, the relationship is a small one, corresponding to <2% explained variance[146].

A dissociation between the saccadic suppression of conscious vision and other forms of visual responses was previously proposed in Watson and Krekelberg's study[117], where the suppression of a line stimulus from conscious perception did not eliminate its 'shape contrast' effect, or the ability to bias the apparent shape of a subsequently presented ellipse. Our results reinforce the evidence that the content of our consciousness

is not the only representation available in the visual system; distinct representations appear to be accessible to support nonconscious responses[118,119]. Pupillary responses are an extreme example of these— even if there is evidence that they are not reflexes[124], they are still completely automatic responses that escape voluntary control[123]. Another example is open-loop pointing, which a previous study showed to differentiate from conscious perception of perisaccadic stimuli [120]. In this case, subjects reported the perceived location—rather than the visibility— of perisaccadic stimuli; there were strong localization biases for both subjective reports and pointing responses, but the two were systematically different.

By suggesting that saccades differentially affect conscious and nonconscious visual processing, these observations may seem incompatible with the hypothesis that saccades affect visual processing by acting very early— even before the visual signal reaches the cortex[67,81]. However, the discrepancy may be resolved by assuming that visual pathways supporting conscious vision vs. other forms of processing diverge even earlier—subcortically, with unconscious responses relying on an extrageniculate pathway possibly involving the superior colliculus[149].

Given that there is no consensus either on the site of saccadic suppression or on the divergence between pathways supporting conscious vs. unconscious visual functions, the neural mechanisms underlying the suppression of pupillary responses we observe here

remain unclear. We nevertheless note that some relatively subtle features of our results fit with the hypothesis that saccadic suppression primarily targets a cortically mediated component of the pupillary light response. The pupillary response we studied is a transient constriction, and this is likely a combination of a light-dependent constriction (which would have been sustained had our stimulus been a constant light increment rather than a brief flash) with a non-luminance dependent transient constriction. The latter can be evoked by stimuli such as changes of chromaticity or motion direction and, primarily, by gratings[150,151]. The "grating" response has a low-pass behavior[152], meaning that it is most responsive to low spatial frequencies (the lowest being a full-screen stimulus like a luminance flash); it is quickly saturated with contrast[152] and its maximal amplitude is usually 0.1-0.2 mm. Thus, assuming that this component is selectively suppressed during saccades would be consistent with an effect of suppression of about 0.2 mm approximately constant across luminance levels, just as we observed here – but note that the limited range of tested luminance levels does not allow for excluding alternative models of the suppression effect, e.g. a divisive effect as seen in psychophysics[76]. It is interesting to note that this grating response has been associated with the magnocellular pathway[152], which is believed to be the main target of saccadic suppression[67]. Also, the grating response is strongly attenuated in patients with lesions of the visual cortex – indicative of a cortical source – and, in some of these patients, a dissociation was found between grating responses and conscious vision – the amplitude of the pupillary

response correlating with unconscious visual discrimination abilities or 'blindsight'[153]. If this component were suppressed during saccades, then, one would not necessarily expect a correlation with the suppression of conscious vision. Whether pupillary suppression correlates better with unconscious visual processing, such as revealed by the Watson and Krekelberg study[117], remains an open question.

Here we focused on pupillary responses to the flash stimuli and have shown that the mere presence of pupil modulation related to saccade execution cannot influence our estimates of saccadic suppression. However, further studies are necessary to investigate this eye movement-related pupil modulation, especially since its cause and function are at present unknown. It cannot be entirely explained either by 1) the eye-position artifact[154], evident as a rapid, small pupil change during the saccade, or 2) the effort of preparing the saccade execution[155], which consists of a progressive dilation preceding the saccade. Neither of these effects explains the prolonged constriction after the eye has reached its final postsaccadic position. Because pupil constriction is known to accompany near focus[123,156], Zuber et al.[136] suggested that this modulation reflects a change of focal plane during a saccade. More recently, Mathot et al.[147] advanced the hypothesis that the constriction reflects a "grating" response instead, elicited by the spurious motion of retinal images produced by the eye movement. Available evidence is insufficient to support any of these proposals. It is also interesting to note that a similar constriction also accompanies eye-blinks[157], which are associated with perceptual suppression like saccades, suggesting that

understanding the nature of this pupil modulation might ultimately be relevant to explaining the suppression of light responses.

In conclusion, the pupillary response to light flashes shows a robust suppression during saccades, with features that deviate in interesting ways from the suppression of conscious vision. This highlights the complexity of pupillary responses, which integrate diverse sources of information. It also provides further support to the idea that saccades may produce different effects on visual pathways supporting conscious perception and those supporting other visual functions, e.g., (oculo)motor responses.

3 RHYTHMIC MODULATION OF VISUAL CONTRAST DISCRIMINATION TRIGGERED BY ACTION[*][64]

3.1 INTRODUCTION

Ongoing brain oscillations modulate perception, suggesting that sensory systems act as discrete mechanisms sampling information from the environment within specific time-windows[7,62,158]. Several electrophysiological studies have demonstrated that neural oscillations preceding the sensory stimulation are causally linked to perceptual performance particularly in the theta range[5,159–161]. Oscillations have also been demonstrated in perceptual performance after the presentation of a sensory stimulation[49,162,163]. These results can be interpreted as a synchronization of the endogenous rhythms of the visual brain by the preceding stimulus, or as a gain modulation due to the stimulus-driven attention that oscillates over time[27]. Whatever the underlying mechanism, oscillatory fluctuation of sensory sensitivity could play a major role in aligning a temporal incoherent flow of sensory events, contributing to the integration of information from different sensory modalities. Similar integration mechanisms may also mediate the synchronization between

---

[*] This chapter refers to the published paper: A. Benedetto, D. Spinelli, M.C. Morrone. (2016). *Rhythmic modulation of visual contrast discrimination triggered by action.* Proc. R. Soc. B.

action and perception, where temporal alignment is particularly important. Although the visual system has developed a selective pathway to dialog optimally with action[119], a visual-motor synchronization mechanism is still needed and sensory oscillations may facilitate this difficult task[164–166]. Recently, Wood et al.[98] have shown that a visual stimulus can reset the phase of alpha oscillations. Complementary, Tomassini et al.[62] showed that action preparation synchronizes visual oscillations in the theta-band, possibly via a coupling between early motor planning and early visual processing. Interestingly, the coupling is independent of the spatial congruency between the visual stimulus and the action, as well as on the kinematics of the movement.

The aim of the present study was to investigate the fine temporal dynamics of visual-motor integration processes. Fi*rstly*, we asked whether a simple voluntary motor "go" signal could synchronize visual oscillations and, if so, how long they would persist; *secondly,* whether the frequency of visual oscillations could be changed by manipulating the endogenous brain rhythms or the neural temporal characteristics of visual processing. To address the second question, we reduced the ambient luminance from photopic to mesopic level. The latency and integration time of visual processing increases at low luminance and the effect is already present at retinal level, becoming stronger at later processing sites. If oscillations are linked to the dynamics of the neuronal response, we predict a decrease in the oscillation frequency: the temporally prolonged responses to the visual inputs in the dark should reduce the capability to modulate the cortical discharge at high

frequencies. On the other hand, we should expect a shift of the perceptual rhythm toward higher frequency, if the oscillations reflect the brain endogenous rhythm that is known to increase in frequency, at low-luminance[167,168] . Our data, being consistent with the second hypothesis, suggest that visual oscillations are a consequence of the network dynamic properties. They further suggest that the phase-locking mechanisms do not depend on visual stimulus processing time.

3.2   MATERIALS AND METHODS

3.2.1 Participants

Eight volunteers (three women; mean age: 27±3 years; including one author) participated in the experiments. All had normal or corrected-to-normal vision. Participants provided an informed consent in accordance with the Declaration of Helsinki (2008).

3.2.2 Apparatus

Subjects sat in front of a monitor screen (40x30°) at a distance of 57 cm. For experiment 1, stimuli and responses were generated and recorded using the ViSaGe and CB6 Response Box (Cambridge Research Systems) controlled via CRS Toolbox for Matlab and presented on a Barco Calibrator monitor with a resolution of 800x600 pixels and a refresh rate of 120 Hz, mean luminance of 38.5 cd/m², ambient light ~0.08 cd/m². For experiment 2, stimuli and responses were generated and recorded by the Matlab psychtoolbox[139] and presented on a CRT monitor with a resolution of 800x600 pixels and a refresh rate of 85 Hz, mean luminance of 51.8 cd/m² ,ambient light ~0.01 cd/m². In the low-luminance experimental condition, neutral filters of 1.5LU were mounted on the goggles worn by the participants. The monitors were gamma calibrated. We also controlled that the physical fluctuations of contrast throughout the time of the trial were too small to be measured by a photometer.

3.2.3 Stimuli and procedure

Participants maintained fixation on a red square (0.25°) in the center of the screen that appeared at the beginning of the block and lasted until the end of the session. The stimulus was a horizontal sinusoidal grating (1c/°, contrast 10%) presented with random phase for 1 frame through a circular window of 5° with smoothed edge. In the upper or lower half of the circular window, a contrast increment was obtained by boosting the sinusoidal amplitude in an ellipsoidal Gaussian window (see stimulus equation from experiment 1).

In the *self-trigger* conditions, participants pressed a button to initiate the trial. After a random delay between 0-1 s, the stimulus was displayed and the subjects reported via button-press whether the contrast increment was up or down. To avoid that the response action could perturb visual oscillations, the subjects were required to delay the response for 2 s after the stimulus presentation in experiment 1 and 0.3 s in experiment 2. In experiment 1, participants had to pause for at least 2 s before pressing again the button to start the next trial; in experiment 2 they had to wait 0.3 s. In the *self-trigger* conditions, data were acquired at high luminance (*self-HL*), and with neutral filters (*self-LL*).

To evaluate the contribution of biological noise and of possible stimulus contrast fluctuation to the oscillation in performance, we repeated experiment 1 with a random trigger (hereafter *random-HL):* the stimulus onset was randomly delivered by the computer between 3-7 s after the subject's response, mimicking the temporal event sequence of the *self-*

trigger conditions. This task was performed only at high luminance. Also in this condition, participants were asked to wait 2 s after stimulus presentation before responding. In experiment 2 we replicated both self-trigger conditions of experiment 1, adding a third condition, where the go stimulus was a sound. The auditory condition was performed under high-luminance viewing (hereafter called *audio-HL)*, and participants were instructed to attend to the auditory cue (noise burst, 12 ms duration). The visual stimulus was presented after a random delay (0-1 s) from the auditory cue, but the majority (80% of total trials) of stimulus delays were in the first 350 ms from the go signal, to optimize sampling. The auditory cue was delivered via external speakers. The inter-trial interval randomly varied between 0.3-0.8 s, mimicking the inter-trial interval of the *self-trigger conditions* for the experiment 2. An auditory feedback informed participants that they did not respect the required delay before responding. These trials were removed from further analysis. No feedback about the correctness of their response about the visual stimulus was provided to the subjects for all conditions. The subjects were required to touch for all the time and condition the button both for the start and the collection of the responses.

A QUEST procedure was adopted to obtain an individual psychometric function of the contrast increment sensitivity. The contrast increment value that elicited about 75% of correct responses was selected and kept constant within each block. In order to balance perceptual learning improvement, the contrast increment was slightly adjusted from block to block to maintain the 75% of correct responses. In experiment 1 the

average number of trials per subject collected over 3-7 sessions were 794±377; in experiment 2 these were reduced at 511±121, given that we collected trials limited to delays ranging from 12-350 ms. The number of independent trials for each delay are shown in the figures. If not stated differently on the text, the number of trials that participated to the bin average was double of those plotted, given the 50% overlap between bins.

3.2.4 Data analysis

To evaluate the presence of an oscillation we performed several analyses both at individual level and by pooling individual data together (hereafter termed *aggregate observer*[169]) or by group-average in experiment 2.

For the experiment 1, in order to verify whether contrast discrimination performance was rhythmically modulated, we calculated the percentage of correct responses in 50 ms bins that overlapped by 50% with the adjoining one. The variability was assessed via a bootstrap procedure (1000 iterations, with replacement and standard deviation of the bootstrap reported as standard error of the mean, s.e.m). The time series were fitted with a sinusoidal function for each condition for the aggregate observer. The best fit statistical significance was evaluated using a bootstrap procedure on surrogated data: the delay of each trial of each subject was scrambled randomly, averaged and fit with the same sinusoidal function used for the aggregate subject[162]. A one-tail non-parametric bootstrap t-test was run to assess if the adjusted-R^2 of the

best fit of the data was statistically higher than the 95%ile of the adjusted-R^2 distribution obtained from the bootstrapped surrogate data.

To evaluate the power spectra of the aggregate observer, we performed a Fourier analysis in the range 3-8.5 Hz, with increment of 0.25 Hz. We averaged the temporal series of performance at the fixed interval under exam; we first binned the trials into 7 contiguous intervals per period to optimize the number of trials per bin and then evaluated the sinusoidal harmonic that best fitted the binned data. A 2D statistical significance test was run on the real and the imaginary components of fundamental harmonic for each frequency in the range between 3-8.5 Hz by bootstrap. A non-parametric one-tail sign test was run to determine whether the distribution of the data points was different from zero in at least one the two (real and imaginary) components (α=0.05), implying that the 2D cloud of bootstrapped data was not centered at the origin. To evaluate the presence of oscillations at individual level, we repeated the same analysis using 6 bins per period to optimize the number of trials per bin and we restricted the frequency to the range where the aggregate observer data were statistically significant.

Figure 3.1: main results
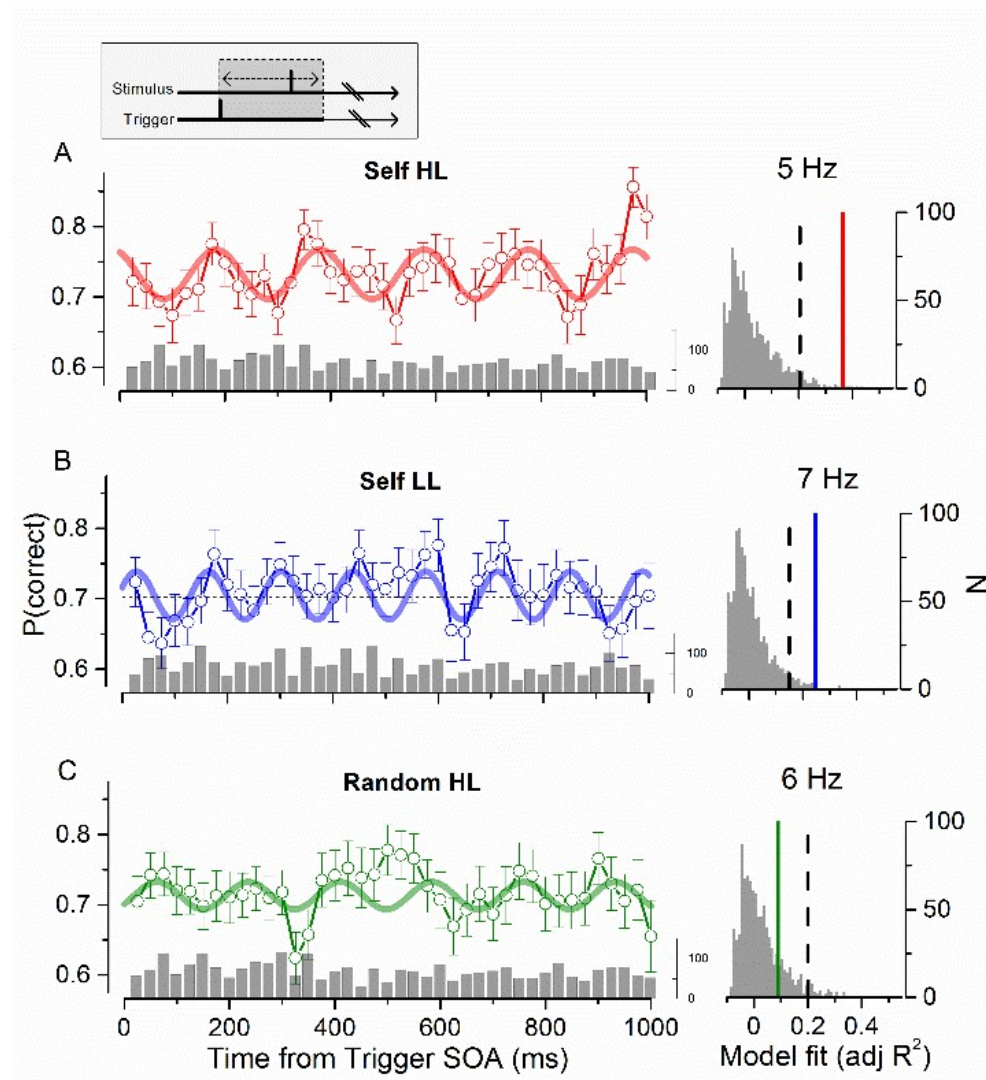
Left. Contrast discrimination performance as function of delay from self-trigger condition at high-luminance (**A**, self-HL; red) and at low-luminance (**B**, self-LL, blue); random-trigger condition at high-luminance (**C**, random-HL, green). Aggregate observer, N=5. Bar plots show the number of independent observations for each bin (on average 74±23). Vertical lines represent the s.e.m from bootstrapping; thick lines represent the best sinusoidal fit to the data; horizontal dashed lines represent the average correct response. **Right**. Adjusted-R^2 distribution obtained by fitting the random shuffled data with the sinusoidal functions of **A**, **B** and **C** respectively. Black lines mark 0.95 probability; colored lines mark the R^2 for self-HL (p=0.005), self-LL (p=0.008) and random-HL condition (p=0.12).

3.3   RESULTS

We measured how contrast discrimination accuracy varied as a function of delay of the motor-go signal in *self-HL* condition (figure 1A), pooling together the data of all subjects in the *aggregate observer.* Performance is not constant over time but it oscillates for up to one second after the movement onset. The difference between the peaks and the troughs performance is more than two standard deviations. To assess whether the oscillations are real and not a consequence of biological noise fluctuations, we fitted the sensitivity data with sinusoidal waveform and compared the goodness of the fit to the same fit applied to surrogate data obtained by random shuffling the time presentation of each trial[162] (see the right panel of figure 1). The best sinusoidal fit for the self-HL condition was obtained at 5 Hz). This fit exceeds the 95%ile of the adjusted-R^2 distribution obtained by best fitting the random shuffled data with the same sinusoidal function, indicating that the oscillation at this frequency is significant (adj-R^2=0.36; $p<0.01$; figure 1A). Other frequencies close to 5 Hz provide statistically significant fit, but not frequencies higher than 6 Hz (see figure 2).

To verify whether the voluntary action was crucial in synchronizing the oscillation, discrimination performance was measured when the subject did not perform the start action, but passively observed a stimulus that was presented randomly (*random-HL)* with a delay of at least 3 s after the preceding response. Figure 1C shows the aggregate observer accuracy data for this condition. The best-fit was obtained at 5.7 Hz,

however, the adjusted-R^2 was low and confined below the 95% limit indicating that the oscillation is not significantly different from random noise (adj-R^2=0.08; p>0.05). The overall variance of the temporal series for the *random-HL* is lower than that for the *self-HL* (9.5 vs. 14.8 respectively). The reduced variance for the random-HL is consistent with the result of the statistical analysis reported in figure 1C.

To investigate whether the frequency could be changed by manipulating the dynamics of the processing of temporal stimuli, we repeated the experiment at low-mesopic luminance (*self-LL*). Reliable oscillations were also detected at this luminance (figure 1B). However, the best-fitting sinusoidal function had a higher frequency than at photopic luminance, being now 7.2 Hz) instead of 5Hz observed at *self-HL*. Also for the *self-LL* conditions, the one-tail bootstrap t-test revealed that the adjusted-R^2 distribution of the fit was significantly higher than expected for noise (adj-R^2=0.24; p<0.01). The fit of the low-luminance performance with a 5 Hz sinusoidal function was very poor (see also figure 2). Despite the fact that the low luminance increases the processing latency of the sensory input, we observed an increase in frequency of the performance oscillation (see discussion).

Figure 3.2: spectral analysis
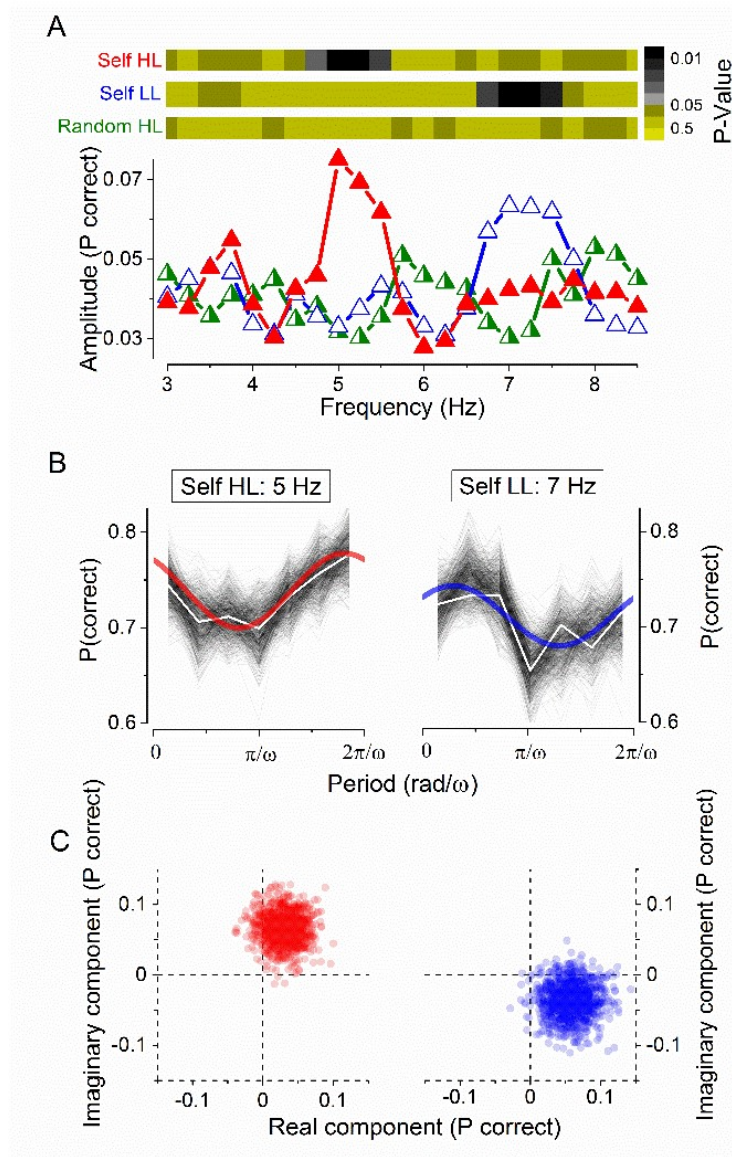
Spectral analysis of visual performance of the aggregate observer. **A**. **Bottom**: Amplitude for self-HL (red filled triangles), self-LL (blue empty triangles) and random-HL (green half-filled triangles) conditions. **Top**: statistical significance in color code for the three conditions calculated by a 2D cluster spread derived by bootstrap as shown in C. **B**. Spectral analysis applied to the most significant harmonic component for self-HL and self-LL (5 and 7Hz respectively). Bootstrap simulations (thin lines), their mean (white line) and best-fit model (continuous colored lines) for the self-HL and self-LL conditions. **C**. 2D polar statistics for the two most significant frequencies analyzed. Real and imaginary components of each bootstrap for the self-trigger conditions. Points clustered away from the origin, indicating statistical significance as reported in A top row.

Figure 3.3: single subject results
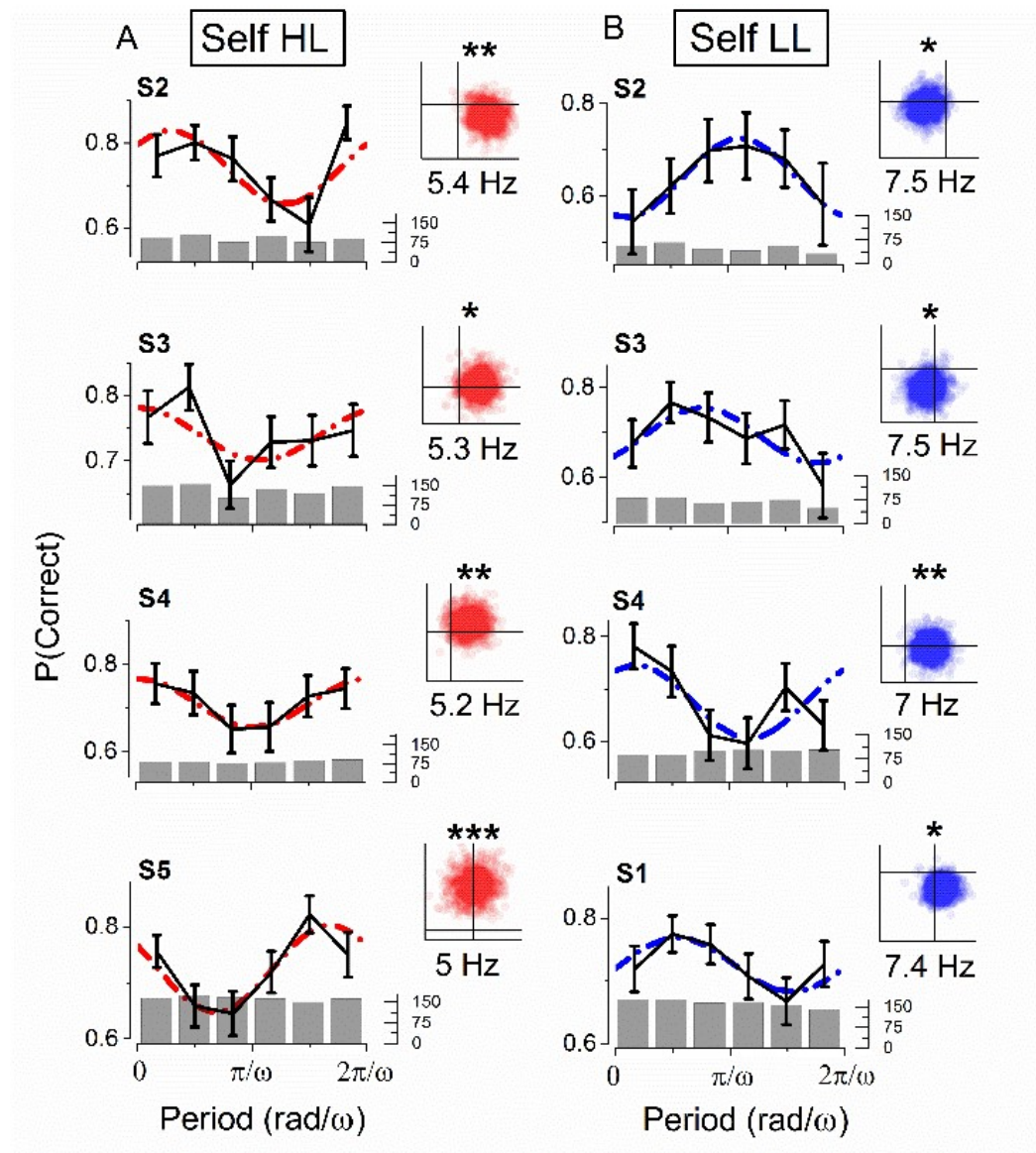
Single subject spectral analysis of visual performance in experiment 1 for self-HL (**A**) and self-LL (**B**) conditions. Each panel shows the most significant frequency modulation in the range between 4.8-5.5 and 6.8-7.5 for self-HL and self-LL respectively. 6 equal bins for each frequency. Dashed lines: Best-fit model. Black lines: means and s.e.m. Bar plot shows the number of independent observations for each bin. Insets on the left: the 2D statistics for the individual frequencies, each point correspond to a bootstrap iteration. P-values significant levels: 0.05 (*) 0.01 (**) 0.001 (***).

Figure 2A illustrates the Fourier transform of the time series in the range between 3-8.5 Hz. We calculated the amplitude at each frequency by averaging corresponding bins for the various periods in the time series and best fitting the sinusoidal function. We kept the bin number equal to 7 per period. Examples of the procedure are shown in fig 2B for the most representative frequencies of the aggregate observer data for the two conditions. Black thin lines in figure 2B represent the percentage of correct responses from each bootstrap iteration; the white line represents their mean; the best sinusoidal fit is superimposed in red for the *self-HL* and in blue for the *self-LL* condition, respectively. The average amplitude as function of frequency is reported in figure 2A (bottom panel). *Self-HL* (filled triangles) and *self-LL* (empty triangles) conditions show an amplitude peak around 5 Hz and 7 Hz, respectively. Random-HL condition (half-filled triangles) shows lower amplitude across all frequencies. In order to estimate the significance of the oscillations, we run 2D statistics, illustrated in figure 2C for the two most significant frequencies for the self-HL (5 Hz, left panels) and self-LL (7 Hz, right panels). Each point in figure 2C corresponds to the real and imaginary component of the best sinusoidal fit for each bootstrap iteration for the *self-HL* (red dots) and *self-LL* (blue dots) condition, respectively. The points cluster together and the cloud of points is offset from the origin of the plot. Consistently with the previous analysis of figure 1, only a small range of frequencies around 5 Hz for the *self-HL* and around 7 Hz for the *self-LL* condition were higher than noise level (non-parametric one-tail

sign test on the real or the imaginary component: *self-HL*: 5 Hz, P=0.003; *self-LL*: 7 Hz, P=0.01, see figure 2A upper panel). No other frequencies reached significance level. Further, the amplitude of oscillations in the *random-HL* conditions was lower than noise at all frequencies.

The oscillations in the self-trigger conditions were strong enough to be detected also in individual subject data. Figure 3 shows the most significant frequencies for the individual subjects for the high and low-luminance conditions in the range corresponding to those demonstrated for the aggregate observer (i.e. 4.8-5.5 Hz and 6.8-7.5 Hz, respectively). Contrast discrimination accuracy oscillates significantly in this range for the majority of subjects for both conditions, with 2 exceptions which reached significance for only one of the two conditions. Subject S1 did not reach statistical significance for the self-HL condition and subject S5 did not reach statistical significance for the self-LL condition. The shift of the oscillatory frequency with luminance was detected in almost all subjects, with higher frequency for the mesopic luminance.

Sensory signals are transiently suppressed in the first hundred milliseconds after an action (*motor-induced suppression*)[170–172]. We investigated more in depth the first 120 ms after action, to evaluate whether a similar transient effect can be detected in our paradigm. Figure 4A plots the same data of figure 1, now binned at 12 ms (50% overlap). Clearly, discrimination performance in both conditions decreases around 100 ms after action (figure 4A). Notably, a two-tail binomial test revealed

that the minimum performance points in the 0-120 ms range were lower

than the average performance (*self-HL*: p=0.03; *self-LL*: p=0.01).

Figure 3.4: motor-induced suppression
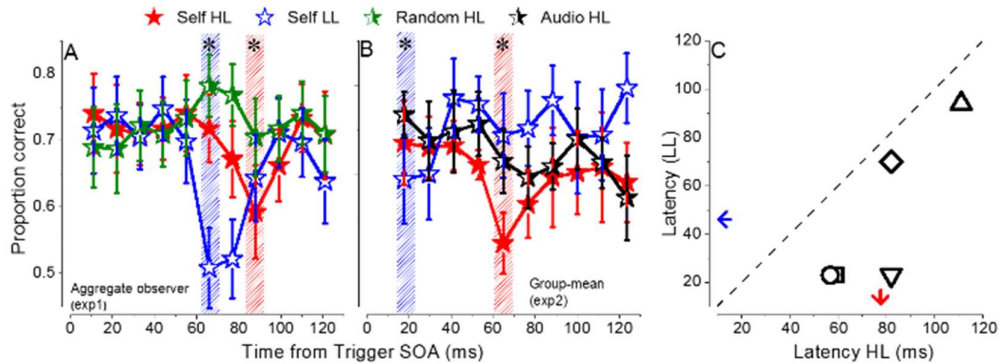
Proportion correct in the first 120 ms from trigger in experiment 1 and 2. **A**, Aggregated observer results for experiment 1 (N=5). **B**, group-subject mean and s.e.m for Experiment 2 (N=5). Red filled stars: self-HL; Blue empty stars: self-LL; Green half-filled stars: random-HL; Black half-filled stars: audio-HL. Dashed bars indicate points statistically different from the mean of the curves (binomial test). Asterisk: p < 0.05. **C**: Scatter plot of individual subjects' latency corresponding to the minimum performance for self-HL and self-LL conditions in experiment 2. The arrows indicate the means across subjects. All points are below the equality line, indicating the minimum performance is reached earlier at low than high luminance. Bin size is equal to 12 ms with 50% overlap.

This suppression was confirmed at the individual level in experiment 2

where sampling was concentrated in the first 350 ms (see methods and

figure 5). Figure 4B shows group means for both *self-HL* (red filled stars)

and *self-LL* (blue empty stars) conditions. Replicating the finding from the

experiment 1, a two-tail binomial test confirmed that both self-HL and self-

LL conditions showed a significant suppression in performance (self-HL: p=0.002, self-LL: p=0.03) in the first 120 ms from action execution. The timing of the individual minimum performance from experiment 2 scatter below the equality line (figure 4C), indicating that the minimum at the low-luminance was anticipated by about 30 ms with respect to the minimum at high-luminance. The paired t-test between the individual latencies reveals that the local minima was about 30 ms earlier in LL than in HL condition (t(4)=-3.81, p=0.01). Comparing the two experiments, there is an anticipation of the timing of both conditions in experiment 2 with respect to experiment 1. Importantly, the relative delay of HL condition with respect to LL condition is about the same.

The green curve (half-filled stars) of figure 4A replots at finer scale the data for the *random-HL* task of figure 1A,B and C. No data point was different from the mean in the first 120 ms of random-HL, suggesting that the minimum performance observed in the two self-trigger conditions cannot be due to artifact. To explore further the contribution of the motor component in producing the sensory suppression, we replaced the internal motor trigger with an external auditory trigger, keeping all the other timing parameters the same. Figure 4B (black half-filled stars) and figure 5C reports the data after auditory trigger at high luminance for the group-mean where we did not observe a reliable decrease of performance in the first 120 ms. Discrimination performance after the auditory cue does not exhibit any statistical significant deviation from its mean (p>0.05).

Figure 3.5: motor-induced suppression for single subject
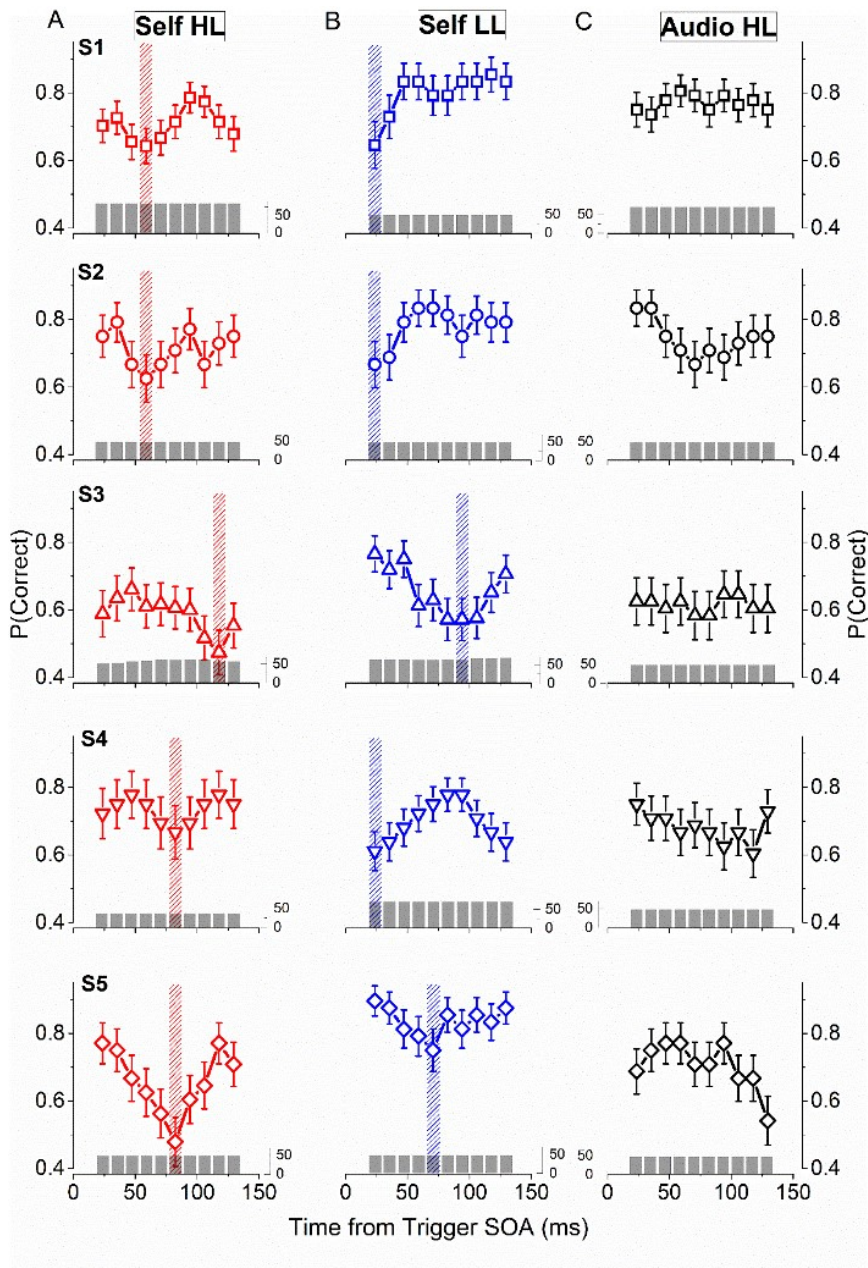
Proportion correct in the first 120 ms in experiment 2 for individual subjects for self-HL (**A**, red), self-LL (**B**, blue) and audio-HL (**C**, black) conditions. Bin size 24 ms, 66% overlap; vertical lines represent the s.e.m of the bootstrapped data. The local performance minimum is highlighted by the dashed bars for both self-HL and self-LL conditions. Bar plot: total number of observations for each bin.

3.4   DISCUSSION

In the present study, we evaluated the effect of action and luminance on visual accuracy in a contrast discrimination task. In line with Tomassini et al.[62], we found that action synchronizes oscillations of visual sensitivity in the theta-band; in addition, we found three novel results. *First*, the action-synchronized oscillatory activity persists for up to one second after execution. *Second*, the frequency of the oscillations varies within theta-range with luminance, i.e. the frequency is higher in mesopic than photopic vision. *Third*, the action produces a sensory-motor suppressive effect in the first 100 ms that is earlier in time at low-luminance compared to high-luminance.

We found that button-press that started the trial synchronizes visual oscillations in the theta-range for up to one second from action onset. Performance oscillations emerged also at the group-level analysis, suggesting commonalities in oscillatory frequency and phase across participants. Crucially, no significant oscillations were detected when the stimulus was randomly delivered by the computer in the absence of a motor act, suggesting that the origin of the phase-locking signal is genuinely linked with the motor act. This interpretation is also corroborated by the finding that theta oscillations are specifically involved in sensory-motor integration functions[28,50]. It is also probable that this phase-resetting mechanism acts over visual rhythms at a very low-level of cortical processing The subject's task was a contrast discrimination, and several evidence suggests that it is limited by the activity of V1,

whose neurons have a contrast threshold[173,174] (unlike those of the retina or LGN).

Phase-resetting mechanisms can be also activated by external sensory stimuli[49,162,163]. We compared the effect of a sound-trigger with that of the motor act. Results from audio-HL did not show any significant deviation from the mean performance in the individual subjects and in the group-mean. This suggests that, if there exists a phase-resetting modulation of visual oscillation by sound[49,162], this must be lower in amplitude and reliability than the one induced by voluntary action. Comparing the effect of voluntary motor action between the two experiments, we observed that the overall delay of the motor suppression was reduced when using shorter trial intervals (as in experiment 2). This may be a consequence of the different attentional and hazard rate characteristics of the two experiments. It is also possible that attention allocation not only change the overall motor-visual timing but also mediates the phase-reset. Action and visual attention are strongly linked[175–178] and attention can reset the phase of the ongoing activity in visual areas, or exert an oscillatory gain of the sensory processing[41,46–48]. However, visual attention was clearly allocated also in the random-HL condition in experiment 1. Crucially, it was identical between the sound-HL and the self-trigger conditions of experiment 2. Nevertheless we did not observe the suppressive motor effect neither in the random-HL nor in the sound-HL conditions. If attention has a role in promoting oscillation, as it has been recently demonstrated[46,47], it must be tightly coupled with the motor system to explain the present data. It may well be that attention is the common

mechanism that synchronizes both the motor and the visual system and its gain, if modulated in time, generates the oscillation observed here.

Besides the role of attention and of voluntary motor action, other mechanisms could be involved in generating visual oscillations. Microsaccades might produce either enhancement or suppression of visual sensitivity, depending on the spatio-temporal characteristic of the stimuli[93,179]. Microsaccade rate increases around the start of a voluntary action[180], but the increase is too earlier and too weak to explain the suppressive effect shown here. Microsaccades possess an intrinsic rhythmicity at around 2-3 Hz. This is a frequency range much lower than the one reported here, making microsaccades involvement unlikely. Although we cannot completely exclude the role of microsaccades, our result would indicate that microsaccadic frequency oscillation should be synchronized with the preparatory activity of a hand voluntary action and not with a sound cue or another visual cue (see also Tomassini et al.[62]).

We measured visual oscillations in photopic and mesopic vision and found that both are in the theta-range. Surprisingly, the frequency was higher in mesopic than photopic conditions (7 vs. 5 Hz). This is in striking contrast with the temporal frequency neuronal selectivity that shift towards lower values at low luminance[66,181], and with neuronal temporal processing that is slower at lower luminance[182]. If visual oscillations are a consequence of the endogenous rhythms of the visual cortex[62] being phase-reset by action preparation, then the most likely frequency of the visual oscillation should be the lowest with the highest power. Brain

rhythms exhibit an enhancement of alpha-power activity at low, compared with high, luminance[167,168]. This increase could induce the shift towards higher frequency of the visual oscillation at mesopic conditions. If so, the frequency shift would imply that the frequency of visual oscillations is determined by endogenous visual rhythms. This conclusion is also consistent with the other important finding of this study: the advance in the first minimum of the oscillations with respect to the action onset. At low-luminance, visual processing is slowed down and delayed. If the frequency of visual oscillations is determined by endogenous rhythms, the response delay should produce an advance of the phase of the oscillation (shorter latency of the minimum) as we observed. Interestingly, the time difference between the two minima for the two luminance conditions is about 30+18 ms, a value consistent with the physiological delay of about 15 ms for each log-unit attenuation of luminance[181,183]. In summary, this interpretation suggests the oscillation frequency is determined by the endogenous rhythms and not by the stimulus processing. Although this interpretation may appear counterintuitive against the general idea that slower processing and slower temporal integration should produce a lower frequency oscillation, it fits nicely with the increase of the alpha-band power at low luminance.

Brain alpha-oscillatory activity is generally linked to inhibition of cortical areas, and thus strongly coupled with stimulus processing[41,184,185]. Indeed, it has been proposed that both the phase and amplitude of alpha activity reflect the amount of inhibitory cortical influxes over the cortex, and consequently these parameters are strongly correlated with temporal

integration processes[186–188]. We could hypothesize that the increase of alpha-band (and hence also theta) power at low luminance results from the decrease of cortical inhibition necessary to process optimally the slow temporal response evoked at low luminance. The typical impulse response of cortical neurons comprises two lobes, one excitatory and one inhibitory. At low luminance, the second inhibitory lobe becomes very weak, given the reduced cortical inhibition[182]. Action exerts a profound influence over perception. For example, it has been shown that eye movements generate a strong visual suppression[67]. In general, stimuli triggered by a self-initiated action can exhibit the so called *motor-induced suppression* that is a suppression of stimulus processing caused by a gain reduction of neural response[171]. This suppressive effect interacts with sensory areas via feed-forward connections and generates sensory suppression in a time window of few hundred of milliseconds after movement. Moreover, action controls also the temporal properties of perception by influencing the temporal integration timing[103,189,190]. We found that when the subject intentionally started the trial by an action, contrast discrimination was clearly impaired in the first 100 ms after button-press. Crucially, no suppressive effect was found in the *random-HL* condition or in the *audio-HL* condition. Given that we reported a motor-induced suppression on a contrast discrimination task that it is thought to be limited by V1 neuronal processing[173,174], this sensory-motor interaction likely takes place at very low-level cortical processing stages as V1. However, this interpretation seems to falter when we consider the phenomenon across the whole one-second interval after action: the

suppressive dip is only the first of many other rhythmical dips. Present finding may suggest that the motor-induced visual suppression does not occur only once, soon after the action, but rhythmically several times. It should be interpreted as an expression of a more general phenomenon of phase-reset of visual oscillations by action.

Taken together, our results suggest that action resets the phase of visual oscillations and that the frequency of such oscillations is modulated by luminance level and governed by endogenous brain rhythm. The functional role of this mechanism is still not clear. We may speculate that higher-theta visual oscillations could play a key role in determining our ability of synchronizing visual-motor processing at different luminance viewing conditions. White et al.[191] found that while low-luminance stimuli exhibit delayed processing, the visual-motor system is able to compensate this perceptual lag and accurately synchronize the action with moving dim stimuli. In the light of the data above, we may speculate that the goal of phase-reset by action of visual oscillations is to achieve maximum sensitivity at specific time during the action. Indeed, the present oscillations exhibit a minimum within the first 100 ms from the motor action regardless of the frequency and luminance viewing conditions (see figure 4A, B). Interestingly the synchronization takes place well before action execution, as showed by Tomassini et al.[62], possibly allowing to reach visuo-motor phase-coherence before action onset. We could even speculate further that this mechanism is tuned to favor vision during specific phases of repetitive moments, such as walking or running with rhythms in the 3-7 Hz range.

Visual discrimination thresholds fluctuate rhythmically over time in the theta range with systematic differences in photopic and mesopic light conditions. These visual oscillations are phase-reset by a voluntary action and not by an external sensory stimulus, such as a sound. The visual rhythmic activity could play a key role in optimizing sensory-motor integration, and may be instrumental in achieving a dynamic compensation of the sensory delay at low luminance.

4 AMBIENT LUMINANCE CHANGES MODULATE OSCILLATORY PROPERTIES OF THE VISUAL SYSTEM[*]

4.1 INTRODUCTION

The human brain can be conceived as a dynamical system where billions of neurons synchronize their activity to generate a coherent and stable representation of the world. Neuronal oscillations play a special role in this synchronization, and in particular, alpha oscillations (8-13 Hz) are known to shape perception[6,7]. Ongoing alpha amplitude and phase are related to stimulus processing and cortical excitability[5,42,159,192,193]. Furthermore, alpha rhythm peak frequency was linked to visual temporal resolution[186,188]. Recently, by applying a reverse-correlation technique, the electroencephalogram "impulse-response function" (EEG IRF, or echo function) of the visual system has been modeled[194]. Briefly, a white-noise luminance sequence was displayed to participants while electroencephalogram was simultaneously acquired. To extract the IRF, single-trial cross-correlations between luminance values and all EEG channels were computed and later averaged[194,195]. This echo function revealed a strong reverberation of visual stimuli shaped in a prolonged

---

alpha oscillatory fashion that might reveal peculiar visuo-temporal properties.

The amplitude and the frequency of the echo function are correlated with the resting alpha[194]. However, it is known that spontaneous alpha amplitude is inversely correlated to attentional allocation[196]; conversely, the echo function amplitude positively correlates with attentional allocation[194]. This suggest that the two rhythms reflect partially independent functions.

Luminance viewing conditions strongly influence visual and cognitive abilities[197,198]. The latency and integration time of visual processing – from retinal to higher processing sites – progressively increases at low-luminance[199], as well as the alpha amplitude[167,200]. Moreover, brief dark exposure produces adaptive changes in cortical excitability[201]. Recently, contrast sensitivity was reported to oscillate[62,64], with faster frequencies under low-luminance viewing[64], likely reflecting a modulation in endogenous brain rhythms caused by luminance changes. However, the link between ambient luminance and neuronal oscillation is still not clear.

Here, we investigated the effect of ambient luminance on alpha amplitude and frequency during spontaneous brain activity at rest (experiment 1) and during the measurement of echo functions (experiment 2). We found that luminance affected the alpha characteristics for both indices, but in a non-trivial way. During resting (experiment 1), low-luminances increased alpha amplitude, but did not affect alpha frequency. Yet, in experiment 2 the echo amplitude was lower under low-luminance, and its

frequency was slightly faster. This effect is distinct from the modulation of evoked alpha activity recorded in the same experiment. In fact, evoked alpha and echo functions showed a similar amplitude modulation; however, luminance changes influenced only the echo peak frequency.

Critical flicker frequency (CFF) was reported to correlate with alpha activity[202–204], although this relation is debated[205,206]. Samaha et al. showed that the individual alpha frequency predicts visual temporal resolution[188], supporting a correlation between CFF and alpha. In experiment 3, we compared the monocular CFF under contralateral dark-adaptation, with the monocular CFF under binocular light-adaptation. We thus assured an identical retinal adaptation of the tested eye, but a different cortical excitability state for the two conditions. Behavioral results showed a CFF increase during monocular dark adaptation, suggesting a close link with the finding of the EEG IRF frequency increase shown in the previous experiment.

Our results confirm that echo functions are fundamental aspects of vision, only partially related to EEG alpha. Importantly, we show that ambient luminance changes affect the visual system oscillatory properties.

4.2 MATERIAL AND METHODS

All experiments were conducted in a quiet, dark room (mean ambient luminance < 0.01 cd\m^2). For experiment 1 and 2, electrophysiological activity was continuously acquired at 1024 Hz using a 64 channel ActiveTwo Biosemi system. Horizontal and vertical eye movements were recorded by three additional electrodes: one below the left eye and two at bilateral outer canthi. Overall, 16, 12 and 13 subjects took part in experiments 1, 2 and 3, respectively (including two authors). All had normal or corrected-to-normal vision. Two subjects from experiment 1 did not show alpha activity and were discarded from further analyses. For experiments 1 and 2, stimuli were generated using the MATLAB Psychophysics toolbox[207] and displayed at 57 cm on a gamma corrected CRT monitor (640×480 pixels, 160 Hz). For experiment 3, stimuli were presented using Python[208] on a gamma corrected CRT monitor (800×600 pixels, 60 Hz) and a white LED controlled by Arduino Uno serially connected to the PC (115200 baud rate)[209]. For experiment 3, responses were recorded via a potentiometer driven by Arduino Uno. Data were analyzed with EEGLAB[210], FieldTrip[211] and custom Matlab code. The low-luminance viewing condition was obtained by applying a neutral-density filter (NDF) in front of the monitor (NDF: 2.5 LU, experiments 1 and 2), or in front of the left eye (NDF: 1.5 LU, experiment 3). All experiments were performed with approval of the local ethical committee.

4.2.1 Experiment 1: resting state

We recorded blocks of one minute of EEG activity while participants (N=14) maintained fixation on a dot presented on a gray screen (*resting*

state, with eyes open). To maintain alertness, after each resting period participants performed a reaction time (RT) task to a visual target presented above a movie shown in the screen center (*active task*, 2-minutes long). The experiment consisted in three consecutive sessions. In the first and the third sessions, 5 resting blocks of one minute per session were recorded for each participant over 13 minutes, under high-luminance viewing conditions (mean luminance of 51.8 cd/m^2). The second session was performed under low-luminance viewing condition, obtained by positioning a NDF (2.5 LU) in front of the monitor. 14 minutes of resting were collected for each participant over 40 minutes. The experimental procedure is shown in figure 1A.

The EEG was re-referenced to the common average and band-passed filtered (1-256 Hz, 4th order Butterworth IIR filter). Each 1-minute recording was split in 5 s epochs (from 5 to 60 s). Firstly, epochs were visually inspected and those with gross muscular artifacts were rejected. Secondly, artifacts were removed from the signal via ICA[212]. For each participant and condition, we investigated two main indices: the individual alpha amplitude (resting EEG IAA) and the individual alpha frequency (resting EEG IAF). The analysis was restricted to the three occipital electrodes: Oz, POz, Pz. To compute the resting EEG IAA, we firstly band-passed the single epochs in the alpha range (ideal band-pass filter, 7-14 Hz), and we computed for each epoch the alpha amplitude envelope via a Hilbert transform. The resting EEG IAA was defined for both high- and low-luminance condition, as the area under the mean alpha amplitude curve. To determine the resting EEG IAF we computed the

mean amplitude spectrum in the alpha range, within 8 and 13 Hz via a Fast Fourier transform. The resting EEG IAF was defined as the center of mass of the alpha frequency spectrum[213].

4.2.2 Experiment 2: echo function

White-noise visual luminance sequences were displayed on a CRT monitor (640×480 pixels, 160 Hz), within a disc of 3.5º radius presented in the vertical meridian centered at 7.5º above the fovea on a black background. Each randomly generated luminance sequence (6.25 s) was tailored to have equal power at all frequencies, by normalizing the amplitudes of its Fourier components before applying an inverse Fourier transform. Sequences ranged from black (0.02 cd/m2) to white (110 cd/m2). Observers (N=12) covertly monitored the stimulus to detect a 1 s long target square (3.75 degrees) appearing inside the disc on a random 25% of trials. The target onset occurred at a random time (uniform distribution, excluding the first and last 0.25 s) within the sequence. The area within the square followed the same sequence of luminance changes as the disc stimulus, but scaled in amplitude using a QUEST procedure so that detection performance was fixed at approximately 82%[214]. A schematic of the procedure is shown in figure 1B. Observers were instructed to press a button at the end of the sequence if they had detected the target. The experiment consisted in 250 trials and each participant performed the experiment both under high- and low-luminance viewing condition. The order of the condition was random, and 5 minutes of dark-adaptation preceded the low-luminance recordings. Both target-present and target-absent trials were included in the cross-

correlation analysis, since it was verified elsewhere that the echo function is consistent in both conditions[194].

The EEG was re-referenced to the common average and down sampled to 160 Hz before cross-correlation with the stimulus sequences. To obtain the "impulse response function" of the EEG we averaged the single-trial cross-correlations[194,195] between the luminance sequence and the simultaneously acquired EEG time series at all lags between -0.2 to 1.5 s. Individual alpha amplitude (echo IAA) and individual alpha frequency (echo IAF) were computed for the echo function at the electrode POz, on the delays between 0.1 and 1.5 s. For echo IAF, the signal was previously zero-padded to increase frequency resolution (30 s). Moreover, we investigated the phase difference between the two conditions. We selected a time-window from 0.1 to 0.5, where the alpha amplitude was maximal for both conditions (see figure 4D). Instantaneous analytic phase was obtained by taking the angle of the Hilbert-transform of the band-pass filtered echo functions (7-14 Hz) within this window of interest. Finally, we investigated the evoked EEG IAA and the evoked EEG IAF for the raw EEG recorded during the stimulation, in the same way described above. Given that the EEG was not phase-locked trial-to-trial, the evoked EEG IAF was directly computed for each subject by estimating the center of mass of the mean spectrum at POz, between 8 and 13 Hz.

4.2.3 Experiment 3: monocular critical flicker frequency

The experiment consisted in a monocular *critical flicker frequency* (CFF) measurement performed during binocular light-adaptation (LA) and contralateral monocular dark-adaptation (DA) conditions. The stimulus was a white LED flickering (square wave from 20 to 70 Hz, 65 cd/m^2) 20° right to the center and visible only by the right eye thanks to a board positioned between the subject's nose (head fixed on a chin-rest) and the center of the screen. Participants (N=13) were asked to adjust online the frequency of the flicker with a potentiometer, until reaching the subjective fusion frequency threshold. Each trial lasted for 6 s and the starting flickering frequency was fixed at 70 Hz. 10 trials were acquired for each testing session. After a training period, a baseline was computed for each individual subject right before the beginning of the experiment. In the monocular dark-adaptation condition (30-minute duration, 70 trials) a NDF (1.5 LU) was applied in front of the left eye. The filter was removed in the subsequent light-adaptation condition where all subjects performed the same task (8-minute duration, 40 trials). 6 subjects were additionally tested three times more at 8, 10 and 12 minutes after DA. The procedure details are shown in figure 1C, and D. After each CFF session, the board was removed and participants performed a reaction time task to a black blob (3 cpd) presented beside a movie shown in the screen center (2.5x2 deg). The *RT task* lasted for 5' and 2' under DA and LA condition, respectively. Only data from CFF were analyzed. A linear mixed-effect model analysis was run on the logarithm of the CFF, with subject variability modeled as a random effect, while condition (baseline,

monocular dark adaptation and binocular light adaptation) and session as fixed effects. For the analysis on the effect of session, we contrasted the baselines with the following sessions.

4.2.4 Regression analysis

To statistically evaluate linear regressions and to assess the effect of single correlations as well as the interactions between regressors, we performed a linear mixed-effect model analysis. When possible, we modeled the dependent variable (e.g. echo IAF) via two regressors (e.g. the main effect – evoked EEG IAF - and the condition effect - ambient luminance) and their interaction, otherwise we only evaluated the effect of the main regressor (i.e. figure 4D). The analysis was implemented using the Matlab function "fitlme" on the model: Y = regressor1 + regressor2 + regressor1:regressor2. When the main effect was statistically significant, we reported the slope and the Pearson's r of the regression between the dependent variable and the main effect.

Figure 4.1: experimental procedures
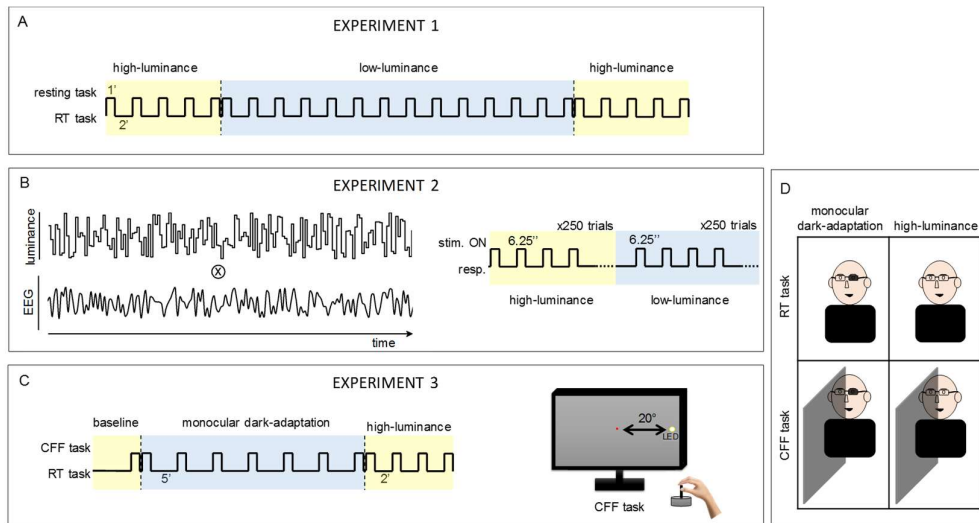
A, schematic of the procedure of experiment 1. One minute of resting state was followed by 2 minutes of RT task. Globally, 10' of resting state was recorded under high-luminance and 14' under low-luminance viewing condition. **B**, schematic of experiment 2. For each participant, we computed the individual echo by cross-correlating the random luminance sequence of the visual stimulation with the EEG response of the POz electrode. Each stimulation lasted for 6.5 s, and 250 trials were recorded under high- and low-luminance viewing condition. **C**, schematic of experiment 3. After a training conducted under high-luminance viewing condition, 10 CFF thresholds were recorded as a baseline, right before starting the monocular dark-adaptation. During the monocular dark-adaptation CFF thresholds were acquired followed by 5 minutes of RT task. CFF threshold was tested 7 times over 30 minutes of global monocular dark-adaptation, for a total of 70 CFF threshold values. CFF was then computed 7 times more under high-luminance viewing condition, again after CFF task participants performed 2' of RT task. The right insert shows an example of the CFF task: the flickering LED was 20° distant from the center, participants had 6'' to select with a potentiometer the CFF threshold. **D**, an example showing the experimental apparatus for the CFF experiment. During monocular dark-adaptation participants wore googles with a NDF on the left eye. During the CFF task, a board was positioned between the subject's nose and the center of the screen and the stimulus was presented on the right hemi-field. Only the right (non-adapted) eye was tested. Note that in this way, the retinal adaptation of the tested eye was identical between the monocular dark-adaptation and the light-adaptation condition.

4.3 RESULTS

4.3.1 Experiment 1: resting state

We analyzed the effect of ambient luminance on resting EEG alpha for 14 participants at three occipital electrodes of interest (Oz, POz, Pz). The resting EEG IAA was computed for both high- and low-luminance recordings (figure 2A, and B). A two-tailed paired t-test showed that alpha amplitude – for all three electrodes - was higher at low-luminance compared to high-luminance viewing conditions (t(13) = [-4.74, -6.04, -3.22], p-val = [<0.001, <0.001, 0.006] for Oz, POz and Pz electrodes, respectively. Bonferroni-Holm corrected for multiple comparison). Similarly, we compared the resting EEG IAF at the three electrodes for the two luminance conditions (figure 2C, and D). No differences were found in resting EEG IAF for high- and low-luminance conditions at any electrode (uncorrected p-val > 0.05).

Figure 4.2: experiment 1 – resting state
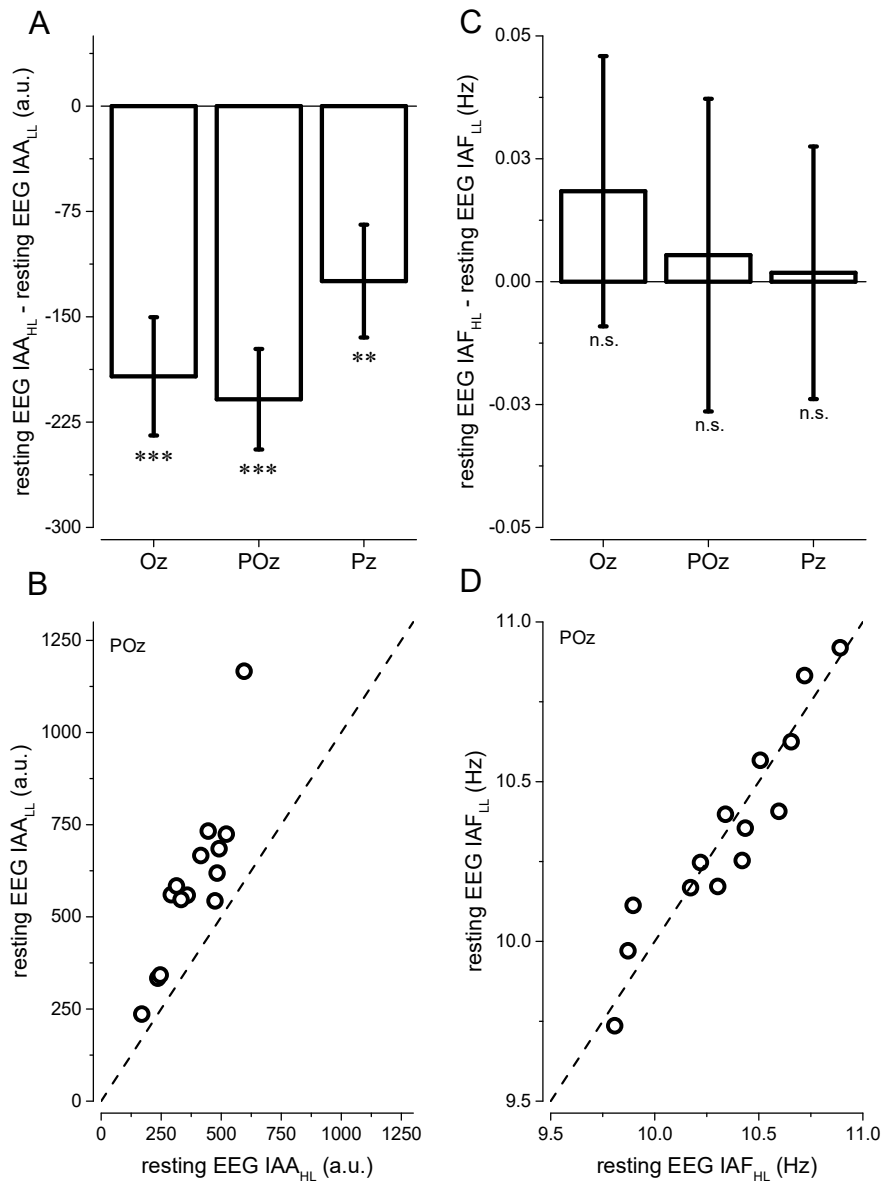
Main results from experiment 1. **A**, Group-mean difference and s.e.m. between IAA at high- and low-luminance for three electrodes (Oz, POz, Pz). **B**, IAA at high- and low-luminance for individual subjects, at the POz electrode. All the points cluster above the equality line (dashed line) confirming a strong IAA difference for the two luminance conditions. **C**, histogram of the IAF difference (±1 s.e.m.) between high- and low-luminance for the electrodes Oz, POz and Pz. **D**, scatter plot of the IAF computed on POz at high- and low-luminance. The points are distributed around the equality line (dashed line), confirming no differences in IAF for the two conditions. Asterisks mark the statistical significance (n.s. > 0.05 > * > 0.01 > ** > 0.001 > ***).

4.3.2 Experiment 2: echo function

For each participant (N = 12) we computed the echo function at high- and low-luminance for the POz electrode (two representative subjects are shown in figure 4A,B). Figure 3A shows the mean spectrum ±1 s.e.m. of the echoes, for both viewing conditions.

Figure 4.3: experiment 2 – echo function I
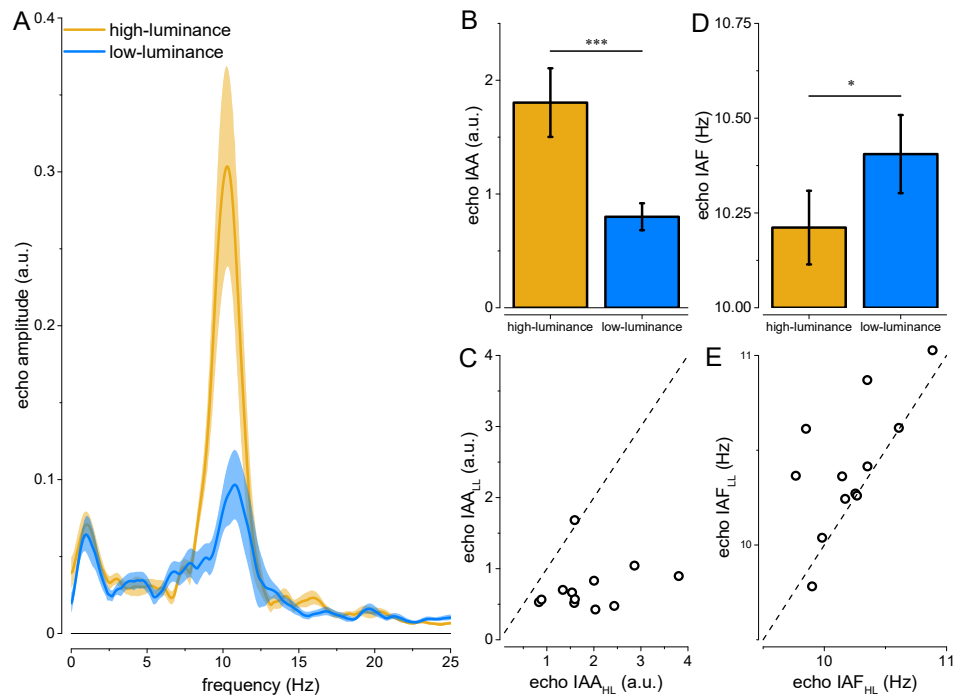
A, Group-mean echo spectrum and s.e.m. at high- and low-luminance (yellow and blue lines, respectively) for the POz electrode. **B**, Bar plot of the echo IAA (±1 s.e.m.) at high- and low-luminance. **C**, scatter plot of the echo IAA at high- and low-luminance. The points cluster below the equality line (dashed line), indicating a difference in echo IAA for the two conditions. **D**, Bar plot of the echo IAF (±1 s.e.m.) at high- and low-luminance. **E**, scatter plot of the echo IAF across single subjects for the two luminance conditions. The cloud of dots scatter above the equality line, indicating that the echo IAF was higher at low-luminance. Asterisks mark the statistical significance (n.s. > 0.05 > * > 0.01 > ** > 0.001 > ***).

We compared the echo IAA for the two luminance conditions with a two tailed t-test, and we found that alpha echo amplitude was higher at high-luminance compared to low-luminance ($t(11) = 4.68$, p-val < 0.001. See figure 3B, and C). Thus, we investigated the effect of luminance on echo IAF (figure 3D, and E) and we found a significant echo IAF shift of about 0.2 Hz towards higher frequencies at low-luminance compared to high-luminance ($t(11) = -2.41$, p-val = 0.03).

Finally, we selected a time window of 400 ms which contained the maximal echo alpha activity, from 0.1 to 0.5 s (figure 4C), and we computed the phase difference between the high- and low-luminance echoes (figure 4G). We found that during the maximal amplitude of the echo function there was a strong phase opposition (2.99 ± 0.4 rad) maximally expressed over the occipital electrodes, and particularly at POz (figure 4F). To verify that the phase-difference was significant, we performed a Rayleigh test that confirmed the presence of a non-uniform phase distribution centered around π (i.e. phase opposition, p-val < 0.001).

Thus, we investigated the correlation between the echo IAF difference and the phase difference (figure 4D) via a linear mixed-effect model analysis. The test revealed a non-significant correlation between phase difference and echo IAF difference (slope = 0.25 ± 0.62, Pearson's r = 0.12; $F(1,10) = 0.203$, p-val = 0.66), indicating that the phase shift between high- and low-luminance conditions was not driven by echo IAF differences. Finally, we asked whether the phase shift could be driven by

a fixed physiological neural delay, caused e.g. by luminance differences
[199]. We performed a linear mixed-effect model analysis on the phase
difference, modeling the effects of echo IAFs, of the ambient luminance
conditions, and their interaction (figure 4E). Note that it was possible here
to perform a linear regression on circular phase data, because the
measured phase differences were all comprised between π/2 and 3π/2,
so there was no "wraparound" issue around 0 or 2π. The analysis
revealed a significant effect of the echo IAF (slope = 0.91±0.27,
Pearson's r = 0.57; F(1,20)=8.131, p-val = 0.009) and no effect of ambient
luminance condition or interaction (p-val > 0.05), suggesting that the
phase delay could have been mainly determined by the constant neural
delay caused by luminance reduction. The phase lags, when expressed
in ms (taking into account the echo IAF for each subject/condition) were
clustered around 45±7 ms, a value consistent with the physiological delay
of about 15 ms fore each log-unit attenuation of luminance [181,183],
predicting here a neural delay around 40 ms.

Figure 4.4: experiment 2 – echo function II
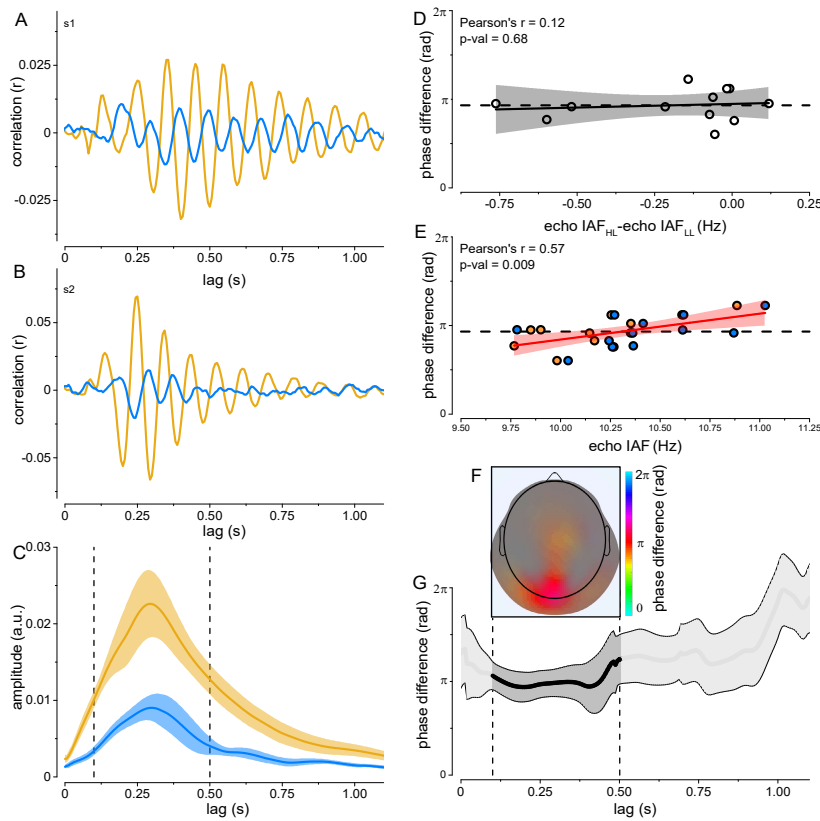
Example of echoes for two representative subjects (**A**, and **B**) at high- and low-luminance (yellow and blue line, respectively). **C**, Alpha amplitude envelope for both high-and low-luminance echoes. Dashed lines mark the temporal window of interest for the phase analysis in panels D, E, F, G (between 0.1 and 0.5 s). **D**, scatterplot for echo phase difference as a function of echo IAF difference. The black line (95% confidence intervals in gray area) reports the linear regression model, showing a non-significant correlation between the two variables (p>0.05), indicating the phase lag was independent from the frequency shift previously reported. Dashed line shows the mean phase difference. **E**, scatterplot for echo phase difference as a function of echo IAF. Yellow and blue dots report the single subject data for the high- and low-luminance conditions, respectively. The red line (red area as 95% confidence intervals) reports the linear regression model, showing a significant positive correlation between the two variables (p<0.05), suggesting the phase lag was mainly driven by the physiological neural delay (estimated at around 40 ms). Dashed line shows the mean phase difference. **F**, Grand-mean topographic representation of phase differences averaged over the temporal window of interest. Color code represents phase differences in radians. Topography was masked (gray transparency) by the averaged amplitude of perceptual echoes. **G**, Phase difference mean and s.e.m. between the two echo functions. Dashed lines mark the temporal window of interest for the phase analysis (shown in C).

We also investigated the EEG spectrum obtained during the stimulation. Figure 5A shows the main results of these analyses for high- and low-luminance conditions. We evaluated the relation between echo IAA and the evoked EEG IAA using our linear mixed-effect model analysis (figure 5B). We found a main effect of evoked EEG IAA (with dependent variable echo IAA; Pearson's r = 0.54; $F(1,20) = 17.75$, p-val < 0.001) and a significant interaction between ambient luminance condition and evoked EEG IAA ($F(1,20) = 5.35$, p-val = 0.03), with no main effect of ambient luminance condition (p-val = 0.15). The same analysis was run for the echo IAF (figure 5C) and revealed a significant main effect of evoked EEG IAF (with dependent variable echo IAF; slope = 1.34±0.21, Pearson's r = 0.796; $F(1,20) = 24.205$, p-val < 0.001), and no main effect of ambient luminance condition or interaction (p-val > 0.05). Similarly to what was found for the echo, results showed a decrease in evoked EEG IAA for the low-luminance condition (t(11) = 2.868; p-val = 0.015. Figure 5D). However, this difference was much reduced, compared to the one found for the echo function. Interestingly, no difference was found regarding the evoked EEG IAF (t(11) = -0.305; p-val = 0.76. Figure 5E).

Figure 4.5: experiment 2 – EEG and echo function
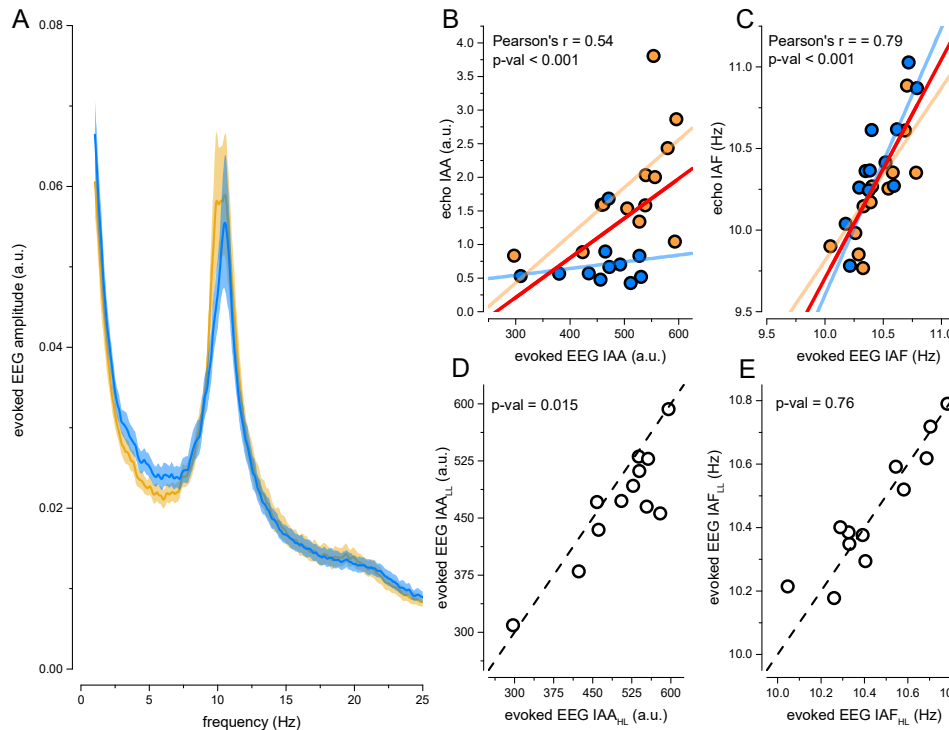
A, Group-mean and s.e.m. spectrum of the evoked EEG recorded at POz, at low-luminance (blue line) and high-luminance (yellow line) during the echo experiment. **B**, and **C**, correlation between the IAA and IAF computed for the echo and the evoked EEG signal. Dots represent the IAA for single subject at high- and low-luminance (yellow and blue, respectively). Red lines report the global linear model. Yellow and blue lines in panel B show separately the correlation under high- and low-luminance. P-values report the main effect of the main regressor (red line), irrespective of the ambient luminance condition. **D**, scatter showing evoked EEG IAA for single subjects under different luminance viewing conditions. EEG amplitude was higher at high-luminance. Dashed line marks the equality points. **E**, same as **D** but for evoked EEG IAF. No differences were found between evoked EEG IAF for the two conditions. Dashed line marks the equality points.

4.3.3 Experiment 3: monocular critical flicker frequency

We next investigated on 13 participants the potential perceptual consequences of alpha modulations in a monocular CFF task. A linear mixed-effect model on the CFF timecourse showed a significant effect of

time session (fixed effect 'time session' with 'subject' as random effect. $F(14,1725) = 4.4208$, p-val < 0.001. See figure 6A). Post-hoc contrasts between session and baseline revealed that the CFF in the first session of the binocular light-adaptation was the only threshold significantly different from the baseline (p-val = 0.047). We next investigated the global effect of monocular dark-adaptation on CFF. Figure 6B shows the group-mean CFF shifts between the two conditions. The test between monocular dark-adaptation and binocular light adaptation conditions revealed a significant difference between conditions (fixed effect 'condition', random effect 'subject'. $F (2,1737) = 14.592$, p-val < 0.001), indicating that CFF was consistently higher during DA compared to LA, of about 3-4 Hz. No differences were present between DA and baseline or LA and baseline (p > 0.05). Figure 6C shows this result for single subjects, tested with a bootstrap t-test (10000 repetitions with replacement, n=40). 9 subjects showed a statistically significant difference in CFF between monocular dark-adaptation and binocular light adaptation conditions (p-val < 0.01), while 4 participants showed a trend without reaching significance (p-val > 0.05).

Figure 4.6: experiment 3 - CFF
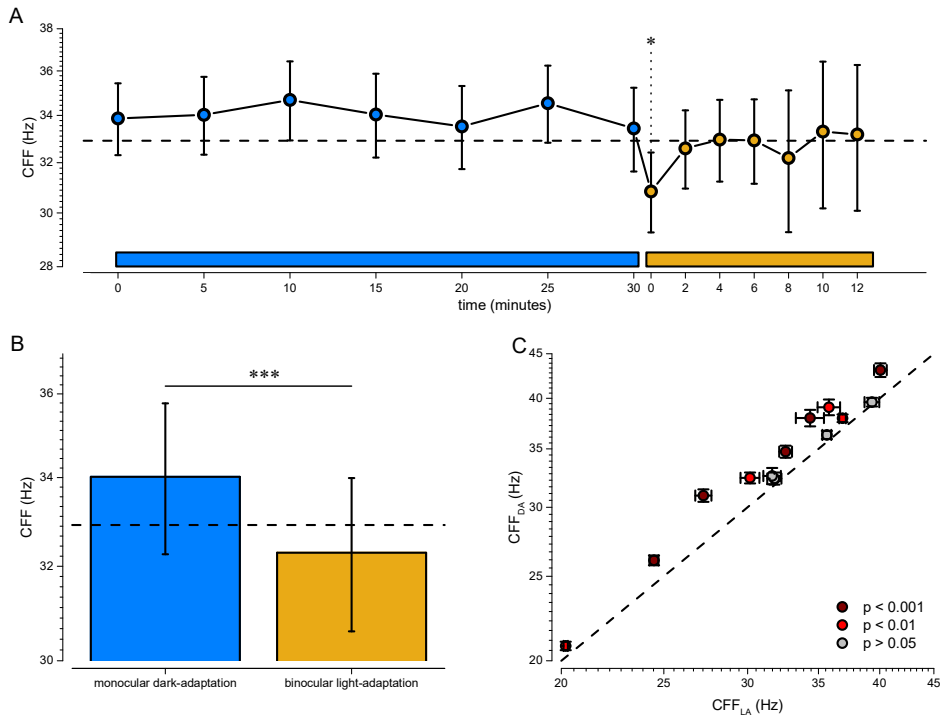
A, CFF and s.e.m. timecourse as a function of time from monocular dark-adaptation (DA, blue bar) and binocular light-adaptation (LA, yellow bar). Horizontal dashed line shows the baseline computed before DA. Horizontal blue and yellow lines mark the duration of the DA period (blue dots) and of the LA (yellow dots), respectively. **B**, grand-mean and s.e.m. of the CFF shift for DA (blue bar) and LA (yellow bar). Horizontal dashed line shows the baseline. **C**, CFF and standard error for DA and LA for all subjects. Confidence intervals were computed via a bootstrap procedure. Equality line shown as dashed line. Asterisks (in **A** and **B**) indicate the statistical significance (p-val: 0.05 > * > 0.01 > ** > 0.001 > ***). Color codes (in **C**) mark the statistical significance of the difference.

Additionally, we investigated the existing correlations between all the frequency indices computed in all three experiments (i.e. resting/evoked EEG IAF for experiment 1 and 2, echo IAF for experiment 2, and CFF for experiment 3). For each regression, we selected those subjects that had both indices. This resulted in 6 participants included for experiments 1 and 2, 8 participants for experiments 1 and 3, and 5 participants for experiments 2 and 3. The limited amount of observations poses a challenge in establishing a definitive regression analysis; however, we found the global regression analysis be informative. A linear mixed-model effect analysis was run for each comparison (figure 7). We found significant correlations between resting EEG IAF and evoked EEG IAF (slope = 1.21 ± 0.37, Pearson's r = 0.76; $F(1,8)$ = 8.351, p-val = 0.02), between resting IAF and echo IAF (slope = 0.56 ± 0.21, Pearson's r = 0.64; $F(1,8)$ = 12.072, p-val = 0.008), between echo IAF and evoked EEG IAF (slope = 1.34 ± 0.21, Pearson's r = 0.79; $F(1,20)$ = 24.205, p-val < 0.001), and between CFF and echo IAF (slope = 5.67 ± 1.8, Pearson's r = 0.74; $F(1,6)$ = 7.12, p-val < 0.037). Non-significant correlation was found between CFF and resting EEG IAF (p = 0.89), and between CFF and evoked EEG IAF (p > 0.05). No effects of condition and no interaction were detected for any regression (p > 0.05).

Figure 4.7: regression analysis

Linear regression analysis for several frequency indices: IAF for the EEG recorded at rest (resting EEG IAF, experiment 1), for the EEG recorded during a visual task (evoked EEG IAF, experiment 2), for the perceptual echo (echo IAF, experiment 2), and CFF (experiment 3). Statistically significant correlations and their confidence interval (95 percentile) are indicated by a red regression line, non-significant correlations in gray. Dots report single subject results at high- and low-luminance (yellow and blue, respectively). Correlation coefficient (Pearson's r) and p-values are shown for each comparison.

4.4 DISCUSSION

We evaluated the influence of ambient luminance changes on the rhythmic and dynamic characteristics of visual processing. Firstly, we investigated the effect of luminance changes on the ongoing alpha rhythm recorded during resting and during a white noise stimulation paradigm (experiments 1 and 2). In agreement with the existing literature[167], we found that ambient luminance alters the spectral amplitude in the alpha range during resting. We found – for all the occipital electrodes investigated – a strong resting EEG IAA enhancement at low-luminance compared to high-luminance. Traditionally, this alpha power enhancement is interpreted as a consequence of the metabolic deactivation of the underlying cortex at low luminance[200], reflected in a strong occipital alpha-synchronization in the EEG. Interestingly, luminance changes produced no effects on the resting EEG IAF for spontaneous activity (experiment 1). As regards the echo function, we found a very different neural response across luminance changes. In opposition to what we reported for the spontaneous alpha rhythm at rest, the echo IAA was strongly attenuated during low-luminance viewing conditions. A similar, but much reduced effect, was confirmed for the evoked EEG IAA recorded during visual stimulation in experiment 2. Furthermore, we found that the alpha frequency of the IRF (echo IAF) shifted towards higher frequencies at low luminance compared to high-luminance viewing. The alpha amplitude modulation might reflect a reduced capability of the visual system to synchronize its responses to the stimuli, due to a degradation of the

signal-to-noise ratio at low luminance. It has been suggested that the echo function could reveal a key brain function connected with the maintaining of sensory representations over time[194]. In this respect, the weaker and shortened correlation between the neural responses and the stimulation under low-luminance viewing could reveal a reduced system capability in retaining perceptual information. In line with this interpretation, it has been shown that luminance reduction impairs memory performance[215]. Additionally, it has been shown that the dwell-time of visual attention – i.e. the attentional blink – is different under high- or low-luminance viewing conditions[216]. Crucially, we found that IAF - for the perceptual echo only – was lower at high- compared to low-luminance viewing. We may speculate that this shift could reveal a basic adaptive strategy to balance the reduced inflow of good quality visual information under low luminance, with an oversampling of the visual inputs. In other words, when the visual inputs are reliable (i.e. under high-luminance viewing) the system facilitates the retention of the sensory representation over time; conversely, when the visual inputs are degraded (i.e. under low-luminance viewing), the system underweights its sensory representations and updates them more quickly. Additionally, we found a consistent phase opposition between the perceptual echoes at high- and low-luminance. We tested the possibility that the phase shift was merely due to the reported frequency shift between the two tested conditions (figure 4D). No correlation was found between the phase and the echo IAF difference, indicating that the phase shift was not (solely) driven by the frequency shift. At low-luminance, visual processing is

slowed down and delayed by about 15 ms for each log-unit attenuation of luminance[181,183,199], resulting in a constant delay of about 40 ms, in our experiment. To test whether this delay could also account for the observed phase shift, we computed the phase difference for each echo IAF (figure 4E). As a matter of fact, we found a positive correlation between the phase difference and the echo IAFs, suggesting that the phase shift reported here could be mainly assigned to a constant neural delay.

Finally, we compared the echo IAA and IAF with the evoked EEG IAA and IAF. We found that IAF values are strongly correlated for both high- and low-luminance condition; on the other hand, the IAA shows a strong correlation at high-luminance for the echo and the evoked EEG indexes, but a weak correlation at low-luminance. This ambient luminance interaction for the IAA, together with a lack of frequency shifts at low-luminance for the EEG IAF, indicates that the echo and the evoked alpha possess peculiar and independent properties.

Next, we tested the behavioral effect of luminance changes with a monocular CFF task. It is known that CFF is modulated by both retinal and central visual processes[217], and that binocular light adaptation modulates the critical flicker frequency: it decreases during dark adaptation, and increases in the course of light adaptation[218]. Interestingly, it has also been shown that the light adaptation of one eye can modulate the CFF of the other eye in an opposite way[219]. In his experiment, Lipkin[219] adapted one eye with a steady light and tested the

non-adapted eye. He found that an adapting luminance on one eye progressively reduced the CFF on the contralateral eye. Here, we adopted a similar procedure: we dark-adapted the left eye of the subjects for 30 minutes by applying a NDF patch, while testing the non-deprived right eye. Next, we removed the patch and continued testing the right eye for 12 minutes. Note that in this way we kept constant the retinal adaptation of the tested eye, while manipulating only the extraretinal light adaptation. In agreement with Lipkin[219], we showed that monocular CFF was higher during contralateral dark-adaptation, compared to binocular light adaptation. Much evidence suggests that this phenomenon could be considered as a plasticity response of the primary visual cortex to luminance changes. Recently, it has been shown that dark exposure reduces tonic inhibition in visual cortex[201], and that monocular deprivation alters early components of visual evoked potentials as well as producing a GABA concentration decrement in the primary visual cortex of adult humans[220,221]. Moreover, 3 hours of monocular light-deprivation are known to produce a decrease in the CFF for the non-occluded eye[222]. Here, we studied the temporal dynamics of CFF during monocular dark adaptation and binocular light adaptation and we found that only 30 minutes of monocular dark-adaptation induced a fast and consistent decrease of CFF threshold that gradually disappeared after about 12 minutes. It has been suggested that CFF and alpha activity might correlate[202–204], however the majority of the reported effects are shown for clinical populations[204,205], rely on somatosensory tasks[204], or their results have been questioned[205,206]. We suggest here that monocular

CFF in healthy subjects might indeed positively correlate with the frequency of the EEG IRF (echo IAF), while CFF and resting\evoked EEG IAF only displayed a positive correlation that did not reach statistical significance. This result does not only suggest that the echo function plays a key role in determining the temporal resolution of our vision, but it also shows a dissociation between the resting\evoked alpha and the echo function. Moreover, CFF estimation is important to evaluate the stage and gravity of some pathologies[203,204]; the positive correlation shown here between CFF and echo IAF (although problematic for the lack of enough data points, see methods and results) could potentially have clinical implications, for example when there is no possibility to measure the CFF (e.g. unresponsive patient). To sum up, we might speculate that the EEG IRF changes across different luminance conditions reflect an important plasticity phenomenon: the visual cortex modulates its IRF depending on the luminance viewing condition, and these modulations impact on very low-level stages of visual processing (such as flicker perception). However, future experiments would be needed to provide more concrete evidence for this hypothesis.

5   GENERAL CONCLUSIONS

There are several ways to create predictions about upcoming events: for example, we are able to extract temporal regularities from perceptual events (entrainment); alternatively, we can identify specific and informative perceptual cues that direct our predictions in space and time. All these options rely on attentive mechanisms, however – sometime – we cannot take advantages from regularities or cues to drive our predictions. Another likely mechanism is linked with voluntary actions. When we act in the environment we are interfering with the external events, increasing the probabilities to produce effects or to detect relevant\salient information. For this reason, we might expect that an efficient predictive mechanism would operate in the temporal proximity of our voluntary actions, i.e. when the environmental changes are more likely to occur. In agreement with this hypothesis, we have shown here that visual perception is synchronized with very simple voluntary movements such as saccades or button-press (studies 1 and 3). Interestingly, this synchronization revealed a long lasting oscillatory modulation of visual sensitivity starting even before the actual movement onset, suggesting the presence of a phase-locking mechanisms starting during motor planning. In other words, we hypothesize the presence of an early visuo-motor coupling taking advantages of endogenous rhythm to maintain coordination between the two systems; this coordination is expressed by neural oscillations and impacts visual sensitivity; we hypothesize that these coupling – likely driven by predictive top-down mechanisms – act by resetting the phases of endogenous oscillations

during motor preparation (action planning processing stages). Moreover, the frequency of these oscillations seems to depend on the motor effector timing: at around 3 Hz for eye movements and about 6 Hz for finger\hand movements, corresponding to the natural action rating of eye and finger movement, respectively[80,105,106]. A perfect action-perception coupling is fundamental for our normal behavior, as revealed by pathologies in which this coupling is compromised, as in Parkinson's disease and Schizophrenia[223,224]. Moreover, it has been shown that hallucinatory events (e.g. auditory hallucinations, tinnitus) correlate with abnormal oscillatory activity in the theta, alpha and gamma range[225–228]. Thus, a better comprehension of these sensorimotor oscillatory mechanisms might increase our comprehension of the severe and impairing motor and perceptual deficits derived from their abnormal functioning.

We also investigated the effect of action on the dynamics of pupillary light response and the correlation between the perceptual suppression and the pupillary one (study 2). We found that saccades modulate pupillary constriction, suppressing its constrictive response for stimuli presented at around the time of the eye movement. This response was much dilated compared to the visual suppression and it was not correlated with perception: the pupillary constriction was independent from the perceptual awareness of the subjects and their perceptual report. This suggests that visual and pupillary suppressions rely on different efference copy signals, indicating that the oscillatory modulation reported in the perceptual tasks (study 1,2 and 3) likely depends on the geniculate pathway, while the modulation reported for the pupillary response (study

2) depends on the extra-geniculate pathway possibly involving the superior colliculus[149]. Moreover, we suggest here that the pupillary signal is uncorrelated with perceptual awareness and likely possessing intrinsic and different dynamics from the ones reported for perception.

Moreover, we investigated the possible relationship between the characteristics of these oscillations and the ambient luminance (study 3 and 4). It is known that luminance profoundly impacts vision by delaying and slowing down its processing[181,182]. On the other hand, ambient luminance changes also modulate endogenous oscillations, increasing the EEG power spectrum (especially in the alpha range) and potentially speeding up some of its components[167,168]. We found that the dynamics of visual oscillations were different under high or low ambient luminance, resulting in faster oscillations at low-luminance compared to high-luminance viewing (study 3). Traditionally, it is assumed that our visual timing under mesopic and scotopic viewing condition is worst compared to the timing under photopic viewing[183]. An important factor determining this effect is the retinal adaptation that impairs a fast inputs transmission at low luminance. Thus, we investigated the extraretinal effects of ambient luminance, by selectively dark\light adapting one eye and measuring the monocular CFF on the contralateral eye. We found that the monocular CFF was higher under low-luminance compared to high-luminance (study 4-III), suggesting a positive effect of extraretinal dark adaptation over visual temporal resolution. To better understand this light modulation, we analyzed the electrophysiological activity under low and high ambient luminance viewing (study 4-I and 4-II). We found a strong

modulation of brain rhythms as a function of ambient luminance. We computed the EEG brain response at rest and the EEG visual impulse response function (echo function) under high- and low-luminance viewing and we found a dissociation between the resting EEG response and the EEG IRF: at low luminance, the resting EEG activity shows higher alpha power compared to high-luminance, while the echo function shows the opposite pattern; on the other hand, only the echo function shows a shift of the alpha frequency towards higher frequency at low-luminance compared to high-luminance. This influence of ambient luminance over intrinsic visual oscillatory activity might suggest that our vision – or the endogenous rhythms of vision – actively fits environmental viewing condition. In other words, endogenous oscillations seem to balance\compensate the internal neural delay caused by scotopic viewing by increasing the amplitude of higher frequencies and slightly shifting the center of gravity of the endogenous rhythms towards faster oscillations.

To sum up, we have shown here the importance of visual oscillations for action and perception. We investigated the temporal dynamics of action and perception coupling, and we hypothesized the presence of an ongoing oscillatory modulation of vision triggered by action planning or the intention to move. We found that this rhythmic modulation affects early stages of visual processing and likely relies on the geniculate pathway. Finally, we found that these oscillations can adapt their characteristics based on the relevant effector to synchronize with vision

(i.e. eye or finger in our studies) and based on the ambient luminance condition.

Sense of agency, free will and consciousness are crucial concepts implicated in these investigations. Firstly, it is important to keep in mind that these concepts rely on ambiguous terms, referring to many different phenomena[229,230]. For this complexity, and the widespread impression of an inherently subjective experience as a fundamental aspect of these cognitive processes the actual possibility of a scientific investigation of these phenomena has been long debated[229,231,232]. However, from the early 90s of the last century, there have been several attempts to address the problem of consciousness within a scientific framework. Crucially, neural oscillations represented the biological core of these neurobiological theory of consciousness[233–236]: thanks to their ability to bind different information together, neural oscillations were reported to play a key role in generating awareness. As a logical consequence, it follows that our consciousness (e.g. perceptual awareness) floats rhythmically over time and it is intrinsically non-linear. This strongly contrasts with our naïve psychological assumption on consciousness as a continue process that - as an all-or-nothing process – is time invariant. Moreover, as mentioned above, this idea has profound consequences on our sense of agency (or our self-consciousness), and our free will assumptions as well. Libet et al.[86] found that the wish to move (i.e. the self-reported timepoint in which the subject consciously feels the intention to move) is preceded by a so called "readiness potential" that precedes the subject's volition to move from up to one second. These

results suggested that – unconsciously – subjects action planning starts much before the conscious intention to move. Here, and in agreement with a similar experiment[62], we reported that vision is synchronized with action from up to one second before the voluntary movement. This might imply two opposite interpretations. On the one hand, an intention to move signal (no matter whether conscious or unconscious) could trigger visual oscillations by resetting their phases; on the other hand, it is also likely that our will (and thus our consciousness) is constrained within certain phases of ongoing endogenous oscillations. In the latter case, our will would not be entirely free but shaped and constrained by the phases of ongoing brain oscillations.

However, further experiments will be necessary to better understand the basic nature of these oscillatory phenomena and to approach such high-dimensional and complex concepts.

ACKNOWLEDGMENTS

Several people have had a direct or indirect impact on the development of this thesis, and I would like to thank them for their help.

I thank all the PisaVisionLab[*] for the help I received during these years and, in particular, I would like to thank my supervisors Prof. M.C. Morrone and Prof. D. Burr which followed closely all of my projects and gave crucial advises throughout the whole duration of the Ph.D. A special thanks to Prof. G.M. Cicchini for his unconditional and trustworthy help, and to Prof. P. Binda who was never too busy to answer all my questions and problems.

A thank goes to Prof. R. Vanrullen, who hosted me in his PAF team[†] in Toulouse, and guided me for the whole duration of my formative French stage; thanks also to D. Lonzano-Soldevilla, B. Zoefel, and all the PAF team for their helpful comments and support.

Finally, a special thanks my family and Valeria for their unmeasurable support during these years (and surely for the one are going to come), and to all my friends (they are too numerous to be individually quoted).

---

[*] www.pisavisionlab.org
[†] www.cerco.ups-tlse.fr/~rufin

BIBLIOGRAPHY

1. Gibson, J. The perception of the visual world. (1950).

2. Tsodyks, M., Kenet, T., Grinvald, A. & Arieli, A. Linking Spontaneous Activity of Single Cortical Neurons and the Underlying Functional Architecture. *Science (80-.).* **286,** (1999).

3. Arieli, A., Sterkin, A., Grinvald, A. & Aertsen, A. Dynamics of ongoing activity: explanation of the large variability in evoked cortical responses. *Science* **273,** 1868–71 (1996).

4. Softky, W. R. & Koch, C. The highly irregular firing of cortical cells is inconsistent with temporal integration of random EPSPs. *J. Neurosci.* **13,** 334–50 (1993).

5. Busch, N. A., Dubois, J. & VanRullen, R. The Phase of Ongoing EEG Oscillations Predicts Visual Perception. *J. Neurosci.* **29,** 7869–7876 (2009).

6. VanRullen, R. Perceptual Cycles. *Trends Cogn. Sci.* **20,** 723–735 (2016).

7. VanRullen, R. & Koch, C. Is perception discrete or continuous? *Trends Cogn. Sci.* **7,** 207–213 (2003).

8. Chiel, H. J. & Beer, R. D. The brain has a body: adaptive behavior emerges from interactions of nervous system, body and environment. *Trends Neurosci.* **20,** 553–557 (1997).

9. Muckli, L. What are we missing here? Brain imaging evidence for higher cognitive functions in primary visual cortex V1. *Int. J.*

Imaging Syst. Technol. **20,** 131–139 (2010).

10. Burr, D. C. & Cicchini, G. M. Vision: efficient adaptive coding. *Curr. Biol.* **24,** R1096-8 (2014).

11. Carandini, M. *et al.* Do we know what the early visual system does? *J. Neurosci.* **25,** 10577–97 (2005).

12. Enroth-Cugell, C. & Robson, J. G. The contrast sensitivity of retinal ganglion cells of the cat. *J. Physiol.* **187,** 517–52 (1966).

13. Movshon, J. A., Thompson, I. D. & Tolhurst, D. J. Receptive field organization of complex cells in the cat's striate cortex. *J. Physiol.* **283,** 79–99 (1978).

14. Hubel, D. H. & Wiesel, T. N. Receptive fields, binocular interaction and functional architecture in the cat's visual cortex. *J. Physiol.* **160,** 106–54 (1962).

15. Hubel, D. H. & Wiesel, T. N. Receptive fields of single neurones in the cat's striate cortex. *J. Physiol.* **148,** 574–91 (1959).

16. Somers, D. C., Dale, A. M., Seiffert, A. E. & Tootell, R. B. Functional MRI reveals spatially specific attentional modulation in human primary visual cortex. *Proc. Natl. Acad. Sci. U. S. A.* **96,** 1663–8 (1999).

17. Tootell, R. B. *et al.* The retinotopy of visual spatial attention. *Neuron* **21,** 1409–22 (1998).

18. Kastner, S., De Weerd, P., Desimone, R. & Ungerleider, L. G. Mechanisms of directed attention in the human extrastriate cortex as revealed by functional MRI. *Science* **282,** 108–11 (1998).

19. Brefczynski, J. A. & DeYoe, E. A. A physiological correlate of the 'spotlight' of visual attention. *Nat. Neurosci.* **2,** 370–4 (1999).

20. O'Connor, D. H., Fukui, M. M., Pinsk, M. A. & Kastner, S. Attention modulates responses in the human lateral geniculate nucleus. *Nat. Neurosci.* **5,** 1203–1209 (2002).

21. Silver, M. A., Ress, D. & Heeger, D. J. Neural correlates of sustained spatial attention in human early visual cortex. *J. Neurophysiol.* **97,** 229–37 (2007).

22. Rensink, R. A., O'Regan, J. K. & Clark, J. J. To See or not to See: The Need for Attention to Perceive Changes in Scenes. *Psychol. Sci.* **8,** 368–373 (1997).

23. Simons, D. J. & Levin, D. T. Change blindness. *Trends Cogn. Sci.* **1,** 261–267 (1997).

24. Helmholtz, H. von & von, H. in *Readings in the history of psychology.* 214–230 (Appleton-Century-Crofts, 1948). doi:10.1037/11304-027

25. Gregory, R. L. Perceptions as hypotheses. *Philos. Trans. R. Soc. Lond. B. Biol. Sci.* **290,** 181–97 (1980).

26. Friston, K. & Kiebel, S. Predictive coding under the free-energy principle. *Philos. Trans. R. Soc. B Biol. Sci.* **364,** 1211–1221 (2009).

27. Engel, A. K., Fries, P. & Singer, W. Dynamic predictions: Oscillations and synchrony in top–down processing. *Nat. Rev. Neurosci.* **2,** 704–716 (2001).

28. Caplan, J. B. *et al.* Human theta oscillations related to sensorimotor integration and spatial learning. *J. Neurosci.* **23,** 4726–36 (2003).

29. Bland, B. H. The physiology and pharmacology of hippocampal formation theta rhythms. *Prog. Neurobiol.* **26,** 1–54 (1986).

30. Buzsáki, G. *Rhythms of the Brain - Gyorgy Buzsaki - Oxford University Press*. (Oxford University Press, 2006).

31. Jensen, O., Bonnefond, M., Marshall, T. R. & Tiesinga, P. Oscillatory mechanisms of feedforward and feedback visual processing. *Trends Neurosci.* **38,** 192–194 (2015).

32. van Kerkoerle, T. *et al.* Alpha and gamma oscillations characterize feedback and feedforward processing in monkey visual cortex. *Proc. Natl. Acad. Sci. U. S. A.* **111,** 14332–41 (2014).

33. von Stein, A., Chiang, C. & König, P. Top-down processing mediated by interareal synchronization. *Proc. Natl. Acad. Sci. U. S. A.* **97,** 14748–53 (2000).

34. Heusser, A. C., Poeppel, D., Ezzyat, Y. & Davachi, L. Episodic sequence memory is supported by a theta–gamma phase code. *Nat. Neurosci.* **19,** 1374–1380 (2016).

35. McLelland, D. & VanRullen, R. Theta-Gamma Coding Meets Communication-through-Coherence: Neuronal Oscillatory Multiplexing Theories Reconciled. *PLoS Comput. Biol.* **12,** e1005162 (2016).

138

36.   Fries, P. A mechanism for cognitive dynamics: neuronal
       communication through neuronal coherence. *Trends Cogn. Sci.* **9,**
       474–480 (2005).

37.   Womelsdorf, T. & Fries, P. The role of neuronal synchronization
       in selective attention. *Curr. Opin. Neurobiol.* **17,** 154–160 (2007).

38.   Lisman, J. The theta/gamma discrete phase code occuring during
       the hippocampal phase precession may be a more general brain
       coding scheme. *Hippocampus* **15,** 913–922 (2005).

39.   Jensen, O., Bonnefond, M. & VanRullen, R. An oscillatory
       mechanism for prioritizing salient unattended stimuli. *Trends
       Cogn. Sci.* **16,** 200–206 (2012).

40.   Lisman, J. & Idiart, M. Storage of 7 +/- 2 short-term memories in
       oscillatory subcycles. *Science (80-.).* **267,** (1995).

41.   Dugué, L., Marque, P. & VanRullen, R. The phase of ongoing
       oscillations mediates the causal relation between brain excitation
       and visual perception. *J. Neurosci.* **31,** 11889–93 (2011).

42.   Hanslmayr, S. *et al. Visual discrimination performance is related
       to decreased alpha amplitude but increased phase locking.
       Neuroscience Letters* **375,** (2005).

43.   Milton, A. & Pleydell-Pearce, C. W. The phase of pre-stimulus
       alpha oscillations influences the visual perception of stimulus
       timing. *Neuroimage* **133,** 53–61 (2016).

44.   Drewes, J. & VanRullen, R. This Is the Rhythm of Your Eyes: The
       Phase of Ongoing Electroencephalogram Oscillations Modulates

Saccadic Reaction Time. *J. Neurosci.* **31,** 4698–4708 (2011).

45. VanRullen, R. & Dubois, J. The Psychophysics of Brain Rhythms. *Front. Psychol.* **2,** 203 (2011).

46. Fiebelkorn, I. C., Saalmann, Y. B. & Kastner, S. Rhythmic Sampling within and between Objects despite Sustained Attention at a Cued Location. *Curr. Biol.* **23,** 2553–2558 (2013).

47. Landau, A. N. & Fries, P. Attention Samples Stimuli Rhythmically. *Curr. Biol.* **22,** 1000–1004 (2012).

48. Huang, Y., Chen, L. & Luo, H. Behavioral oscillation in priming: competing perceptual predictions conveyed in alternating theta-band rhythms. *J. Neurosci.* **35,** 2830–7 (2015).

49. Romei, V., Gross, J. & Thut, G. *Sounds Reset Rhythms of Visual Cortex and Corresponding Human Visual Perception*. *Current Biology* **22,** (2012).

50. Bland, B. H. & Oddie, S. D. Theta band oscillation and synchrony in the hippocampal formation and associated structures: the case for its role in sensorimotor integration. *Behav. Brain Res.* **127,** 119–36 (2001).

51. Bland, B. H. in *Information Processing by Neuronal Populations* (eds. Holscher, C. & Munk, M.) 283–325 (Cambridge University Press, 2008). doi:10.1017/CBO9780511541650.012

52. Numan, R. A Prefrontal-Hippocampal Comparator for Goal-Directed Behavior: The Intentional Self and Episodic Memory. *Front. Behav. Neurosci.* **9,** 323 (2015).

140

53. Sirota, A. *et al.* Entrainment of neocortical neurons and gamma oscillations by the hippocampal theta rhythm. *Neuron* **60,** 683–97 (2008).

54. Sławińska, U. & Kasicki, S. The frequency of rat's hippocampal theta rhythm is related to the speed of locomotion. *Brain Res.* **796,** 327–331 (1998).

55. Rivas, J., Gaztelu, J. M. & García-Austt, E. Changes in hippocampal cell discharge patterns and theta rhythm spectral properties as a function of walking velocity in the guinea pig. *Exp. brain Res.* **108,** 113–8 (1996).

56. Kahana, M. J., Sekuler, R., Caplan, J. B., Kirschen, M. & Madsen, J. R. Human theta oscillations exhibit task dependence during virtual maze navigation. *Nature* **399,** 781–4 (1999).

57. Cruikshank, L. C., Singhal, A., Hueppelsheuser, M. & Caplan, J. B. Theta oscillations reflect a putative neural mechanism for human sensorimotor integration. *J. Neurophysiol.* **107,** 65–77 (2012).

58. Rawle, C. J., Miall, R. C. & Praamstra, P. Frontoparietal theta activity supports behavioral decisions in movement-target selection. *Front. Hum. Neurosci.* **6,** 138 (2012).

59. Grent-'t-Jong, T., Oostenveld, R., Jensen, O., Medendorp, W. P. & Praamstra, P. Competitive interactions in sensorimotor cortex: oscillations express separation between alternative movement targets. *J. Neurophysiol.* **112,** 224–32 (2014).

60.   Mitchell, D. J., McNaughton, N., Flanagan, D. & Kirk, I. J. Frontal-midline theta from the perspective of hippocampal 'theta'. *Prog. Neurobiol.* **86,** 156–185 (2008).

61.   Watrous, A. J., Fried, I. & Ekstrom, A. D. Behavioral correlates of human hippocampal delta and theta oscillations during navigation. *J. Neurophysiol.* **105,** (2011).

62.   Tomassini, A., Spinelli, D., Jacono, M., Sandini, G. & Morrone, M. C. Rhythmic Oscillations of Visual Contrast Sensitivity Synchronized with Action. *J. Neurosci.* **35,** 7019–7029 (2015).

63.   Benedetto, A. & Morrone, M. C. Saccadic suppression is embedded within extended oscillatory modulation of sensitivity. *J. Neurosci.*

64.   Benedetto, A., Spinelli, D. & Morrone, M. C. Rhythmic modulation of visual contrast discrimination triggered by action. *Proc. Biol. Sci.* **283,** 3536–3544 (2016).

65.   Latour, P. L. Visual Threshold During Eye Movements. *Vision Res.* **2,** 261–262 (1962).

66.   Burr, D. C., Holt, J., Johnstone, J. R. & Ross, J. Selective depression of motion sensitivity during saccades. *J. Physiol.* **333,** 1–15 (1982).

67.   Burr, D. C., Morrone, M. C. & Ross, J. Selective suppression of the magnocellular visual pathway during saccadic eye movements. *Nature* **371,** 511–3 (1994).

68.   Diamond, M. R., Ross, J. & Morrone, M. C. Extraretinal Control of

Saccadic Suppression. *J. Neurosci.* **20,** 3449–3455 (2000).

69. Gezeck, S., Fischer, B. & Timmer, J. Saccadic reaction times: a statistical analysis of multimodal distributions. *Vision Res.* **37,** 2119–2131 (1997).

70. Carpenter, R. H. S. *Movements of the eyes*. (Pion Ltd., 1988).

71. Morrone, M. C. in *The new visual neurosciences* (ed. J.S. Werner & L.M. Chalupa) 947–962 (The MIT press, 2014).

72. Ibbotson, M. R., Crowder, N. A., Cloherty, S. L., Price, N. S. C. & Mustari, M. J. Saccadic Modulation of Neural Responses: Possible Roles in Saccadic Suppression, Enhancement, and Time Compression. *J. Neurosci.* **28,** 10952–10960 (2008).

73. Reppas, J. B., Usrey, W. M. & Reid, R. C. Saccadic Eye Movements Modulate Visual Responses in the Lateral Geniculate Nucleus. *Neuron* **35,** 961–974 (2002).

74. Leopold, D. A. & Logothetis, N. K. Microsaccades differentially modulate neural activity in the striate and extrastriate visual cortex. *Exp. brain Res.* **123,** 341–5 (1998).

75. Royal, D. W., Sáry, G., Schall, J. D. & Casagrande, V. A. Correlates of motor planning and postsaccadic fixation in the macaque monkey lateral geniculate nucleus. *Exp. Brain Res.* **168,** 62–75 (2006).

76. Knöll, J., Binda, P., Morrone, M. C. & Bremmer, F. Spatiotemporal profile of peri-saccadic contrast sensitivity. *J. Vis.* **11,** 15–15 (2011).

77. Kowler, E., Anderson, E., Dosher, B. A. & Blaser, E. The role of attention in the programming of saccades. *Vision Res.* **35,** 1897–1916 (1995).

78. Deubel, H. & Schneider, W. X. Saccade target selection and object recognition: Evidence for a common attentional mechanism. *Vision Res.* **36,** 1827–1837 (1996).

79. Rolfs, M. & Carrasco, M. Rapid Simultaneous Enhancement of Visual Sensitivity and Perceived Contrast during Saccade Preparation. *J. Neurosci.* **32,** 13744–13752a (2012).

80. Morrone, M. C. & Burr, D. C. in *The Cognitive Neurosciences* (ed. Gazzaniga, M. S.) 511–524 (The MIT press, 2009).

81. Wurtz, R. H. Neuronal mechanisms of visual stability. *Vision Res.* **48,** 2070–2089 (2008).

82. Bremmer, F., Kubischik, M., Hoffmann, K.-P. & Krekelberg, B. Neural Dynamics of Saccadic Suppression. *J. Neurosci.* **29,** 12374–12383 (2009).

83. Bozzacchi, C., Giusti, M. A., Pitzalis, S., Spinelli, D. & Di Russo, F. Awareness affects motor planning for goal-oriented actions. *Biol. Psychol.* **89,** 503–514 (2012).

84. Deecke, L., Scheid, P. & Kornhuber, H. Distribution of readiness potential, pre-motion positivity, and motor potential of the human cerebral cortex preceding voluntary finger movements. *Exp. Brain Res.* **7,** 158–168 (1969).

85. Ball, T. *et al.* The Role of Higher-Order Motor Areas in Voluntary

144

Movement as Revealed by High-Resolution EEG and fMRI. *Neuroimage* **10,** 682–694 (1999).

86. Libet, B., Gleason, C. A., Wright, E. W. & Pearl, D. K. Time of conscious intention to act in relation to onset of cerebral activity (readiness-potential). The unconscious initiation of a freely voluntary act. *Brain* **106 (Pt 3),** 623–42 (1983).

87. Toma, K. *et al.* Generators of Movement-Related Cortical Potentials: fMRI-Constrained EEG Dipole Source Analysis. *Neuroimage* **17,** 161–173 (2002).

88. Hogendoorn, H. Voluntary Saccadic Eye Movements Ride the Attentional Rhythm. *J. Cogn. Neurosci.* (2016).

89. Wutz, A., Muschter, E., van Koningsbruggen, M. G., Weisz, N. & Melcher, D. Temporal Integration Windows in Neural Processing and Perception Aligned to Saccadic Eye Movements. *Curr. Biol.* **26,** 1659–1668 (2016).

90. Benjamini, Y. & Hochberg, Y. Controlling the False Discovery Rate: A Practical and Powerful Approach to Multiple Testing. *J. R. Stat. Soc. Ser. B* **57,** 289–300 (1995).

91. Michels, L. & Lappe, M. Contrast dependency of saccadic compression and suppression. *Vision Res.* **44,** 2327–2336 (2004).

92. Rucci, M. & Poletti, M. Control and Functions of Fixational Eye Movements. *Annu. Rev. Vis. Sci.* **1,** 499–518 (2015).

93. Rucci, M., Iovin, R., Poletti, M. & Santini, F. Miniature eye

movements enhance fine spatial detail. *Nature* **447,** 852–855 (2007).

94. Campbell, F. W. & Wurtz, R. H. Saccadic omission: Why we do not see a grey-out during a saccadic eye movement. *Vision Res.* **18,** 1297–1303 (1978).

95. Nobre, A. C., Correa, A. & Coull, J. The hazards of time. *Curr. Opin. Neurobiol.* **17,** 465–470 (2007).

96. Kapoula, Z. A., Robinson, D. A. & Hain, T. C. Motion of the eye immediately after a saccade. *Exp. Brain Res.* **61,** 386–394 (1986).

97. Gupta, D. S. & Chen, L. Brain oscillations in perception, timing and action. *Curr. Opin. Behav. Sci.* **8,** 161–166 (2016).

98. Wood, D. K., Gu, C., Corneil, B. D., Gribble, P. L. & Goodale, M. A. Transient visual responses reset the phase of low-frequency oscillations in the skeletomotor periphery. *Eur. J. Neurosci.* **42,** 1919–1932 (2015).

99. Stevens, L. T. On the time-sense. *Mind* **11,** 393–404 (1886).

100. Joiner, W. M. & Shelhamer, M. An internal clock generates repetitive predictive saccades. *Exp. Brain Res.* **175,** 305–320 (2006).

101. Binda, P., Cicchini, G. M., Burr, D. C. & Morrone, M. C. Spatiotemporal Distortions of Visual Perception at the Time of Saccades. *J. Neurosci.* **29,** 13147–13157 (2009).

102. Yarrow, K., Haggard, P., Heal, R., Brown, P. & Rothwell, J. C.

146

Illusory perceptions of space and time preserve cross-saccadic perceptual continuity. *Nature* **414,** 302–305 (2001).

103. Morrone, M. C., Ross, J. & Burr, D. C. Saccadic eye movements cause compression of time as well as space. *Nat. Neurosci.* **8,** 950–954 (2005).

104. Dugué, L., Marque, P. & VanRullen, R. The Phase of Ongoing Oscillations Mediates the Causal Relation between Brain Excitation and Visual Perception. *J. Neurosci.* **31,** 11889–11893 (2011).

105. Findlay, J. M. & Gilchrist, I. D. *Active Vision*. (Oxford University Press, 2003). doi:10.1093/acprof:oso/9780198524793.001.0001

106. Repp, B. H. Sensorimotor synchronization: A review of the tapping literature. *Psychon. Bull. Rev.* **12,** 969–992 (2005).

107. Sommer, M. A. & Wurtz, R. H. Visual perception and corollary discharge. *Perception* **37,** 408–18 (2008).

108. Sommer, M. A. & Wurtz, R. H. Influence of the thalamus on spatial visual processing in frontal cortex. *Nature* **444,** 374–7 (2006).

109. Hanes, D. P. & Schall, J. D. Neural control of voluntary movement initiation. *Science* **274,** 427–30 (1996).

110. Rajkai, C. *et al.* Transient Cortical Excitation at the Onset of Visual Fixation. *Cereb. Cortex* **18,** 200–209 (2008).

111. Bosman, C. A., Womelsdorf, T., Desimone, R. & Fries, P. A Microsaccadic Rhythm Modulates Gamma-Band Synchronization

and Behavior. *J. Neurosci.* **29,** 9471–9480 (2009).

112. Dorr, M. & Bex, P. J. Peri-Saccadic Natural Vision. *J. Neurosci.* **33,** 1211–1217 (2013).

113. Schroeder, C. E., Wilson, D. A., Radman, T., Scharfman, H. & Lakatos, P. Dynamics of Active Sensing and perceptual selection. *Curr. Opin. Neurobiol.* **20,** 172–176 (2010).

114. Benedetto, A. & Binda, P. Dissociable saccadic suppression of pupillary and perceptual responses to light. *J. Neurophysiol.* **115,** 1243–51 (2016).

115. Ross, J., Morrone, M. C., Goldberg, M. E. & Burr, D. C. Changes in visual perception at the time of saccades. *Trends Neurosci.* **24,** 113–121 (2001).

116. Wurtz, R. H., Joiner, W. M. & Berman, R. A. Neuronal mechanisms for visual stability: progress and problems. *Philos. Trans. R. Soc. London B Biol. Sci.* **366,** (2011).

117. Watson, T. L. & Krekelberg, B. The relationship between saccadic suppression and perceptual stability. *Curr. Biol.* **19,** 1040–3 (2009).

118. Mishkin, M., Ungerleider, L. G. & Macko, K. A. Object vision and spatial vision: two cortical pathways. *Trends Neurosci.* **6,** 414–417 (1983).

119. Goodale, M. A. & Milner, A. D. Separate visual pathways for perception and action. *Trends Neurosci.* **15,** 20–5 (1992).

120. Burr, D. C., Morrone, M. C. & Ross, J. Separate visual

148

representations for perception and action revealed by saccadic eye movements. *Curr. Biol.* **11,** 798–802 (2001).

121. de'Sperati, C. & Baud-Bovy, G. Blind Saccades: An Asynchrony between Seeing and Looking. *J. Neurosci.* **28,** 4317–4321 (2008).

122. Gamlin, P. D. & Clarke, R. J. The pupillary light reflex pathway of the primate. *J. Am. Optom. Assoc.* **66,** 415–8 (1995).

123. Loewenfeld, I. *The pupil : anatomy, physiology, and clinical applications*. (Waybe State Univ. Press, 1993).

124. Binda, P. & Murray, S. O. Keeping a large-pupilled eye on high-level visual processing. *Trends in Cognitive Sciences* **19,** 1–3 (2015).

125. Bárány, E. H. & Halldén, U. Phasic inhibition of the light reflex of the pupil during retinal rivalry. *J. Neurophysiol.* **11,** (1948).

126. Richards, W. Attenuation of the pupil response during binocular rivalry. *Vision Res.* **6,** 239–IN5 (1966).

127. Laeng, B. & Endestad, T. Bright illusions reduce the eye's pupil. *Proc. Natl. Acad. Sci. U. S. A.* **109,** 2162–7 (2012).

128. Binda, P., Pereverzeva, M. & Murray, S. O. Pupil constrictions to photographs of the sun. *J. Vis.* **13,** 8–8 (2013).

129. Naber, M. & Nakayama, K. Pupil responses to high-level image content. *J. Vis.* **13,** (2013).

130. Laeng, B. & Sulutvedt, U. The eye pupil adjusts to imaginary light. *Psychol. Sci.* **25,** 188–97 (2014).

131. Mathôt, S., van der Linden, L., Grainger, J. & Vitu, F. The pupillary light response reveals the focus of covert visual attention. *PLoS One* **8,** e78168 (2013).

132. Naber, M., Alvarez, G. A. & Nakayama, K. Tracking the allocation of attention using human pupillary oscillations. *Front. Psychol.* **4,** 919 (2013).

133. Mathôt, S., Dalmaijer, E., Grainger, J. & Van der Stigchel, S. The pupillary light response reflects exogenous attention and inhibition of return. *J. Vis.* **14,** 7 (2014).

134. Binda, P., Pereverzeva, M. & Murray, S. O. Pupil size reflects the focus of feature-based attention. *J. Neurophysiol.* **112,** 3046–52 (2014).

135. Lorber, M., Zuber, B. L. & Stark, L. Suppression of the Pupillary Light Reflex in Binocular Rivalry and Saccadic Suppression. *Nature* **208,** 558–560 (1965).

136. Zuber, B. L., Stark, L. & Lorber, M. Saccadic suppression of the pupillary light reflex. *Exp. Neurol.* **14,** 351–370 (1966).

137. Barbur, J. L. in *The Visual Neurosciences* 641–656 (The MIT press, 2004).

138. Diamond, M. R., Ross, J. & Morrone, M. C. Extraretinal control of saccadic suppression. *J. Neurosci.* **20,** 3449–55 (2000).

139. Pelli, D. G. The VideoToolbox software for visual psychophysics: transforming numbers into movies. *Spat. Vis.* **10,** 437–42 (1997).

140. Cornelissen, F. W., Peters, E. M. & Palmer, J. The Eyelink

Toolbox: eye tracking with MATLAB and the Psychophysics Toolbox. *Behav. Res. Methods. Instrum. Comput.* **34,** 613–7 (2002).

141. Reingold, E. M. & Stampe, D. M. Saccadic Inhibition in Voluntary and Reflexive Saccades. *J. Cogn. Neurosci.* **14,** 371–388 (2002).

142. Wang, C.-A., Brien, D. C. & Munoz, D. P. Pupil size reveals preparatory processes in the generation of pro-saccades and anti-saccades. *Eur. J. Neurosci.* **41,** 1102–10 (2015).

143. Watson, T. L. & Krekelberg, B. An equivalent noise investigation of saccadic suppression. *J. Neurosci.* **31,** 6535–41 (2011).

144. Volkmann, F. C. Human visual suppression. *Vision Res.* **26,** 1401–16 (1986).

145. Osaka, N. Variation of saccadic suppression with target eccentricity. *Ophthalmic Physiol. Opt.* **7,** 499–501 (1987).

146. Cohen, J. *Statistical power analysis for the behavioral sciences*. (Academic Press, 1977).

147. Mathôt, S., Melmi, J.-B. & Castet, E. Intrasaccadic perception triggers pupillary constriction. *PeerJ* **3,** e1150 (2015).

148. Bitsios, P., Prettyman, R. & Szabadi, E. Changes in autonomic function with age: a study of pupillary kinetics in healthy young and old people. *Age Ageing* **25,** 432–8 (1996).

149. Tamietto, M. *et al.* Collicular vision guides nonconscious behavior. *J. Cogn. Neurosci.* **22,** 888–902 (2010).

150. Barbur, J. L., Harlow, A. J. & Sahraie, A. Pupillary responses to

stimulus structure, colour and movement. *Ophthalmic Physiol. Opt.* **12,** 137–141 (2007).

151. Sahraie, A. & Barbur, J. L. Pupil response triggered by the onset of coherent motion. *Graefe's Arch. Clin. Exp. Ophthalmol.* **235,** 494–500 (1997).

152. Young, R. S. & Kennish, J. Transient and sustained components of the pupil response evoked by achromatic spatial patterns. *Vision Res.* **33,** 2239–52 (1993).

153. Sahraie, A., Trevethan, C. T., MacLeod, M. J., Urquhart, J. & Weiskrantz, L. Pupil response as a predictor of blindsight in hemianopia. *Proc. Natl. Acad. Sci. U. S. A.* **110,** 18333–8 (2013).

154. Hayes, T. R. & Petrov, A. A. Mapping and correcting the influence of gaze position on pupil size measurements. *Behav. Res. Methods* **48,** 510–27 (2016).

155. Wang, C.-A. & Munoz, D. P. A circuit for pupil orienting responses: implications for cognitive modulation of pupil size. *Curr. Opin. Neurobiol.* **33,** 134–40 (2015).

156. Marg, E. & Morgan, M. W. The pupillary near reflex; the relation of pupillary diameter to accommodation and the various components of convergence. *Am. J. Optom. Arch. Am. Acad. Optom.* **26,** 183–98 (1949).

157. Hupé, J.-M., Lamirel, C. & Lorenceau, J. Pupil dynamics during bistable motion perception. *J. Vis.* **9,** 10 (2009).

158. Spaak, E., de Lange, F. P. & Jensen, O. Local Entrainment of

Alpha Oscillations by Visual Stimuli Causes Cyclic Modulation of Perception. *J. Neurosci.* **34,** (2014).

159. Linkenkaer-Hansen, K., Nikulin, V. V, Palva, S., Ilmoniemi, R. J. & Palva, J. M. Prestimulus oscillations enhance psychophysical performance in humans. *J. Neurosci.* **24,** 10186–90 (2004).

160. Hanslmayr, S., Volberg, G., Wimber, M., Dalal, S. S. & Greenlee, M. W. Prestimulus Oscillatory Phase at 7 Hz Gates Cortical Information Flow and Visual Perception. *Curr. Biol.* **23,** 2273–2278 (2013).

161. de Lange, F. P., Rahnev, D. A., Donner, T. H. & Lau, H. Prestimulus Oscillatory Activity over Motor Cortex Reflects Perceptual Expectations. *J. Neurosci.* **33,** 1400–1410 (2013).

162. Fiebelkorn, I. C. *et al.* Ready, set, reset: stimulus-locked periodicity in behavioral performance demonstrates the consequences of cross-sensory phase reset. *J. Neurosci.* **31,** 9971–81 (2011).

163. Lakatos, P., Chen, C.-M., O'Connell, M. N., Mills, A. & Schroeder, C. E. Neuronal Oscillations and Multisensory Interaction in Primary Auditory Cortex. *Neuron* **53,** 279–292 (2007).

164. Haegens, S., Nácher, V., Luna, R., Romo, R. & Jensen, O. α-Oscillations in the monkey sensorimotor network influence discrimination performance by rhythmical inhibition of neuronal spiking. *Proc. Natl. Acad. Sci. U. S. A.* **108,** 19377–82 (2011).

165. Stenner, M.-P., Bauer, M., Haggard, P., Heinze, H.-J. & Dolan, R.

Enhanced Alpha-oscillations in Visual Cortex during Anticipation of Self-generated Visual Stimulation. *J. Cogn. Neurosci.* **26,** 2540–2551 (2014).

166. Zanos, T. P., Mineault, P. J., Nasiotis, K. T., Guitton, D. & Pack, C. C. A Sensorimotor Role for Traveling Waves in Primate Visual Cortex. *Neuron* **85,** 615–627 (2015).

167. Min, B.-K., Jung, Y.-C., Kim, E. & Park, J. Y. Bright illumination reduces parietal EEG alpha activity during a sustained attention task. *Brain Res.* **1538,** 83–92 (2013).

168. Nathan, R. D. & Hanley, J. Spectral analysis of the EEG recorded during stimulation of the human fovea. *Brain Res.* **91,** 65–77 (1975).

169. Pascucci, D., Megna, N., Panichi, M. & Baldassi, S. Acoustic cues to visual detection: A classification image study. *J. Vis.* **11,** (2011).

170. Aliu, S. O., Houde, J. F. & Nagarajan, S. S. Motor-induced Suppression of the Auditory Cortex. *J. Cogn. Neurosci.* **21,** 791–802 (2009).

171. Blakemore, S.-J., Wolpert, D. M. & Frith, C. D. Central cancellation of self-produced tickle sensation. *Nat. Neurosci.* **1,** 635–640 (1998).

172. Schafer, E. W. & Marcus, M. M. Self-stimulation alters human sensory brain responses. *Science* **181,** 175–7 (1973).

173. Campbell, F. W. & Maffei, L. Electrophysiological evidence for the

existence of orientation and size detectors in the human visual system. *J. Physiol.* **207,** 635–52 (1970).

174. Boynton, G. M., Demb, J. B., Glover, G. H. & Heeger, D. J. Neuronal basis of contrast discrimination. *Vision Res.* **39,** 257–69 (1999).

175. Anderson, K. L. & Ding, M. Attentional modulation of the somatosensory mu rhythm. *Neuroscience* **180,** 165–180 (2011).

176. Craighero, L., Fadiga, L., Rizzolatti, G. & Umiltà, C. Action for perception: a motor-visual attentional effect. *J. Exp. Psychol. Hum. Percept. Perform.* **25,** 1673–92 (1999).

177. Gutteling, T. P., Kenemans, J. L. & Neggers, S. F. W. Grasping Preparation Enhances Orientation Change Detection. *PLoS One* **6,** e17675 (2011).

178. Rolfs, M., Lawrence, B. M. & Carrasco, M. Reach preparation enhances visual performance and appearance. *Philos. Trans. R. Soc. Lond. B. Biol. Sci.* **368,** 20130057 (2013).

179. Martinez-Conde, S., Otero-Millan, J. & Macknik, S. L. The impact of microsaccades on vision: towards a unified theory of saccadic function. *Nat. Rev. Neurosci.* **14,** 83–96 (2013).

180. Yuval-Greenberg, S., Merriam, E. P. & Heeger, D. J. Spontaneous Microsaccades Reflect Shifts in Covert Attention. *J. Neurosci.* **34,** 13693–13700 (2014).

181. Julesz, B. & White, B. Short Term Visual Memory and the Pulfrich Phenomenon. *Nature* **222,** 639–641 (1969).

182. Swanson, W. H., Ueno, T., Smith, V. C. & Pokorny, J. Temporal modulation sensitivity and pulse-detection thresholds for chromatic and luminance perturbations. *J. Opt. Soc. Am. A.* **4,** 1992–2005 (1987).

183. Williams, J. M. & Lit, A. Luminance-dependent visual latency for the Hess effect, the Pulfrich effect, and simple reaction time. *Vision Res.* **23,** 171–9 (1983).

184. Jensen, O., Gips, B., Bergmann, T. O. & Bonnefond, M. Temporal coding organized by coupled alpha and gamma oscillations prioritize visual processing. *Trends Neurosci.* **37,** 357–69 (2014).

185. Scheeringa, R., Mazaheri, A., Bojak, I., Norris, D. G. & Kleinschmidt, A. Modulation of Visually Evoked Cortical fMRI Responses by Phase of Ongoing Occipital Alpha Oscillations. *J. Neurosci.* **31,** 3813–3820 (2011).

186. Cecere, R., Rees, G. & Romei, V. *Individual Differences in Alpha Frequency Drive Crossmodal Illusory Perception*. *Current Biology* **25,** (2015).

187. Lunghi, C., Berchicci, M., Morrone, M. C. & Di Russo, F. Short-term monocular deprivation alters early components of visual evoked potentials. *J. Physiol.* **593,** 4361–4372 (2015).

188. Samaha, J. & Postle, B. R. *The Speed of Alpha-Band Oscillations Predicts the Temporal Resolution of Visual Perception*. *Current Biology* **25,** (2015).

189. Cicchini, G. M., Binda, P., Burr, D. C. & Morrone, M. C. Transient

spatiotopic integration across saccadic eye movements mediates visual stability. *J. Neurophysiol.* **109,** 1117–25 (2013).

190. Wenke, D. & Haggard, P. How voluntary actions modulate time perception. *Exp. Brain Res.* **196,** 311–318 (2009).

191. White, A. L., Linares, D. & Holcombe, A. O. Visuomotor timing compensates for changes in perceptual latency. *Curr. Biol.* **18,** R951–R953 (2008).

192. Nunn, C. M. H. & Osselton, J. W. The Influence of the EEG Alpha Rhythm on the Perception of Visual Stimuli. *Psychophysiology* **11,** 294–303 (1974).

193. Romei, V., Rihs, T., Brodbeck, V. & Thut, G. Resting electroencephalogram alpha-power over posterior sites indexes baseline visual cortex excitability. *Neuroreport* **19,** 203–208 (2008).

194. VanRullen, R. & Macdonald, J. S. P. *Perceptual Echoes at 10 Hz in the Human Brain. Current Biology* **22,** (2012).

195. Lalor, E. C., Pearlmutter, B. A., Reilly, R. B., McDarby, G. & Foxe, J. J. The VESPA: A method for the rapid estimation of a visual evoked potential. *Neuroimage* **32,** 1549–1561 (2006).

196. Sauseng, P. *et al.* A shift of visual spatial attention is selectively associated with human EEG alpha activity. *Eur. J. Neurosci.* **22,** 2917–2926 (2005).

197. Barbur, J. L. & Stockman, A. in *Encyclopedia of Eye* (ed. Besharse J Dana R Dartt D) 323–331 (Elsevier/Academic Press,

2010).

198. Vandewalle, G., Maquet, P. & Dijk, D.-J. Light as a modulator of cognitive brain function. *Trends Cogn. Sci.* **13,** 429–38 (2009).

199. Kammer, T., Lehr, L. & Kirschfeld, K. Cortical visual processing is temporally dispersed by luminance in human subjects. *Neurosci. Lett.* **263,** 133–6 (1999).

200. Brodoehl, S., Klingner, C. M. & Witte, O. W. Eye closure enhances dark night perceptions. *Sci. Rep.* **5,** 10515 (2015).

201. Huang, S., Hokenson, K., Bandyopadhyay, S., Russek, S. J. & Kirkwood, A. Brief Dark Exposure Reduces Tonic Inhibition in Visual Cortex. *J. Neurosci.* **35,** 15916–20 (2015).

202. Chyatte, C. A note on the relationship of alpha index to critical flicker frequency. *Electroencephalogr. Clin. Neurophysiol.* **10,** 553–554 (1958).

203. Kooi, K., Boswell, R. & Thomas, M. Critical flicker frequency and EEG findings in patients with brain damage. *Neurology* **8,** 764–768 (1958).

204. May, E. S. *et al.* Hepatic encephalopathy is associated with slowed and delayed stimulus-associated somatosensory alpha activity. *Clin. Neurophysiol.* **125,** 2427–2435 (2014).

205. Karp, E., Pollack, M. & Fink, M. Critical flicker frequency and EEG alpha: A reliability study. *Electroencephalogr. Clin. Neurophysiol.* **14,** 60–63 (1962).

206. Dondero, A., Hofstaetter, P. R. & O'Connor, P. Critical flicker

frequency and cortical alpha. *Electroencephalogr. Clin. Neurophysiol.* **8,** 465–466 (1956).

207. Brainard, D. H. The Psychophysics Toolbox. *Spat. Vis.* **10,** 433–6 (1997).

208. Peirce, J. W. PsychoPy—Psychophysics software in Python. *J. Neurosci. Methods* **162,** 8–13 (2007).

209. Teikari, P. *et al.* An inexpensive Arduino-based LED stimulator system for vision research. *J. Neurosci. Methods* **211,** 227–236 (2012).

210. Delorme, A. & Makeig, S. EEGLAB: an open source toolbox for analysis of single-trial EEG dynamics including independent component analysis. *J. Neurosci. Methods* **134,** 9–21 (2004).

211. Oostenveld, R., Fries, P., Maris, E. & Schoffelen, J.-M. FieldTrip: Open source software for advanced analysis of MEG, EEG, and invasive electrophysiological data. *Comput. Intell. Neurosci.* **2011,** 156869 (2011).

212. Jung, T. *et al.* Removing electroencephalographic artifacts by blind source separation. *Psychophysiology* **37,** (2000).

213. Klimesch, W., Schimke, H. & Pfurtscheller, G. Alpha frequency, cognitive load and memory performance. *Brain Topogr.* **5,** 241–251 (1993).

214. Watson, A. B. & Pelli, D. G. QUEST: a Bayesian adaptive psychometric method. *Percept. Psychophys.* **33,** 113–20 (1983).

215. Loftus, G. R. Picture perception: Effects of luminance on available

information and information-extraction rate. *J. Exp. Psychol. Gen.* **114,** 342–356 (1985).

216. Giesbrecht, B., Bischof, W. F. & Kingstone, A. Seeing the light: Adapting luminance reveals low-level visual processes in the attentional blink. *Brain Cogn.* **55,** 307–309 (2004).

217. Wells, E. F., Bernstein, G. M., Scott, B. W., Bennett, P. J. & Mendelson, J. R. Critical flicker frequency responses in visual cortex. *Exp. brain Res.* **139,** 106–10 (2001).

218. Fedorov, N. T. & Mkrticheva, L. Mechanism of Light Flicker Fusion during the Course of Dark and Light Adaptation. *Nature* **142,** 750–751 (1938).

219. Lipkin, B. Monocular Flicker Discrimination as a Function of the Luminance and Area of Contralateral Steady Light II Area. *J. Opt. Soc. Am.* **52,** (1962).

220. Lunghi, C., Berchicci, M., Morrone, M. C. & Di Russo, F. Short-term monocular deprivation alters early components of visual evoked potentials. *J. Physiol.* **593,** 4361–4372 (2015).

221. Lunghi, C., Emir, U. E., Morrone, M. C. & Bridge, H. *Short-Term Monocular Deprivation Alters GABA in the Adult Human Visual Cortex*. *Current Biology* **25,** (2015).

222. Allen, F. On Reflex Visual Sensations*. *J. Opt. Soc. Am.* **7,** 583 (1923).

223. Moore, A. P. Impaired sensorimotor integration in parkinsonism and dyskinesia: a role for corollary discharges? *J. Neurol.*

Neurosurg. Psychiatry **50,** 544–52 (1987).

224. Mathalon, D. H. & Ford, J. M. Corollary discharge dysfunction in schizophrenia: evidence for an elemental deficit. *Clin. EEG Neurosci.* **39,** 82–6 (2008).

225. Ishii, R. *et al.* Theta rhythm increases in left superior temporal cortex during auditory hallucinations in schizophrenia: a case report. *Neuroreport* **11,** 3283–7 (2000).

226. Uhlhaas, P. J., Haenschel, C., Nikolić, D. & Singer, W. The role of oscillations and synchrony in cortical networks and their putative relevance for the pathophysiology of schizophrenia. *Schizophr. Bull.* **34,** 927–43 (2008).

227. Behrendt, R. . Hallucinations: Synchronisation of thalamocortical γ oscillations underconstrained by sensory input. *Conscious. Cogn.* **12,** 413–451 (2003).

228. Lorenz, I., Müller, N., Schlee, W., Hartmann, T. & Weisz, N. *Loss of alpha power is related to increased gamma synchronization—A marker of reduced inhibition in tinnitus? Neuroscience Letters* **453,** (2009).

229. Block, N. *et al.* How many concepts of consciousness? *Behav. Brain Sci.* **18,** 272 (1995).

230. Chalmers, D. J. Facing up to the problem of consciousness. *J. Conscious. Stud.* **2,** 200–219 (1995).

231. Nagel, T. What Is It Like to Be a Bat? *Philos. Rev.* **83,** 435 (1974).

232. Dennett, D. Are we explaining consciousness yet? *Cognition* **79,**

221–237 (2001).

233. Crick, F. & Koch, C. Towards a Neurobiological Theory of Consciousness. *Semin. Neurosci.* **2,** 263–275 (1990).

234. Damasio, A. The brain binds entities and events by multiregional activation from convergence zones. *Neural Comput.* **1,** 123–132 (1989).

235. Engel, A. K. & Singer, W. Temporal binding and the neural correlates of sensory awareness. *Trends Cogn. Sci.* **5,** 16–25 (2001).

236. Mathewson, K. E. *et al.* Making Waves in the Stream of Consciousness: Entraining Oscillations in EEG Alpha and Fluctuations in Visual Awareness with Rhythmic Visual Stimulation. *J. Cogn. Neurosci.* **24,** 2321–2333 (2012).